UNIVERSITA' DEGLI STUDI DI MILANO

PhD program in

Experimental Medicine and Medical Biotechnologies

(XXXIII cycle)

Department of Medical Biotechnology and Translational Medicine

Transcriptomic analysis of human circulating monocytes: focus on membrane-spanning 4A gene family members

Thesis of

Alessandra Rigamonti

Matr. N°: R12093

Directors of studies: Prof. Federica MARCHESI
Prof. Massimo LOCATI

Coordinator: Prof. Massimo LOCATI

Academic year 2020/2021

TABLE OF CONTENTS

1 ABSTRACT 3

2 LIST OF ABBREVIATIONS 5

3 NOTE TO THE READER 7

4 INTRODUCTION 8

4.1 MONOCYTES 8

4.1.1 Subsets of monocytes 8

4.1.2 Origin of monocytes 11

4.1.3 Development and functions in homeostasis 14

4.1.4 Function during infection and diseases 17

4.1.4.1 Monocytes in cancer 21

4.1.4.2 Emergency monopoiesis and trained immunity 24

4.2 THE MS4A FAMILY 25

4.2.1 MS4A family structure 26

4.2.2 MS4A1 (CD20) 28

4.2.3 MS4A2 (FcεRIβ) 29

4.2.4 MS4A4A and other MS4A proteins expressed on myeloid cells 29

5 AIM OF STUDY 31

6 METHODS 32

6.1 SINGLE CELL RNA SEQUENCING 32

6.1.1 Sample collection and isolation of peripheral blood mononuclear cells (PBMCs) 32

6.1.2 Fluorescence-Activated Cell Sorting (FACS) staining 32

6.1.3 cDNA library construction and single cell RNA sequencing 33

6.1.4 Single cell mapping and clustering 33

6.2 CLUSTER ANNOTATION 34

6.2.1 Trajectories analysis 36

6.2.2 Statistics 36

6.3 FACS ANALYSIS 36

6.3.1 Sample collection, isolation of PBMCs and FACS staining 36

6.3.2 Cytospin 37

6.4 BULK RNA SEQUENCING 37

6.4.1 Sample collection and isolation of PBMCs 37

6.4.2 FACS sorting and bulk rna sequencing 38

6.4.3 Sequence data processing 38

6.4.4 Data Analysis *39*
6.4.5 Gene Clustering *40*
6.5 GSE130157 DATASET ANALYSIS 40
7 RESULTS 42
7.1 SINGLE-CELL ANALYSIS OF HUMAN CIRCULATING MONONUCLEAR CELLS 42
7.2 CIRCULATING MONOCYTES PRESENT DISTINCT PROFILES IN HOMEOSTATIC CONDITIONS 46
7.3 TRAJECTORY RECONSTRUCTION OF MONOCYTE POPULATIONS 53
7.4 MS4A GENE FAMILY IN HUMAN MONOCYTES 57
7.5 FOCUS ON MS4A4A IN HUMAN MONOCYTES 61
7.5.1 MS4A4A protein is expressed by a fraction of CD16^{+} monocytes 61
7.5.2 Transcriptomic analysis of MS4A4A positive monocytes 64
7.6 A PRELIMINARY TRANSLATION TO PATHOLOGY SETTING: I.E. RELEVANCE OF MONOCYTE DIVERSITY IN PATHOLOGY . 71
8 DISCUSSION 76
9 BIBLIOGRAPHY 82

1 ABSTRACT

Within the mononuclear phagocyte system (MPS), monocytes represent the unique population able to operate as both effector and precursor cells. These incredibly plastic cells, mainly present in peripheral blood, are essential components of the innate immune system and play central roles both in homeostatic and pathological conditions. Monocytes are key determinants for the surveillance of endothelial integrity and repair, regulation of wound healing and replenishment of tissue resident macrophages (TRMs). Moreover, they serve as first line of defence against infections and hold a key position in several human diseases. Despite the fact that current classification distinguishes three major subsets (classical, intermediate and non-classical), monocytes represent an extremely heterogeneous population in terms of phenotype and specialized functions.

To overcome the remarkable lack of consensus on the identity and interrelationship of monocyte subsets, we have performed a single cell RNA sequencing analysis on circulating mononuclear cells of healthy donors. We identified 8 cluster of monocytes. C0 and c2 resembled neutrophil-like monocytes (NeuMo) and, together with c1, displayed distinct inflammatory programs and activation states. Of the two other clusters of classical monocytes, c7 significantly expressed high levels of antiviral genes, including IFN-related genes, while c12 corresponded to circulating monocyte-platelet aggregates (MPA). C6 and c3 resembled the intermediate and non-classical monocyte populations, respectively. Finally, a small cluster of $CD16^+$ cells (c13) was characterized by the specific expression of genes of the complement system. We then moved to the analyses of a public transcriptomic dataset obtained from peripheral blood mononuclear cells (PBMCs) of gastrointestinal cancer patients at 3 time points of treatment. We were able to identify all previously defined monocyte subsets. Preliminary data showed the specific expansion of the IFN-related cluster c7 exclusively in responder patients after treatment with immunotherapy, suggesting a potential role of this population in response to therapy.

Analyses of the Membrane-Spanning 4-domain subfamily A (MS4A) protein family, representing a set of proteins whose roles in regulating myeloid cell function are now emerging, identified *MS4A4A* as potential markers for the commitment to circulating non-classical monocytes in humans. The expression of MS4A4A on a fraction of $CD16^+$ monocytes was further confirmed at the protein level by flow cytometry. Given the selective expression of this protein on $CD16^+$ cells and based on solid preliminary data from our laboratory, we hypothesized that MS4A4A may play a role in the biology of this subset of cells. Interestingly,

bulk RNA sequencing of $CD16^{-}MS4A4A^{-}$, $CD16^{+}MS4A4A^{-}$ and $CD16^{+}MS4A4A^{+}$ monocytes revealed enrichment of the Fc gamma receptor (FcγR) and Fc epsilon receptor (FcεR) pathways in $MS4A4A^{pos}$ cells. Implementation of these findings with functional assays is in program and will be essential to deeper investigate a possible role of MS4A4A as modulator of FcRs function in monocytes.

2 LIST OF ABBREVIATIONS

AD	Alzheimer disease
ADCC	antibody-dependent cellular cytotoxicity
BCR	B-cell receptor
BM	bone marrow
cMoP	common monocyte progenitor
CMP	common myeloid progenitor
Csf-1	colony-stimulating factor 1
CyTOF	cytometry by time-of-flight
DC	dendritic cell
DCMo	dendritic cell-like monocyte
DEGs	differential expressed genes
EAE	experimental autoimmune encephalomyelitis
EMP	erythro-myeloid precursor
FcεR	Fc epsilon receptor
FcγR	Fc gamma receptor
GMP	granulocyte and macrophage progenitor
HLA	human leukocyte antigen
HSC	hematopoietic stem cell
HSPCs	hematopoietic stem and progenitor cells
IFN	interferon
IRF8	interferon regulatory factor 8
KLF4	Kruppel-like factor-4
LDTF	lineage-determining transcription factor
LMPs	lympho-myeloid progenitors
LOAD	late-onset Alzheimer's disease
LPS	lipopolysaccharide
mAbs	monoclonal antibody
MDP	monocyte/dendritic cell progenitor
Mφ	macrophage/s
MHCII	major histocompatibility complex class II
moDC	monocyte-derived dendritic cell

MP monocyte precursor

MPA monocyte-platelet aggregates

MPP multipotent progenitor

MPS mononuclear phagocyte system

MS4A Membrane-Spanning 4-domain subfamily A

NeuMo neutrophil-like monocytes

PBMCs peripheral blood mononuclear cells

PSGL-1 P-selectin glycoprotein ligand-1

SatM segregated-nucleus-containing atypical monocyte

scRNA-seq single-cell RNA sequencing

SLAN 6-sulfo LacNAc

ssGSEA single sample Gene Set Enrichment Analysis

STREAM Single-cell Trajectories Reconstruction, Exploration And Mapping

TipDC TNF/iNOS-producing dendritic cell

TLR toll-like receptor

TRM tissue resident macrophage

Tspans tetraspanins

WAM wound-associated macrophage

3 NOTE TO THE READER

This thesis provides an insight into the heterogeneity of human monocytes. In view of the lack of consensus about the multiple subtypes and the exact task-division among them, we chose to dissect the diversity of monocytes taking advantage from the power of single cell and RNA sequencing technologies in dissecting lineage heterogeneities and cellular process. The work described in this dissertation originates from the closed collaboration with the bioinformatician engineer Alessandra Castagna, who works in our laboratory and handled the dataset under my continuous inputs and supervision.

In pathological conditions, including tumours, monocytes are amply recruited into tissues, where they may differentiate into monocyte-derived macrophages. Given the long-standing interest of the laboratory in the biology of macrophages in tumours, the data originated from previous studies and our recent data on monocytes, we have begun to explore the phenotype, tissue distribution and localization of macrophages in human cancers. However, since this part is still in its infancy, we preferred not to report this preliminary data in this thesis.

4 INTRODUCTION

4.1 MONOCYTES

Monocytes represent a population of innate immune cells belonging to the so called "mononuclear phagocyte system" (MPS). The definition of this system dates back to the 1972 and was motivated by the necessity to classify populations of cells, including macrophages (Mφ), monocytes and their precursors, which are different in terms of localization, maturation state, phenotype and specialized functions, but with a certain degree of similarities in their origin, morphology and phagocytic capacity [1]. The subsequent extensive collection of literature on this subject has highlighted the vast heterogeneity within these and other immune cells, from the characterization of macrophage states with poor phagocytic activities [2], to the increasingly emerging closed relation between MPS members and dendritic cells (DCs). More research efforts are thus needed to deepen our understanding on this branch of the innate immune system, both in health and disease.

4.1.1 *SUBSETS OF MONOCYTES*

Monocytes have been considered a homogeneous cell population for almost a century, since their identification in 1880 by Paul Ehrlich [3]. The advent of multiparametric technologies, like flow cytometry, and the generation of engineered mice to perform fate-mapping studies [4], allowed the first description of different monocyte subsets. Both in humans and in mice, two populations were initially characterized based on cell function, morphology and the expression of surface markers, namely "inflammatory" monocytes ($CD14^+CD16^-$ in human, $Ly6C^+CX_3CR1^{lo}CCR2^+$ in mice) and "patrolling" monocytes ($CD14^{lo}CD16^+$ in human, $Ly6C^-CX_3CR1^{hi}CCR2^-$ in mice) [5-7]. However, the term "inflammatory", used to identify $CD14^+$ monocytes in the steady state, soon became a source of confusion, and subsequent studies showed that also $CD16^+$ cells exert pro-inflammatory activities in different contexts, such as in response to viruses [8, 9]. Moreover, monocyte complexity was further evidenced by the description of a third major intermediate population, characterized by high levels of both CD14 and CD16 [10, 11]. The functional distinction between inflammatory and non-inflammatory monocytes was therefore considered too simplistic, leading to the adoption, in

2010, of a more general nomenclature: the "classical", "intermediate" and "non-classical" monocytes (**Table 4.1**) [12]. This classification is now widely adopted for humans, where the proportion of classical, intermediate and non-classical monocytes in peripheral blood is respectively, 85-90%, ~5% and ~10% [9]. Conversely, in mice, the intermediate population has not been fully recognized as a distinctive monocyte subset, despite the fact that cells with an intermediate phenotype have been described [13, 14]. For instance, it has been shown a differential expression of the triggering receptor Treml4 within the three subpopulations, and that Ly6C$^{hi/mid}$Treml4^{+} monocytes represent an intermediate subset between Ly6C^{hi}Treml4^{-} and Ly6C^{lo}Treml4^{+} cells [15].

	Human	*Mouse*
Classical	CD14^{++}CD16^{-}	Ly6C^{hi}CD43^{lo}CX$_3$CR1^{lo}CCR2^{hi}
Intermediate	CD14^{++}CD16^{+}	Ly6C^{int}CD43^{hi}CX$_3$CR1^{hi}CCR2^{hi}
Non-classical	CD14^{lo}CD16^{hi}	Ly6C^{lo}CD43^{hi}CX$_3$CR1^{hi}CCR2^{-}

Table 4.1. Three major subtypes of human and mouse monocytes.

Monocyte subsets are typically determined by flow cytometry, using either a trapezoid- or rectangular-based gating strategy. However, this system appears to be imprecise and subjective, especially in the separation of the intermediate and non-classical populations. Such difficulties arise from the evidence that, as well as the lipopolysaccharide receptor (CD14) and the FcγRIII (CD16), the vast majority of monocyte markers are expressed as a continuum along the three subsets. One possible approach to overcome this problem is to set the gate separating the intermediates and non-classicals in correspondence of the endpoint of CD14 expression by classical monocytes [16]. In addition, using cytometry by time-of-flight (CyTOF) and mass spectrometry, it has been shown that the addition of others cell markers, including CCR2, CD36, HLA-DR, and CD11c, to the conventional panel improves subset definition and purity [17, 18]. Recently, 6-sulfo LacNAc (SLAN) has been proposed as a marker for human non-classical monocytes [19]. SLAN identifies a specific O-linked glycosylation of the P-selectin glycoprotein ligand-1 (PSGL-1), not found in mice [20]. At the time of its discovery, when this antigen was first targeted by the monoclonal antibody M-DC8, SLAN^{+} cells were classified as a novel circulating dendritic cell (DC) subset [21, 22]. Later on, several studies demonstrated that these blood cells actually belong to the monocyte lineage, sharing the same phenotype and functional properties of the non-classical subtype, including a lack of the CCR2 chemokine receptor and low levels of CD14 expression [23-26]. Additionally, more recent studies have

demonstrated that $SLAN^+$ monocytes represent only a fraction of $CD16^{++}$ [27, 28], questioning the idea of nominating SLAN as a marker for the distinction between intermediate and non-classical monocytes, whilst also highlighting the vast heterogeneity within human monocytes. TIE-2 angiopoietin receptor is another protein that has been suggested as cell marker for segregating the monocyte populations, even independently of the official system based on CD14 and CD16. It is expressed by a portion of monocytes, representing around 20% of the total [29]. TIE-2 has been long considered an endothelial cell-specific marker, till the identification of proangiogenic and pro-tumoral $TIE2^{pos}$ monocytes, both in human and in mouse. Lacking CD146 and AD133, human $Tie\text{-}2^+$ monocytes can be distinguished by rare peripheral blood endothelial and endothelial progenitor cells [30, 31]. Numerous subsequent studies demonstrated the role that Tie-2 positive monocytes play within the tumour microenvironment, with a consequence for local tumour progression and distant spreading, as discussed in more detail in paragraph 4.1.4.1.

Given all the above, it is now clear how current monocyte classification masks the extensive inter-cellular heterogeneity within classical, intermediate and non-classical subsets. With the advent of powerful single-cell profiling techniques, such heterogeneity becomes more and more evident, however an exact task-division among the different subsets has not been defined yet, and there are still many open questions regarding the distinct monocyte functional phenotypes, as discussed below. Recently, single-cell RNA sequencing (scRNA-seq) of human blood monocytes identified four clusters: Mono1 and Mono2 corresponding to classicals and non-classicals, respectively; Mono3 and Mono4 both containing intermediate cells. These two last subsets were enriched in genes involved in cell cycle, differentiation and trafficking (Mono3) or in cytotoxicity (Mono4) [32]. A deeper analysis of the same scRNA-seq data identified cluster Mono4 as $CD16^+$ contaminating NK cells, and cluster DC4, identified as a population of $CD16^{++}$ DCs in the study by Villani et al., actually corresponding to $SLAN^+$ monocytes [33, 34]. On the same line, but adopting different strategies, investigation by high-dimensional mass cytometry described eight phenotypically different monocyte clusters [28]. Specifically, four subsets were classified as classical monocytes (one small $CD14^+IgE^+$ monocyte population, one group characterized by TREM-1 positivity and two subsets different on the levels of CD93/CD11a), three subsets fell within non-classical monocytes (one $Slan^{neg}$ and two distinct $Slan^{pos}$ populations with increased migration and efferocytosis activities) and one cluster corresponded to the intermediate population. Even in this case, subsequent studies speculated that some cell types had been misclassified. In particular, using flow cytometry, Dutertre *et al*. have suggested that the cluster comprising $CD14^+IgE^+$ cells actually

corresponded to a subset of $CD14^+$ conventional DCs (cDCs) [34]. In the same study, high-dimensional single-cell protein expression analysis of human circulating myeloid cells revealed the presence of 8 clusters of classical-, 2 clusters of intermediate- and 3 clusters of non-classical-monocytes. However, the differences among them have been not discussed. On the other hand, indexed scRNA-seq analysis on monocytes identified only three groups, probably due to the slow number of FACS-sorted cells: two clusters of $CD14^{hi}CD16^-$ (characterized by either high levels of CD14 and inflammatory S100 proteins or high levels of *BNIP3L*, the leukocyte immunoglobulin like receptor A5 and the purinergic receptor P2X 7*)*, and one cluster of $CD16^+$ [34].

Collectively, these studies indicate that the current monocyte classification into three main subtypes provides only a general overview of monocytic cell phenotypes and functions, and that the scenario is likely to be much more complex.

4.1.2 *ORIGIN OF MONOCYTES*

The definition of monocyte origin, development and fates is a very crucial point to understand their biology. Two distinct differentiation pathways characterize foetal and adult monocyte origin.

In the foetus, these mononuclear cells are produced by erythro-myeloid precursors (EMPs). Arising from the yolk-sac blood islands of the embryo at embryonic day 7.0 (E7.0) in mice, EMPs are multipotent progenitors crucial in both the first and the second embryonic hematopoietic programs [35, 36]. Indeed, during the primitive haematopoiesis, c-kit^+ "early" EMPs generate mast cells and macrophage precursors without any intermediate monocytic state. By E9.5, a portion of the c-kit^+ $CD41^+$ "late" EMPs colonize the foetal liver and give rise to different myeloid cells, including erythrocytes, megakaryocytes, granulocytes and monocytes [35, 37-39]. In the specific case of monocytes, they first emerge in the foetal liver during the transient hematopoietic wave, at around E12.5 [40]. Finally, the third (definitive) hematopoietic wave produces, besides functionally active cells derived from either EMPs or lympho-myeloid progenitors (LMPs), a pool of undifferentiated hematopoietic stem cells (HSCs). The latter serves as long-term reservoir to maintain hematopoietic production.

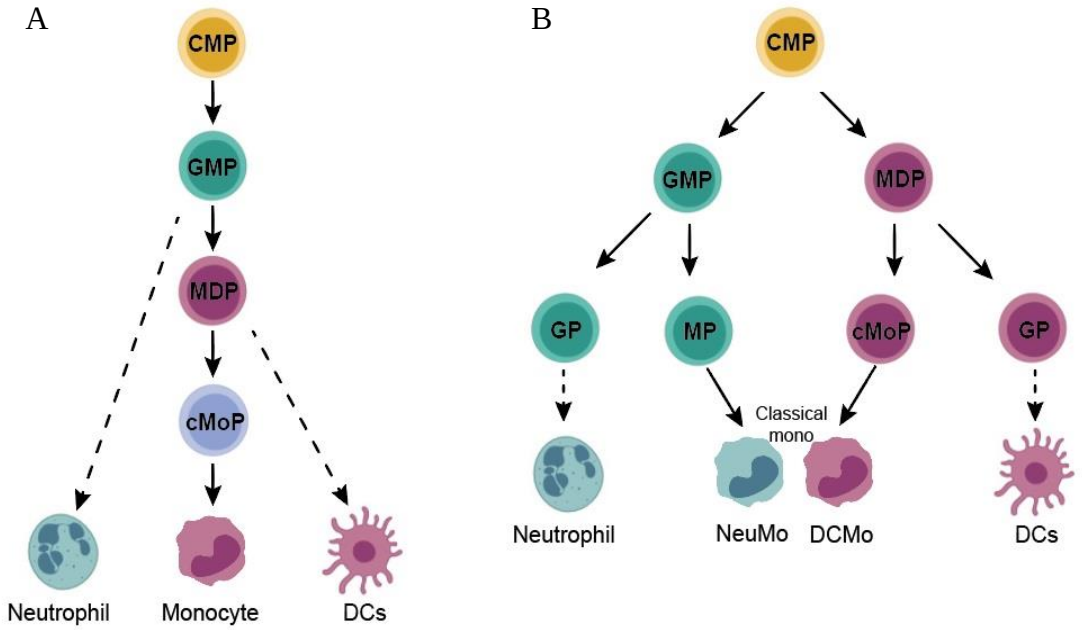

Figure 4.1. Schematic representation of (A) classical model and (B) new proposed model of monopoiesis. In the classical model, different progenitors give rise to monocytes in a linear hierarchy, from the common myeloid progenitor (CMP), via the granulocyte and macrophage progenitor (GMP), the monocyte/DC progenitor (MDP), to the unipotent common monocyte progenitor (cMoP). Recently, a new model of monopoiesis has been proposed. In this scenario, monocytes with characteristic flavours, including neutrophil-like (NeuMo) and DC-like (DCMo) cells, can arise directly from both the GMP and the MDP, respectively. (Mod. from Wolf A.A. et al, Front. Immunol., 2017).

During the perinatal period, HSCs present in the liver migrate to their definitive location in the bone marrow, forming the hematopoietic stem cell niche [41]. Here, multiple commitment steps occur before the release of mature monocytes into the blood circulation. These steps consist of several progenitors at different progressive stages, including multipotent progenitors (MPPs), common myeloid progenitors (CMPs), granulocyte and macrophage progenitors (GMPs), monocyte/DC progenitors (MDPs) and unipotent common monocyte progenitors (cMoPs) [42]. Until recently, these cells have been considered to arise one from another in a linear hierarchy, creating a unique monocyte developmental pathway (**Figure 4.1A**). However, new studies proposed the existence of two distinct routes of monocyte differentiation, each of which resulting into characteristic mature cells, distinguishable on the basis of their phenotype. Adoptive transfer and lineage tracing experiments demonstrated that both GMPs and MDPs can directly and independently give rise to intermediate progenitors that will differentiate into mature monocytes [43]. Specifically, MDPs can differentiate into cMoPs and, subsequently, into mature neutrophil-like monocytes (NeuMo), while immunoregulatory $Ym1^{+}$ $Ly6C^{hi}$ cells

and monocytes with DC-like gene expression (DCMo) derived from the differentiation of GMPs into monocyte precursors (MPs) [43-45] (**Figure 4.1B**). Likewise, lineage trajectory analyses applied to scRNA-seq data reinforce the idea of two routs of monocyte differentiation [46, 47]. Overall, the precise ontogeny of monocytes and whether the different origin of monocyte subpopulations affects their functions remain to be largely elucidated, both in human and in mouse.

Monocyte development in the bone marrow requires the accurate balancing of specific lineage-determining transcription factors (LDTFs) activity. The expression of PU.1, a master LDTF in monocyte production, progressively increases through the development of these cells. During the early stages, PU.1 binds to C/EBPα (CCAAT enhancer-binding protein α), and this complex formation is crucial for the transition of HSC towards the CMPs [48, 49]. At the time of CMP commitment to GMP, the continuous increase of PU.1 coincides with progressively decrease in *Gata2* expression [50], while increasing amount of interferon regulatory factor 8 (*IRF8*) restrains mononuclear phagocyte progenitors from transiting into neutrophils [51, 52]. These two factors play a key role in monocyte differentiation, as indicated by the identification of GATA2 mutation in patients with monocyte deficiencies [53, 54], and the accumulation of monoblasts and monocyte-committed progenitors in *Irf8*-deficient mice [55]. Kruppel-like factor-4 (KLF4) is another key transcription factor for the production of mature monocytes. Accordingly, deletion of *Klf4* led to the absence of classical monocytes [56]. In $Ly6C^{hi}$ monocytes, the levels of both PU.1 and IRF8 are still high, and their active role in the induction of *Klf4* expression has been shown through their binding to the KLF4 enhancer [56]. Both progenitors and mature monocytes relay on colony-stimulating factor 1 (Csf-1) for survival [57].

Mature monocytes produced in the bone marrow (BM) are subsequently released into circulation. CXCR4- and CCR2-signalling are key pathways in the regulation of monocyte retention in the BM or egress to the circulation, respectively. Indeed, the rapid transition of $CXCR4^{+}$ pre-monocytes into $Ly6C^{hi}CXCR4^{-}$ monocytes coincide with the upregulation of CCR2 [58]. These axes are crucial in monocyte trafficking, according to the increase number of trapped $Ly6C^{hi}$ in the BM and the strong reduction of circulating monocytes observed in mice deficient in CCR2 or its ligands [59, 60]. It has been shown that, during inflammatory conditions, different stimuli, such as the lipopolysaccharide (LPS), induce the expression of CCL2 (monocyte chemoattractant protein-1, MCP-1) in $Nestin^{+}$ stromal cells present in the haematopoietic niche, leading to the internalization of CCR2-CXCR4 complexes in the

juxtaposed monocytes. This mechanism causes the desensitization of monocyte response to CXCL12 (ligand of CXCR4), and the consequent egress of cells in the circulation [61, 62]. Regarding non-classical monocytes, it seems that their egress in the blood is dependent on the S1PR5 receptor, according to the lack of circulating $Ly6C^{lo}$ monocytes but normal count in the bone marrow observed in S1PR5-depleted mice [63].

4.1.3 *DEVELOPMENT AND FUNCTIONS IN HOMEOSTASIS*

In recent years, research on monocyte biology has brought to light the extraordinary peculiarity of these MPS cells to serve not only as cellular precursors of tissue Mφ and moDCs, but also to function as effector-cells, each subset exerting distinct activities and retaining peculiar properties [64].

Once in the circulation, classical monocytes, in contrast to the non-classical counterpart, roll along vessels without interacting closely with the endothelium [65]. They present a more pro-inflammatory phenotype compared to the other monocyte subtypes and are involved in tissue repair and immune responses. As it will be explained in the next section, this subpopulation is primed for migration and responsible for efficient phagocytosis, ROS production, response to fungi and bacteria, and secretion of pro-inflammatory cytokines, such as CCL2, CCL3, CCL5, IL-6, IL-8, but also of the anti-inflammatory IL10 [8, 66, 67]. Classical monocytes have a short lifespan of about 20-24h [68]. Among the molecules that regulate the survival of these cells, a recent work has uncovered the crucial role played by the pro-apoptotic protein BIM, whose expression is modulated by the long non-coding RNA *Morrbid* [69]. Such a short lifetime is explained by the fact that classical monocytes represent a transient cell population [42] that can essentially meet three fates.

First of all, these cells can extravasate and migrate into tissues and lymph nodes. Different chemokine receptors highly expressed by classical monocytes, including CXCR1, CXCR2, CCR1, CCR2 and CCR5, are required for their traffic [66, 70]. In the embryo, foetal monocytes colonize essentially every tissue, and differentiate into resident macrophages. For almost half a century, it has been thought that TRMs in adulthood rely exclusively on circulating BM-derived monocytes for replenishment in steady state. However, there is now a consensus on the fact that most tissue Mφ are established prenatally and can be maintained, during the course of life, through self-renewal [71, 72]. Different studies, based largely on fate mapping and

depletion systems in mice, have shown the embryonic origin of TMRs, such as Kupffer cells in the liver, Langerhans cells in the skin, alveolar macrophages in the lung and cardiac macrophages in the heart [73-77]. Notably, in contrast to what happens in adulthood, foetal monocytes traffic into tissues without the involvement of the CCR2-CCL2 axis, and their generation is independent from the expression of the CSF-1 receptor [35, 78]. Growing evidence thus suggests foetal liver monocytes as the main progenitors of almost all adult TRMs. This concept, however, is not in contrast with previous and new findings of TRMs origin, in adult life, from circulating monocytes, as shown, for example, in the dermis, intestine, pancreas and testis [79-84]. Indeed, the current view is that tissue macrophages, both in humans and in mice, are represented by a dual pool of cells: monocyte-derived and self-sustained [85]. Under homeostatic physiological conditions, the proportion between these two populations vary primarily according to the tissue. Example of organs in which contribution of circulating monocytes to the replenishment of TRMs is little or even inconsistent are the epidermis and the central nervous system (with reference to perivascular macrophages, meningeal macrophages, choroid plexus macrophages and microglia) [86, 87]. Conversely, the gut represents a very peculiar district largely dependent on BM-monocytes. Indeed, due to its constant exposure to the commensal microbiota, this organ is in a perpetual status of low-grade inflammation, necessitating a dynamic modulation of the immune compartment [88]. Recently, three gut macrophage populations have been identified on the bases of the apoptotic cell-uptake receptor Tim-4 and CD4: Tim-4^{-}CD4^{+} Mφ had a slow turnover from blood monocytes, Tim-4^{-}CD4^{-} Mφ were found to be the subset with the highest monocyte-replenishment rate, while Tim-4^{+}CD4^{+} Mφ were locally maintained [89]. Interestingly, distinct macrophage populations, located in separate anatomical niches and originating from different monocyte subtypes, have been described also in the lung. Using a humanized mouse model, Evren et al. showed the coexistence of interstitial and alveolar Mφ, derived from classical CD14^{+} circulating monocytes, as well as of pulmonary intravascular Mφ, derived from non-classical CD16^{+} circulating monocytes [90]. Importantly, once in the tissues, circulating monocytes undergo significant epigenetic, transcriptional and phenotypic transformations to adapt to the new environment and to acquire new functions. Indeed, monocyte-to-macrophage differentiation represents a gradual progress through distinct cellular stages defined, for example, by the upregulation of HLA-DR, CD206 and CD209 in the lung; the upregulation of early gene transcription factors (*Rgr1*, *2* and *3*) and the concomitant downregulation of C/EBP, E2F family members and PU.1 in the intestine; the expression of *Nr1h3* (encoding LXRα) upon monocyte interaction with the Nothch ligand DLL4 expressed by the sinusoidal endothelial

cells in the liver [90-92]. It can not be excluded that some monocytes, once in peripheral tissues, maintain their general monocyte-like state without really differentiate into macrophages. However, our notions about tissue monocyte functions are still largely unknown because of the lack of efficient surface markers that can discriminate these cells from their differentiated counterparts [93].

Extravasating classical monocytes, rather than differentiate into TRMs, can also reach specific districts where they accumulate maintaining their monocyte phenotype. These niches act as local monocyte reservoirs [42]. In the lung, the calibre of microvessels is so small that it forces $Ly6^{hi}$ monocytes, whose migration in steady state is regulated by CXCR4 [58], to interact with the vasculature, leading to leukocyte accumulation and the creation of a "marginal pool" [94, 95]. Also, the subcapsular red pulp of the spleen functions as secondary emergency reservoir, besides the BM, for almost all tissues [96]. It has been shown that monocytes egress from the spleen and their migration to atherosclerotic lesions or into the heart during a myocardial infarction are mediated by Angiotensin II-signalling, but not by the classical CCR2 pathway [96, 97].

The last possible fate of circulating classical monocytes is their maturation and progressive transition into non-classical monocytes. In a recent elegant study, Petel et al. have investigate the kinetic of human monocyte maturation and have shown, using *in vivo* deuterium labelling, the transition of classical monocytes into the intermediate cell population. The latter has been found to circulate in the blood for about 4 days before either dye, migrate in tissues or differentiate into non-classical monocytes. Finally, $CD14^{+}CD16^{+}$ monocytes have been reported to have a longer lifespan in blood of around 7 days [98]. These findings are in line with previous evidence about the origin of non-classical monocytes from the classical subtype, both in humans and in mice [14, 74, 99]. However, it is not to be excluded that other routs of development might give rise to $CD16^{+}$ cells [42].

As previously discussed, the intermediate population is less studied than the other subsets, representing the intermediate state between the classical and non-classical populations and, thus, poorly clearly distinguishable among them. One notable exception is represented by a fraction of intermediate monocytes found in mice specifically characterized by the expression of CD209a and major histocompatibility complex class II (MHCII) molecules [13]. Also, human $CD14^{+}CD16^{+}$ double-positive monocytes are characterized by high levels of human leukocyte antigen (HLA)-DR molecules [98, 100, 101]. These cells also express high levels of CCR5, making them susceptible to HIV-1 infection [102], and it has been shown to be

responsive to toll-like receptor (TLR) stimulation, secreting various cytokines, including TNF-α, IL-6, IL-10, IL-17 and IL-1β [103, 104].

Development and survival of non-classical monocytes rely on fractalkine (CX_3CL1), ligand of CX_3CR1 [105, 106], and on the orphan nuclear receptor Nr4a1 and the TF C/EBPβ involved in its regulation, as shown by the phenotypic dysfunctions (abnormal cell cycling and enhanced apoptosis) and the drastic reduced number of $Ly6^{lo}$ cells in both *Nr4a1*-deficient and *C/EBPβ*-deficient mice [13, 107, 108]. Moreover, E2 super-henancer region upstream of Nr4a1 in mice and of $CD16^+$ in humans was found essential for the survival of the non-classical population [109].

In the vasculature, non-classical monocytes exert the specific role of patrolling. This peculiar ability is dependent on CX_3CR1 and the lymphocyte function-associated antigen (LFA)-1. The activated endothelium plays a critical role in stimulating $Ly6^{lo}$ monocytes to scavenge cellular debris in the lumen and to eliminate necrotic endothelial cells by the recruitment of neutrophils *via* the local nucleic-acid-mediated TLR7 "danger" signal [110, 111]. Overall, during homeostatic conditions, non-classical monocytes act as caretakers and sentinels of the vascular tissue, essentials for tissue repair and to maintain homeostasis. Further insight into non-classical monocyte functions and properties will be thus critical to understand their contribution during pathology, such as in hematologic disorders.

In contrast to the classical counterpart, under physiologic conditions, $CD16^+$ cells primarily remain in the vasculature and do not serve as main precursors to TRMs, as indicated by the normal amount of macrophages observed in mice lacking non-classical monocytes in almost all organs [112]. Interestingly though, mice lacking $Ly6^{lo}$ cells lose a typical thymic macrophage population specialized in the clearance of apoptotic thymocytes [107].

4.1.4 *FUNCTION DURING INFECTION AND DISEASES*

Besides their function in TRMs replenishment, wound healing, and surveillance of endothelial integrity and repair during homeostatic conditions, monocytes play a key role in the defence of our organism from pathogens and injuries. The functions of monocytic cells during infection and diseases will be discussed in more detail in the following section, with particular focus on cancer.

Leukocytes, including monocytes, are rapidly recruited into inflamed tissues with the primarily aim to eradicate the inflammatory trigger and, later, restore the damaged tissue. They are attracted at injury sites by different mediators produced by pathogens (pathogen-associated molecular patterns, PAMPs), by the local immune system or by components derived by the injured host cells called damage-associated molecular patterns (DAMPs) [113]. Patrolling monocytes, rolling more closely to the vascular endothelium compared to the classical subset, are suitable for extravasation in a very short time [64]. In transgenic *Cx3cr1*$^{gfp/+}$ mice, Ly6C^{lo} monocytes invade tissues exposed to aseptic wounding, irritants or infection with *Listeria monocytogenes* within 1h [111], while classical cells reach distal tissues slower. CD14^{+} monocytes were enriched in bronchoalveolar lavage following LPS inhalation within 8h, in the nasal mucosa following allergen triggering within 12h, and in skin blister within 24h after its formation [114-116]. Nonetheless, LyC6^{hi} monocytes can also reach rapidly inflammatory sites once meet vascular microhaemorrhages [117].

Once in tissues, crucial mediators like M-CSF, GM-CSF and Flt3 ligand may induce monocyte differentiation into specific subtypes of macrophages and monocyte-derived dendritic cells (moDCs). This transition is supported by transcriptional, morphological and phenotypic changes, including metabolic modifications, increasing in cell size, and, in case of classical monocytes, loss in Ly6C and the concomitant increased expression of F4/80, CX3CR1 and CD11c [112, 118]. However, given that the process of monocyte differentiation into monocyte-derived cells is extremely gradual, the exact distinction between these cells is often very hard. On the other hand, effort in the field has led to the identification of specialized monocytes and tissue Mφ and moDCs, characteristic of specific pathological conditions, timing and/or districts.

TNF/iNOS-producing DCs (TipDCs) were found essential for TNF and iNOS supply and for clearance of primary bacterial infection in a model of *Listeria monocytogenes*-infected mice [119]. Interestingly, monocytes represent the major source of TipDCs, as shown by the absence of these cells in CCR2-deficient mice. TipDCs were subsequently identified during infections caused by many other pathogens and, given their key role in the clearance of microbes, were inferred to actually be part of macrophage-like cells [120-122].

Monocytes are also found to infiltrate atherosclerotic plaques during the very early stages of their formation and are considered essential player in the developmental process of atherosclerosis. Recruited into the intima of arteries by stimuli like CCL2 and lipid deposition, these cells differentiate into inflamed macrophages, DCs and, especially, foam cells, macrophages rich in cholesterol vacuoles derived from monocytes that have phagocytized

lipids, precipitated cholesterol crystals and oxidized lipid species [103]. Using scRNA-seq and genetic fate mapping profile of mouse plaques, Lin et al. characterized several Mφ subtypes in a spectrum of activation states and, interestingly, discovered a new population of proliferating and undifferentiated stem-like monocytes. The authors speculated about their possible persistence in the plaque as a specific self-renewal pool of foam cell progenitors [123].

Aβ42-stimulated PBMCs from Alzheimer disease (AD) patients are enriched in $CD14^{+}$ $CD16^{-}CCR2^{++}CX3CR1^{low}$ monocyte/macrophages compared to aged-matched healthy donors [124]. This cell population expresses higher levels of toll-like receptors (TLR-2, TLR-3, TLR-4 and TLR-8) and superior ability to secrete cytokines like IL-6, CCL2 and IL-23. Interestingly, among all PBMCs, presence of MHC-II/Aβ42 complexes can be detected selectively on monocytes. These results indicate that monocyte/macrophages from AD patients are characterized by a pro-inflammatory phenotype and reveal the possibility for monocytes to be recruited within the proximity of deposited Aβ plaques *in vivo* [124]. However, the presence of BM-derived monocytes in AD brain is still controversial. The role played by these cells in the pathogenesis and progression of Multiple sclerosis (MS), another disease of the central nervous system, is better documented. In an experimental autoimmune encephalomyelitis (EAE) mouse model of MS, monocyte infiltration within the tissue has been sown to correlate with the progression to the paralytic stage of the disease [125]. The blocking of classical monocyte traffic within the blood-brain barrier prevents the progression of the disease. Conversely, *Nr4a1*-depleted mice (lacking the patrolling population) showed increased levels of norepinephrine and leukocyte infiltration, and a general EAE exacerbation [126, 127]. These and other numerous studies provide evidences of the crucial role of monocytes in this neuroinflammatory autoimmune disorder, opening to the possibility of electing specific subpopulations as therapeutic targets in MS [128].

The decisive contribution of monocytes/macrophages, along with other innate immune cells, during the initial and acute phase of inflammation, has been extensively documented in the literature, but these cells are also important mediators of the resolution phase of the inflammatory response. Within the injured tissue, characteristic monocyte-derived Mφ, named wound-associated macrophages (WAMs), represent key players in the control of wound inflammation. These cells transit from an initial inflammatory state, characterized by high production of TNFα and IL6, to an immunoreglatory/tissue remodelling phenotype, defined by substantial secretion of TGFβ [129]. Specifically, 4 WAM populations with distinct dynamics and transcriptomic profiles were identified in the granulation tissues bases on their expression of Ly6C and MHCII: the $Ly6c^{lo}MHCII^{lo}$, the $Ly6c^{lo}MHCII^{hi}$, $Ly6c^{hi}MHCII^{lo}$, and the

Ly6c^{hi}MHCII^{hi}. Of those, Ly6c^{lo}MHCII^{hi} WAMs represent the subpopulations with a non-inflammatory transcriptomic profile, prompt to produced cytokines, including IL-17a, which favoured wound closure [130].

Monocytes have been long considered to be important also during pathological conditions, when they are already within the injured tissue. However, it is increasingly evident that distinct subsets, each with singular functions, begin to have important impacts on the course of disease before their recruitment to the lesion as well, or just remaining in the blood. Indeed, non-classical monocytes were found to be primed for TLR7- and TLR8-mediated immune activities against nucleic acids and viruses, responding with the secretion of cytokines like CCL3, TNF-α and IL-1β [8]. In particular, circulating SLAN^{+} cells triggered by TLR ligands show higher expression of inflammatory cytokines such as IL-1, IL6, TNF, IL-12, but lower levels of IL-10 compared to SLAN negative monocytes [19]. It has been also demonstrated that, during acute gastrointestinal infection, circulating Ly6C^{hi} triggered with *E. coli* lysate express higher levels of IL-10 and PGE_2 even prior to their recruitment to the small intestine lamina propria [131]. In inflamed glomeruli, MHCII^{+} monocytes are retained to patrol the glomerular microvasculature for a prolonged time compared to homeostatic conditions and, within glomerular capillaries, present intravascular antigens to effector CD4^{+} T lymphocytes [131]. Similarly, the number of non-classical monocytes crawling along the lumen of blood vessels with atherosclerotic plaques formation in a CX3CR1-independent fashion is increased in mouse models of hyperlipidaemia and atherosclerosis [132]. The protective role of these cells in the maintainance of the vascular homeostasis was demonstrated by the expanded apoptotic endothelial damage along the vessel wall in Wester diet-fed Nr4a1/ApoE$^{-/-}$ mice compared to controls [132].

Investigations about altered monocyte numbers, frequency and phenotype in the blood of patients are increasing, adding a new dimension to our understanding of their role in disease and may be considered as new prognostic/predictive markers. Only few examples are reviewed below. A retrospective multicentre cohort study proposed the total number of classical monocytes as biomarker of poor prognosis in patients with fibrotic diseases [133]. Patients with Chronic Obstructive Pulmonary Disease (COPD) showed increased levels of total circulating monocytes and of non-classical subset, with reduced M2-like phenotype compared to subjects with moderate COPD [134]. In serum transfer-induced arthritis (STIA) mice, the number of circulating non-classical monocytes positively correlated with mediators of tissue destruction [135]. In both treated and untreated MS patients, it was observed an expansion of

$CD16^+$ monocytes and concomitant reduction in the $CD14^+$ counterpart compared to healthy donors [136]. $SLAN^+CXCR6^+$ monocytes are more frequent in the blood of coronary artery disease subjects, in line with their function as patroller and their augmented responsiveness to CXCL16 produced by the foam cells within the atherosclerotic plaques [28]. Moreover, *ex vivo* stimulation with LPS of monocytes isolated from patients with severe symptomatic coronary atherosclerosis showed higher production of pro-inflammatory cytokines associated with lower histone 3 lysine 4 trimethylation (H3K4me3) and lower H3K27me3 on the TNFα promoter compared to cells from patients with asymptomatic carotid atherosclerosis [137]. Finally, studies from the current coronavirus disease 2019 (COVID-19) pandemic caused by infection with severe acute respiratory syndrome coronavirus 2 (SARS-CoV-2) showed a significant expansion of $CD14^+CD16^+$ monocytes producing IL-6 in PBMCs of COVID-19 patients treated in intensive care units compared with those patients who did not require hospitalization [138].

4.1.4.1 Monocytes in cancer

The role played by an inflammatory tumour microenvironment in cancer progression is now largely recognized, and has led, in 2011, to include cancer-related inflammation within the "hallmarks of cancer" [139]. In the last decades, the role of the tumour microenvironment has been closely investigated, both with focus on the adaptive immune system and on the innate counterpart, bringing a lot of attention to macrophages as critical orchestrators of tumour progression and distal spreading. Nevertheless, the extraordinary ability of Mφ to adapt and respond to different environmental cues enables them to acquire either anti-tumour or tumour-promoting phenotypes in a context-depending manner [140-142]. Recently, monocytes have been also shown to display diverse functions at different stages of tumour growth and progression, depending on their phenotype and cancer type.

Monocytes were found to invade different primary tumours from their early stages, and continue to be recruited within the tissues throughout the process of cancer progression, even in metastatic lesions [93]. Such enrolment is strongly dependent on CCL2, both in mice and humans. Indeed, in MMTV-PyMT mouse models of breast cancer, it was observed an impaired recruitment of $CCR2^{-/-}$ monocytes within the mass [112, 143, 144]. Also, in human lung tumour tissues, the decreased production of CCL2 correlates with increased proportion of dead $CD14^+$ cells [145].

As it happens in homeostatic conditions or during inflammation, once monocytes reach the tumour tissues they can differentiate into moDCs or macrophages. TAMs are thus a mixture of monocyte-derived and resident macrophages, and they also continue to accumulate within the mass thanks to their proliferative capability, as shown by the normal rate of TAM accumulation in CCR2-deficient mice, at least in breast tumours [146]. Though, surprisingly, the inhibition of inflammatory $Ly6C^+/CD14^+$ monocyte recruitment suppresses the formation of metastatic breast cancer in the lung [144, 147]. Interestingly, the differentiation of monocytes into TAMs seem to follow a specific spatial distribution along time. Arwert et al. have recently described this unidirectional transition process: circulating monocytes recruited into the tissue via the CCR2 signalling differentiate into migratory macrophages (a specific subpopulation involved in the guidance of neoplastic cells toward blood vessels), promoted by cancer cells via TGF-β-dependent upregulation of CXCR4 in monocytes; motile TAMs migrate toward the blood vessels promoted by perivascular fibroblast via CXCL12 and, finally, migratory TAMs differentiate into perivascular macrophages (a cell subpopulation that supports cancer vascular invasion) [145]. Angiopoietin 1 receptor (TIE2) is amply expressed by perivascular TAMs, both in mice and humans, and $TIE2^{pos}$ macrophages have been reported as important promoters of angiogenesis and tumour growth [30, 31, 148]. As previously mentioned, TIE2 is also expressed in monocytes, allowing the identification of a specific monocyte subpopulation. It has been shown that tumour endothelial cells recruit $TIE2^+$ monocytes and TAMs via angiopoietin 2 (ANGPT2), leading to their accumulation within blood vessels and thus promoting angiogenesis and blood vessel sprouting [29, 30, 149].

Monocytes represent not only a source of tissue macrophage precursors, but they also exert direct immunological functions, even in the context of cancer biology. In early-stage human lung cancers, it has been observed an accumulation of $HLA\text{-}DR^{hi}CD14^+$ cells within the tumour lesion as compared to blood and distant tissue. Notably, tissue monocytes showed suppressive effects on T cell responses, in contrast to the normal T-cell stimulatory activity displayed by TAMs [150]. Conversely, Namasimhan et at. have recently demonstrated the crucial role played by patrolling monocytic subtype in the prevention of lung tumour metastases via the recruitment and activation of NK cells, according with the increased tumour burden and the impairment of NK cell enrolment observed in E22/2-depleted mice lacking in non-classical monocytes [109]. In a Lewis lung carcinoma mouse model, circulating human TIE2-2 positive monocytes were found to express higher levels of VEGFA, COX-2, WNT5A and metalloproteinase-9 (MMP-9) already in blood in steady state, compared to their counterpart

TIE2^{neg}, indicating that they are innately pro-angiogenetic cells and they exhibit a broader pro-tumoral phenotype [151]. Moreover, in mice bearing lymphoma EL4 and lung LLC tumours, CD11b^{+}Gr1^{+} myeloid cells mediate refractoriness to anti-VEGF treatment, according to the significant reduction of tumour weight and volume after anti-VEGF and anti-Gr1 combined therapy [152]. Monocytes from women with endometrial and breast cancer show significant transcriptional differences compared to healthy donors, including enrichment in pathways involved in angiogenesis, cell communication and cell migration, as well as increased expression of pro-angiogenic factors [153].

Several *in vitro* experiments have demonstrated the capability of monocytes to kill cancer cells. CD16^{+}SLAN^{+} cells from diffuse large B-cell lymphoma (DLBCL) patients performed a very efficient rituximab antibody-dependent cellular cytotoxicity (ADCC) of B lymphoblasts [154]. Conversely, monocytes isolated from peripheral blood or ascites of patients with ovarian cancer showed reduced ADCC and antibody-dependent cellular phagocytosis (ADCP) of neoplastic cells [155]. Activation with INF-α or INF-γ induce the expression of TRAIL in human monocytes, which thus acquire the ability to mediate tumour cell apoptosis. Moreover, interferon stimulation cause a synchronous downregulation of monocyte TRAIL receptor 2, leading to the acquisition of resistance to TRAIL-mediated apoptosis in these cells [156].

To date, antibodies recognizing tumour-associated antigens used in targeted therapies are all IgG. However, the employment of antibodies of other classes could represent a great advantage, since each class exerts peculiar functions through different Fc receptors in different tissues [157]. According to this, evidence has been collected pointing to anti-cancer efficacy of engineered IgE antibodies recognizing tumour antigens [158, 159]. Based on this evidence, a mouse/human chimeric IgE Ab (MOv18-IgE) against folate receptor-alpha has been developed and is in a phase 1 clinical trial in advanced cancers (https://ichgcp.net/clinical-trials-registry/NCT02546921). Of note, monocytes have been shown to play a critical role in MOv18-IgE-dependent anti-tumour functions [160]. Specifically, Pellizzari et al. have shown, in a nude-mouse model of ovarian carcinoma treated with MOv18-IgE, prolonged survival, associated with highly enrichment of injected human PBMCs within the tumour. Notably, monocytes *in vitro* were able to kill ovarian tumour cells in MOv18 IgE Ab-mediated phagocytosis [157].

4.1.4.2 Emergency monopoiesis and trained immunity

Monocytes serve as plastic and reactive immune cells playing a key role during the first line of defence against pathogens or injury, as well as during chronic inflamed conditions. Therefore, the control of their availability, both in blood and tissues, becomes a crucial aspect. Under inflammation, emergency and stress conditions, when the request of rapid monocyte recruitment in the circulation and within the site of injury necessitates accelerated production and mobilization of cells from the bone marrow, the shortened routs of monocyte development are potentiated [42]. Thus, the number of NeuMo, originated from the GMP progenitor bypassing the canonical developmental pathway (4.1.2), is strongly increased [43]. Moreover a population of atypical $Ly6^{lo}$ monocytes directly developing from the GMP without passing through a classical phenotype has been recently reported as relevant in the progression of fibrosis, and it has been named segregated-nucleus-containing atypical monocytes (SatM) [161]. Hematopoietic stem and progenitor cells (HSPCs) can directly respond to different pathogens by expansion, mobilization and differentiation, while some microbes, including *Ehrlichia chaffeensis*, *Anaplasma phagocytophilum* and *Listeria monocytogenes*, lead to the reduction in the number of HSPCs [162]. Different studies in rodents have shown the effect of emerging haematopoiesis in response to different stimuli, both in acute and in chronic scenarios. In a colitis mouse model, IFNγ-dependent HSPCs accumulation and IL-23-dependent skew toward GMP production led to the accumulation of inflammatory monocytes in the intestine [163]. Systemic TLR ligands triggered TLR signalling *via* Myd88 adaptor protein in HSPCs, stimulating the rapid differentiation of myeloid progenitors into monocytes bypassing some usual growth requirements [62, 164]. A recent study showed, in a human experimental endotoxemia model, that LPS injected systemically induced a transient monocytopenia (2h), followed by the replenishment of classical $CD14^{+}CD16^{+}$ monocytes, and, sequentially, of the intermediate and non-classical populations [98].

During emergency monopoiesis, the repertoire of monocytes produced is not only dependent on the velocity of their developmental process, but is even more dependent on the functionality of such distinct monocyte populations [165]. Such selective enhancement is regulated by stimuli produced locally in the bone marrow or reaching the BM niche through the circulation. As an example, during *T. gondii* infection, NK cells in the BM, secreting cytokines like IFNγ, induce the production of $Sca\text{-}1^{+}CXCR1^{-}Ly6C^{hi}$ monocytes [131]. Also, NOD2 triggering in $Ly6C^{high}$ monocytes induce their conversion into patrolling $Ly6C^{low}$ cells [166].

It is now emerging the concept of trained immunity, or rather, the long-term functional reprogramming of non-adoptive immune system (including innate immune cells and tissue-resident stem cells), which results in a stronger or lower response in cells previously challenged by exogenous or endogenous insults [167]. There are different examples of the trained immunity phenomenon. In humans, Bacillus Calmette-Guérin (BCG) vaccination has been associated with the induction of pro-inflammatory phenotype in monocytes with a consequent better protection against malaria and virus infections [168, 169], and with the promotion of monocyte anticancer functions in several tumours, such as leukaemia, lymphoma, melanoma and bladder cancer [170-173]. Superior killing capability of *Mycobacterium tuberculosis* was found in BCG-trained BM-derived macrophages, both *in vitro* and *in vivo*, phenomenon occurring through changes in the transcriptional landscape of hematopoietic stem cells [174]. Furthermore, cases of individual tissue trained immunity have been described [167]. Mice chronically infected with gamma herpesvirus showed mild house dust mite-induced asthma, and this phenotype was found to be associated to the long-term production and maintenance of monocyte-derived regulatory alveolar macrophages in the lung [175]. Instead, adenovirus infection induced immune memory responses in alveolar macrophages, which consequently activated a stronger $CD8^+$ T cell-dependent antibacterial immunity [176].

Interestingly, it seems that the major changes occurring in the trained immunity processes are epigenetic modifications rather than transcriptomic reprogramming, involving, for example, histone modifications of pro-inflammatory genes like TNF and IL-6 [42, 177].

4.2 THE MS4A FAMILY

The capability of a cell to respond to all the different environmental stimuli it is exposed to depends on the translation of extracellular cues into intracellular signalling pathways. Typically, this process is made possible by the formation of signalling complexes in specific subcellular domains of the plasma membrane [178]. Tetraspanins (Tspans), a large family of cell-surface proteins characterized by four α-helical transmembrane regions, are key players in this process, functioning as organizers of peculiar tetraspanin-enriched microdomains (TEMs) [179]. MS4A (membrane-spanning 4-domain family, subfamily A) represents another protein family composed of molecules with similar polypeptide sequence and predicted to span the plasma membrane four times [180]. Differently from Tspans, most of the MS4A proteins are still not well characterized at both the protein and function levels; however, given their

topological similarity with Tspans and the relatively limited literature on the subject, it seems that they play a role as adaptor proteins or ion channels [181].

In the following sections, I will provide a short overview of MS4A members' structure, including the well-known MS4A1 (CD20) and MS4A2, and of our current knowledge about the other members expressed on myeloid cells.

4.2.1 *MS4A FAMILY STRUCTURE*

At the beginning of the century, new genes closely related to CD20, FcεRIβ and HTm4 were identified and cloned, leading to the definition of a new gene family, named MS4A [182-184]. These genes shared an overall amino acidic identity of 25-40% and highly hydrophobic profiles. Subsequently, besides humans and mice, MS4A orthologues have been identified in other species, such as rat, dog and horse [185-187].

In humans, MS4A genes are clustered along a ~600-kb region on chromosome 11q12-13 (chromosome 19 in the mouse genome). In addition, TMEM176B and TMEM176A, two MS4A related genes family, were identified in chromosome region 7q36.1 (chromosome 6 in mice) [181]. They all share typical structure features and common intron/exon splice boundaries [188, 189]. The overall domain organization is consistent among the members, counting four potential transmembrane domains (with the exception of *MS4A6E*, having only two membrane-spanning domains), two extracellular loops and both the short N- and C-terminals, constituted by ~ 20–90 amino acids lacking polar residues, located in the cytosol [180, 183]. **Table 4.2** shows the 18 MS4A family members described to date.

MS4A desgnation	Predicted topology	Alias	Genomic localization
MS4A1	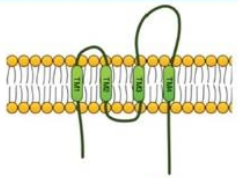	CD20	11q12.2
MS4A2	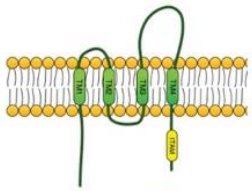	FcεRIβ	11q12.1
MS4A3	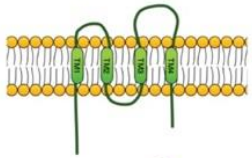	HTm4	11q12.1
MS4A4A	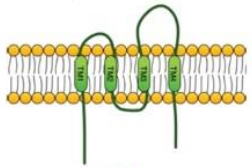	—	11q12.1
MS4A4E	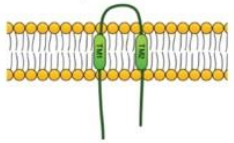	—	11q12.2
MS4A5	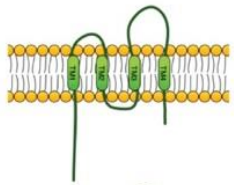	TETM4.1	11q12.2
MS4A6A	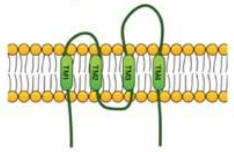	—	11q12.2
MS4A6E	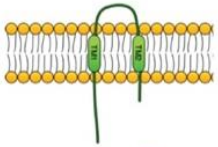	—	11q12.2
MS4A7	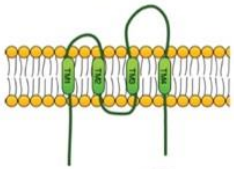	CFFM4	11q12.2
MS4A8B	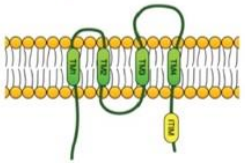	L985P	11q12.2
MS4A10	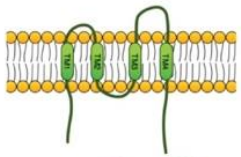	—	11q12.2
MS4A12	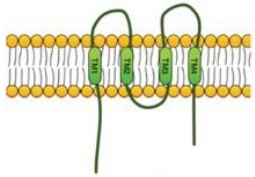	—	11q12.2
MS4A13	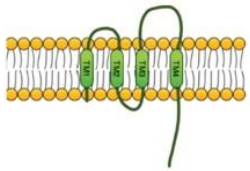	TETM4.2	11q12.2
MS4A14	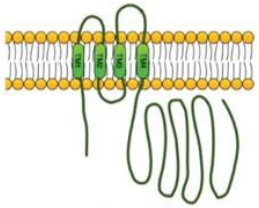	NYD-SP21	11q12.2
MS4A15	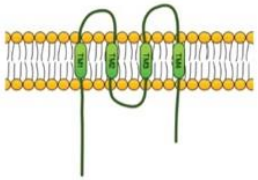	MGC35295	11q12.2
MS4A18	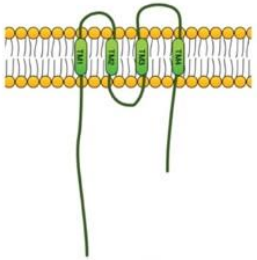	—	11q12.2
TMEM176A	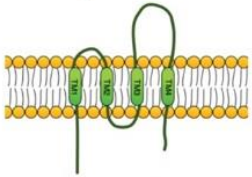	HCA112	7q36.1
TMEM176B	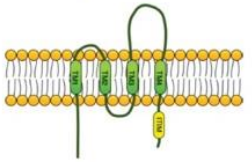	LR8 TORID	7q36.1

Table 4.2. MS4A gene family (Mod. from Kuek et. al, ICB, 2016)

4.2.2 ***MS4A1 (CD20)***

Among the MS4A proteins, CD20 is certainly the most studied. It was first identified in 1994 by Tedder and Engel as a marker involved in the cell signalling and progression of B lymphocytes [190], and it was then adopted as important clinical target. Indeed, given its selective expression on mature and neoplastic B cells but not in mature plasma cells nor early progenitors, different therapeutic monoclonal antibodies (mAbs) against this glycosylated phosphoprotein have been designed (i.e. obinutuzumab, tositumomab, ublituximab, ocrelizumab, ofatumumab and rituximab). CD20 mAbs are now currently adopted in the treatment of B-cell lymphomas, including non-Hodgkin's lymphomas and mantle cell lymphomas, revolutionizing the treatment of $CD20^+$ lymphoid malignancies [191, 192]. Anti-CD20 mAb-mediated B cell depletion therapy is also adopted in the treatment of certain autoimmune diseases, such as systemic lupus erythematosus, rheumatoid arthritis and multiple sclerosis [193].

Curiously, despite decades of studies, the exact role of MS4A1 is not completely elucidated. It has been shown to exist as a homodimer and homotrimer in the plasma membrane, which in turn associated with other proteins within specific microdomains. Similar association was found with other tetraspanins, including CD81, CD82 and CD53, the major histocompatibility complex class I and class II, CD40, the B-cell receptor (BCR) and C-terminal src kinase-binding protein (CBP) [194]. Surprisingly, given the importance of these interactomes, lack in CD20 showed only mild phenotypes. In a patient with loss of MS4A1 production caused by a gene homozygous mutation, normal precursors B-cell differentiation and normal circulating IgM were reported [195]. Conversely, memory B cell impairment was found, indicated by the reduced numbers of these cells and IgG in the blood. Also, different CD20-depleted mouse models didn't show any defects in terms of B-cell differentiation, isotype switch or maturation [196, 197]. Instead, *in vitro* studies came out with more promising results. CD20 silencing in B-cell lines resulted in reduced BCR-activated calcium flux, while CD20 crosslinking induced the opposite result of increased calcium flux in human lymphoma cell lines [198, 199]. Moreover, MS4A1-silencing in malignant B cells demonstrated the importance of this protein in BCR signalling [200].

4.2.3 *MS4A2 (FcεRIβ)*

In humans, the cell-surface Fc receptor for IgE (FcεRI) exists in two molecular forms: as trimer, binding the α-chain (FcεRIα) and a β-chain (FcεRIβ), or as tetramer, binding, in addition to the α- and β- chains, a homodimer of γ-chains (FcεRI γ) [201]. Conversely, in rodents, FcεRI is restricted to its tetrameric form. MS4A2 thus represents a component of the FcεRI, mainly expressed on basophils and mast cells, and takes part to the allergic immune response [202].

Two slice variants of MS4A2 have been described [203, 204]. The $MS4A2_{trunc}$ variant contains a consensus immunoreceptor tyrosine-based activation motif (ITAM) in its C terminus, and functioning as amplifier of the receptor expression and signal transduction. On the contrary, the β_T variant is a truncated proteins that have lost the ITAM motif and significantly reduced the expression of FcεRI on the cell surface of mast cells and basophils by binding to the immature form of the receptor and trafficking it to the proteasome for degradation [180]. Both variants are expressed in cells and compete with each other, and thus the balance between these two proteins play a crucial role in controlling FcεRI expression and efficacy of its signal transduction [202].

MS4A2 has been shown to play a role also in in the pathogenesis of arthritic inflammation, as shown by the exacerbated arthritic inflammation, leukocyte infiltration into the knee joint, and bone erosion and tissue cytokine expression observed in FcRβ-deficient arthritis mouse models (treated by LPS and anti-CII mAbs) [205].

4.2.4 *MS4A4A AND OTHER MS4A PROTEINS EXPRESSED ON MYELOID CELLS*

As mentioned, to date little is known about the function of the other MS4A members. Prevailing literature about these genes associate different polymorphisms from MS4A locus with late-onset Alzheimer's disease (LOAD) risk. The two genes more likely involved in the disease are MS4A4A and MS4A6, whose levels are the most altered in Alzheimer's patients [206, 207]. In the centre nervous system, the expression of these proteins, together with MS4A7, were found to be restricted to microglia [208]. Despite the numerous evidence suggesting a crucial role of MS4A4A, MS4A6A and MS4A7 in the pathology, there is no data about their functions in the brain. The only speculation is that they may act upstream of the receptor expressed on myeloid cells 2 (TREM2), key player in microglial biology and LOAD belonging to the immunoglobulin superfamily [208, 209].

MS4A4A is becoming an emerging protein in other contests. Our laboratory has been very much focused on the biology of phagocytes and interested in their polarization for a long time [85, 210, 211]. Several years ago, a transcriptomic profile performed in the group aimed at deciphering the key pathways regulating differentiation of human macrophages from monocytes and their further polarization toward M1 or M2 [212]. From this study, a complex network emerged, comprehensive of common immune molecules, such as chemokine and cytokine receptors, cytokines and, among others, the tetraspanin-family molecule MS4A4A. Particularly, MS4A4A resulted as the most overexpressed membrane receptor in M2 macrophages, suggesting a role in the transcriptional program of these cells. Based on this evidence, over years, following studies in the group have tested MS4A4A as a critical molecule in tumour-associated macrophages [213]. Its expression was found upregulated in macrophages undergoing IL-4- and dexamethasone-dependent alternative activation *in vitro*, in several human tissue resident and tumour-associated macrophages. Moreover, MS4A4A localized in macrophage lipid rafts where it interacted with MS4A6A, MS4A7 and the pattern recognition beta-glucan receptor Dectin-1, upon its engagement by zymosan. Gene-targeted animals demonstrated that MS4A4A performed a critical role during metastatization, being required for Dectin-1 signalling and NK cell-mediated anti-tumour responses towards tumours with aberrant expression of beta-glucans. These findings are consistent with other studies reporting MS4A4A as an M2-like Mφ and TAM marker [214-217]. Moreover, it has been recently demonstrated that the tetraspanin-like molecule regulate *Arg1* expression without compromising other relevant macrophage genes, such as *Ym-1*, *Mrc-1* and *Marco*, in peritoneal exudate cells from a MS4A4A-delated mouse model [218]. Interestingly, in RAW264.7 cells transfected with the murine sequence for MS4A8B (Ms4a8a), another tetraspanin-like member, the upregulation of *Arg1* and other M2-like markers was detected [219].

MS4A4A is thus emerging as an important player in the formation of lipid raft-associated signalling complexes and receptor regulators. In mast cells, MS4A4A has been shown to regulate the endocytic recycling of the receptor tyrosine kinase KIT. Mechanistically, the tetraspanin-like protein controlled the recruitment of KIT to caveolin-1–enriched lipid rafts and thus regulated its signalling activity [220]. Also, Arthur and colleagues have recently demonstrated that MS4A4A functions in mast cell degranulation through FcεRI, both promoting FcεRI-PLCγ1 complex interaction with signalling molecules in lipid rafts and favouring IgE-dependent store-operated Ca2+ entry (SOCE) [221]. Overall, more research is needed to understand the functions of the MS4A family, exploring the cellular function of its components as scaffold proteins, ion channels or signalling receptors in different contexts.

5 AIM OF STUDY

This dissertation aims to dissect the human monocyte heterogeneity.

Specifically, by this study we had three main objectives:

- characterize circulating monocyte populations during homeostatic conditions;
- investigate the expression and distribution of the MS4A family of proteins within peripheral monocyte subsets;
- determine if alteration in monocyte phenotype and frequency occur during pathological conditions.

6 METHODS

6.1 Single cell RNA sequencing

6.1.1 *SAMPLE COLLECTION AND ISOLATION OF PERIPHERAL BLOOD MONONUCLEAR CELLS (PBMCS)*

Peripheral blood was obtained after informed consent, from 5 male adult healthy donors recruited to the IRCCS-Humanitas Research Hospital and collected in EDTA-coated tubes (BD Vacutainer K2E). Peripheral Blood Mononuclear Cells (PBMCs) were isolated from fresh blood by Lympholyte® Cell Separation density gradient solution (Cederlane Laboratories, Burlington, Canada). Briefly, 15 mL of fresh blood were first diluted in a 1:1 ratio with sodium chloride physiological solution. Diluted blood was added to the Lympholyte® solution in a volume ratio of 1:4 and centrifuged for 25 minutes at 400 rcf at room temperature without brake. The interphase ring containing mononuclear cells was collected, washed with sodium chloride physiological solution and centrifuged two times for 10 minutes at 170 rcf. Any residual erythrocytes were removed via Ammonium-Chloride-Potassium (ACK) Lysing Buffer (Lonza) treatment for 60 seconds at room temperature.

6.1.2 *FLUORESCENCE-ACTIVATED CELL SORTING (FACS) STAINING*

To assess PBMC vitality, cells were stained with viability dye (Zombie NIR; Biolegend) for 15 minutes at room temperature. Fc-block was performed with 1% human serum for 10 minutes at room temperature before staining. For cell sorting prior single cell RNA sequencing (scRNA-seq), PBMCs were stained for 15 minutes at room temperature with the following antibody cocktail: anti-CD45 (BioLegend, clone HI30), anti-CD3 (BioLegend, clone UCHT1), anti-CD19 (BioLegend, clone HIB19), anti-CD56 (Biolegend, clone 51H11), anti-HLA-DR (BD, clone L243), anti-CD66b (BioLegend, clone G10F5), anti-CD14 (BD, clone M5E2), anti-CD16 (Bio-Legend, clone 3G8). Finally, cells were washed in 2% fetal bovine serum/PBS and immediately FACS sorted on a FACSAria III (BD Biosciences).

6.1.3 *cDNA LIBRARY CONSTRUCTION AND SINGLE CELL RNA SEQUENCING*

Cells were FACS-sorted as previously described and resuspended in 0.5 ml PBS 1X plus 0.04% BSA and washed once by centrifugation at 450 rcf for 7 min. Cells were then resuspended in 50 μl and counted with an automatic cell counter (ThermoFisher; Countess II). Approximately 7,000 cells of each sample were loaded into one channel of the Chromium Chip B using the Single Cell reagent kit v3 (10X Genomics) for gel bead emulsion generation into the Chromium system. Following capture and lysis, cDNA was synthesized and amplified for 14 cycles following the manufacturer's protocol. 50 ng of the amplified cDNA was then used for each sample to construct Illumina sequencing libraries. Sequencing was performed on the NextSeq550 Illumina sequencing platform following 10X Genomics' instructions for read generation, reaching at least 35,000 reads as mean reads per cell.

6.1.4 *SINGLE CELL MAPPING AND CLUSTERING*

FASTQ files were generated by demultiplexing raw base call (BCL) files (mkfastq function, Cell Ranger v.3.0.2). Count function allowed alignment, preliminary filtering, barcode counting, and UMI counting; GRCh38 – hg 38 was used as reference genome; chemistry "Single Cell 3′ v3" was specified in the function parameters.

Preliminary filtering, data integration and marker analyses were performed with R (v.3.6.1), using the Seurat package (v.3.1.5). Only genes expressed by at least 3 cells and only cells expressing at least 500 genes were taken into consideration. Moreover, cells were filtered considering mitochondrial expression genes (cells with a mitochondrial expression lower than 10% were considered). A matrix of 21,507 genes per 26,474 cells was obtained. In order to integrate the 5 samples, for each one 2,000 variable genes were determined (FindVariableFeatures; vst method) and used as anchors in FindIntegrationAnchors function. Data were log normalized and scaled (scaling factor: 10,000). Cells were plotted in a UMAP (Uniform Manifold Approximation and Projection).

Clustree package, v.0.4.2 was used to create a plot of a cluster tree (**Figure 6.1**). Clusters were set out with Louvain Algorithm (FindClusters) function. We decided to use the value of 0.45 as it represented the adequate resolution to identify the largest number of cell clusters retaining the possibility to appreciate cluster differences. Finally, The average expression matrices were calculated through the AverageExpression() function. Cells were organized and

averaged considering clustering or donor belonging. Only cells expressing genes participate in mean calculation.

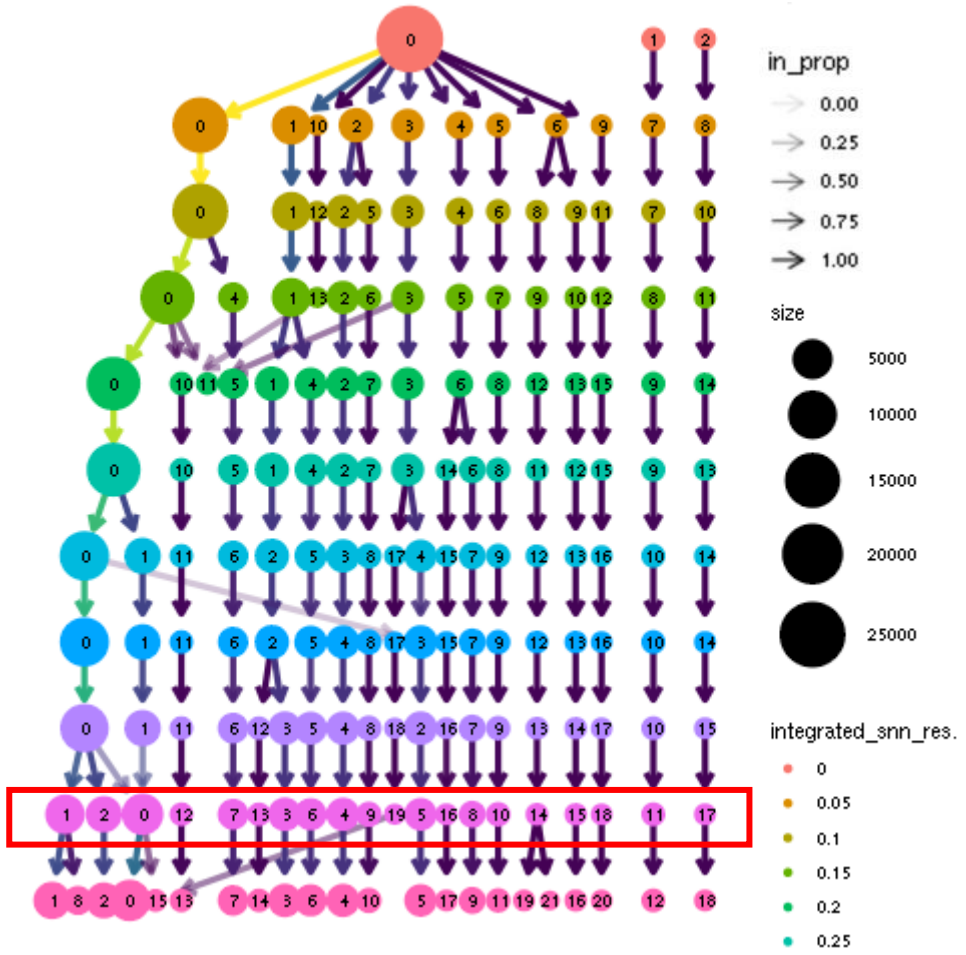

Figure 6.1. Plot of clustering tree at different resolutions (from 0 to 0.5; each level is increased by 0.05). Relationship between clusters at different resolutions and proportion and count of cells within each cluster are shown. Clusters at 0.45 resolution value are pointed out by a red box.

6.2 Cluster annotation

As first approach, the SingleR R package (v.1.0.6) was used to annotate clusters, allowing us to have directions about cluster cell types. Afterwards, cell type-based cluster annotation was performed adopting a scoring signature method. Each cell was firstly subjected to s*ingle sample Gene Set Enrichment Analyses* (GSEA) using manually curated signatures considering canonical cell lineage markers (**Table 6.1**). Scores were elaborated and normalized in order to achieve a cluster-signature score system ranging from 0 to 1.

CD14+ mono	CD16+ mono	DCs	progenitors	NK cells	B cells
CD14	FCGR3A	ID2	KIT	NKG7	BLK
VCAN	LST1	IRF4	CD34	GNLY	BTK
S100A8	AIF1	FCER1A	FLT3	GZMA	CD19
S100A9	IFITM3	CLEC4C	GATA1	GZMH	MS4A1
S100A12	SERPINA1	IL3RA	GATA2	GZMM	CD79A
FCN1	MTSS1	CD1C	MS4A3	KLRD1	IGHM
LYZ	TCF7L2	IRF8	SOX4	NCR3	CD22
RNASE2	CSF1R	CLEC10A	HOXA9	KLRF1	FCRL2
CD36	SIGLEC10	CD74	HOXA10	CTSW	CD24
NCF1	RHOC	HLA-DQA1	CYTL1	IL2RB	
		HLA-DPB1		KLRB1	
		HLA-DPA1		PRF1	
		HLA-DQB1			
		HLA-DRB1			
		HLA-DMA			

Table 6.1. List of gene signatures used to identify distinct cell lineages.

In order to better characterize clusters belonging to the same lineage, we evaluate the expression of selected genes typical of monocyte, NK and dendritic cell subpopulations (**Table 6.2**).

Classical mono	Non-classical mono	Intermediate mono and DCs	cDC2	cDC1	pDC	pre-DC	NK	NKT
CD14	FCGR3A	HLA-DPA1	CD1C	CLEC9A	IL3RA	AXL	GZMA	GZMA
VCAN	CSF1R	HLA-DPB1	FCER1A	CADM1	CLEC4C	SIGLEC6	GZMH	GZMH
		HLA-DQA1	CLEC10A		NRP1	DAB2	GZMM	GZMM
		HLA-DQB1					NKG7	NKG7
		HLA-DRB1					PRF1	PRF1
		HLA-DRA						CD3D
								CD3E
								CD3G

Table 6.2. List of genes used for manual cluster annotation.

We identified markers specific to each cluster using the FindAllMarkers() Seurat function, choosing wilcox as the statistical test. Only genes with $\ln FC$ greater than 0.25 were considered, expressed by at least 3 cells per group (first group: cluster under analysis; second group: all the remaining clusters together). We defined cluster markers only genes with: $pvalue_{adj} \leq 0.05, pct1 \geq 0.1,\ pct2 \geq 0.1,\ \log_2 FC \geq 0.5$.

Markers in a subset of clusters (e.g. in monocytes clusters) were defined with the FindMarkers().. as well as the differential analyses of one versus one cluster.

6.2.1 *TRAJECTORIES ANALYSIS*

With regard to single cell trajectories exploration, the STREAM package (v.1.0) was applied (developed in Python v.3.6.11). The analysis was performed in a subset: only cells previously annotated as progenitors, dendritic cells and monocytes were considered as input raw counts dataset. The variable genes were calculated and applied for branching analysis. The Spectral Embedding (SE) was chosen as reduction method on the basis of the characteristics of our dataset. The model was optimized with finetuning branching nodes, pruning branches, shifting branching nodes and extending leaf nodes as intermediate steps. The 5th state (S5) was chosen as the root node.

6.2.2 *STATISTICS*

Statistical analysis was performed in R (v.3.6.1).

Pearson's correlation was calculated in order to confirm sample homogeneity and investigate MS4 family genes relative behaviour. Plots were performed using tidyverse, GGally and ggplot2 libraries. Enrichment analysis were conducted by using Hallmark, GeneOntology or REACTOME (https://www.gsea-msigdb.org/gsea/msigdb/collections.jsp). ssGSEA was performed with the packages: AnnotationDbi v.1.48.0, org.Hs.eg.db v.3.10.0, qusage, GSVA v.1.34.0.

6.3 FACS analysis

6.3.1 *SAMPLE COLLECTION, ISOLATION OF PBMCS AND FACS STAINING*

Peripheral blood was obtained after informed consent, from adult healthy donors recruited to the Humanitas Clinical and Research Center and collected in EDTA-coated tubes (BD Vacutainer K2E). PBMCs were then isolated and stained as described for scRNAseq experiment (see above), with the following modification:

- addition to the antibody cocktail of anti-MS4A4A (BioLegend, clone C512/MS4A4A) and, in selected experiments, of anti-SLAN (Miltenyi, clone REA1050), anti-CD89 (BD Bioscience, clone A59), anti-FcεRIα (BioLegend, clone AER-37), anti-CD64 (BioLegend,

clone 10.1), anti-CD32 (BioLegend, clone FUN-2) and anti-CD23 (BioLegend, clone EBVCS-5);

- at the end of the staining, cells were fixed in 1% paraformaldehyde/PBS for 15 min and then acquired on a BD LSRFortessa (BD Biosciences).

Data were analyzed with FlowJo v10 software.

6.3.2 *CYTOSPIN*

PBMCs were obtained, stained and FACS sorted as for the bulk RNA sequencing. Cytospins were prepared from 10^4 sorted monocytes, using 300 g for 5 minutes (CytoSpin 4 Cytocentrifuge, Thermo Scientific, Thermo). Cytospin preparations of monocytes were stained by ematoxylin and eosin for morphological evaluation. Representative images were acquired using Widefield BX53 Micrscope (Olimpus).

6.4 Bulk RNA sequencing

6.4.1 *SAMPLE COLLECTION AND ISOLATION OF PBMCS*

Human peripheral blood mononuclear cells were isolated from buffy coats of healthy donors in accordance with clinical protocols approved by the ethical committee of Humanitas Clinical and Research Center. PBMCs were isolated from buffy coats by Lympholyte® Cell Separation density gradient solution (Cederlane Laboratories, Burlington, Canada). Briefly, 15 mL of blood were first diluted with 35 mL of sodium chloride physiological solution and centrigufed for 8 minutes at 1250 rpm at room temperature, acceleration 6 and brake 2. Supernatant plasma was removed and cellular pellet resuspended in sodium chloride physiological solution to 35 mL. Diluted blood was added to the Lympholyte® solution in a volume ratio of 1:2 and centrifuged for 25 minutes at 400 rcf at room temperature without brake. The interphase ring containing mononuclear cells was collected, washed with sodium chloride physiological solution and centrifuged two times for 10 minutes at 170 rcf. Any residual erythrocytes were removed via Ammonium-Chloride-Potassium (ACK) Lysing Buffer (Lonza) treatment for 60 seconds at room temperature.

6.4.2 *FACS SORTING AND BULK RNA SEQUENCING*

Monocytes were stained as for FACS analysis and $CD16^{-}MS4A4A^{-}$ (C), $CD16^{+}MS4A4A^{-}$ (CD16n) and $CD16^{+}MS4A4A^{+}$ (CD16p) monocytes were FACS sorted from 5 healthy donors. Samples were recovered in 0.5ml of $PBS^{-/-}$ with 0.04% BSA (Sigma Aldrich), centrifuged at 450 rcf for 7 min and cells were lysed by TRIzol reagent. Total RNA was isolated using DirectZOL RNA Miniprep kit (ZymoResearch) according to the manufacturer's instruction. Quantification and quality check (RNA integrity number RIN>7) were assessed by using Qubit4 (Invitrogen) instrument. Total RNA extracted from sorted monocytes were subjected to poly(A) mRNA sequencing. Libraries were constructed by SMARTer-Stranded Total RNA Kit (Clontech), according to manufacturer's instructions. Sequencing was performed with the NextSeq 500 (Illumina). All libraries were sequenced twice in paired-end mode (75-bp length) to produce an average of 80M of reads per sample.

6.4.3 *SEQUENCE DATA PROCESSING*

The *bcl2fastq* v2.20.0.422 tool allowed us to demultiplex samples and generate FASTQ files starting from base call (BCL) files. Fastq files were subjected to quality control using *fastQC* version 0.11.8. Mapping and sorting were performed with the *STAR* v.2.7.3a tool, and UMI counting; GRCh38 – hg 38 was used as reference genome. Count matrix was then generated with *featureCounts* (Subread v.2.0.0). Raw counts data was elaborated with the *EdgeR* Bioconductor package. The Principal Component Analysis was performed with the *DESeq2* R libraryand sample clustering was checked calculating Pearson's correlation. Due to the fact that one sample behaved as an outlier, accordingly also with complexity preliminary analysis, we decided to exclude that sample from the data set and outputted for further investigation (**Figure 6.2**Figure 6.2). Genes were filtered by expression with the *filterByExpr()* function. Finally, the count matrix was normalized generating cpm (counts per million) matrix.

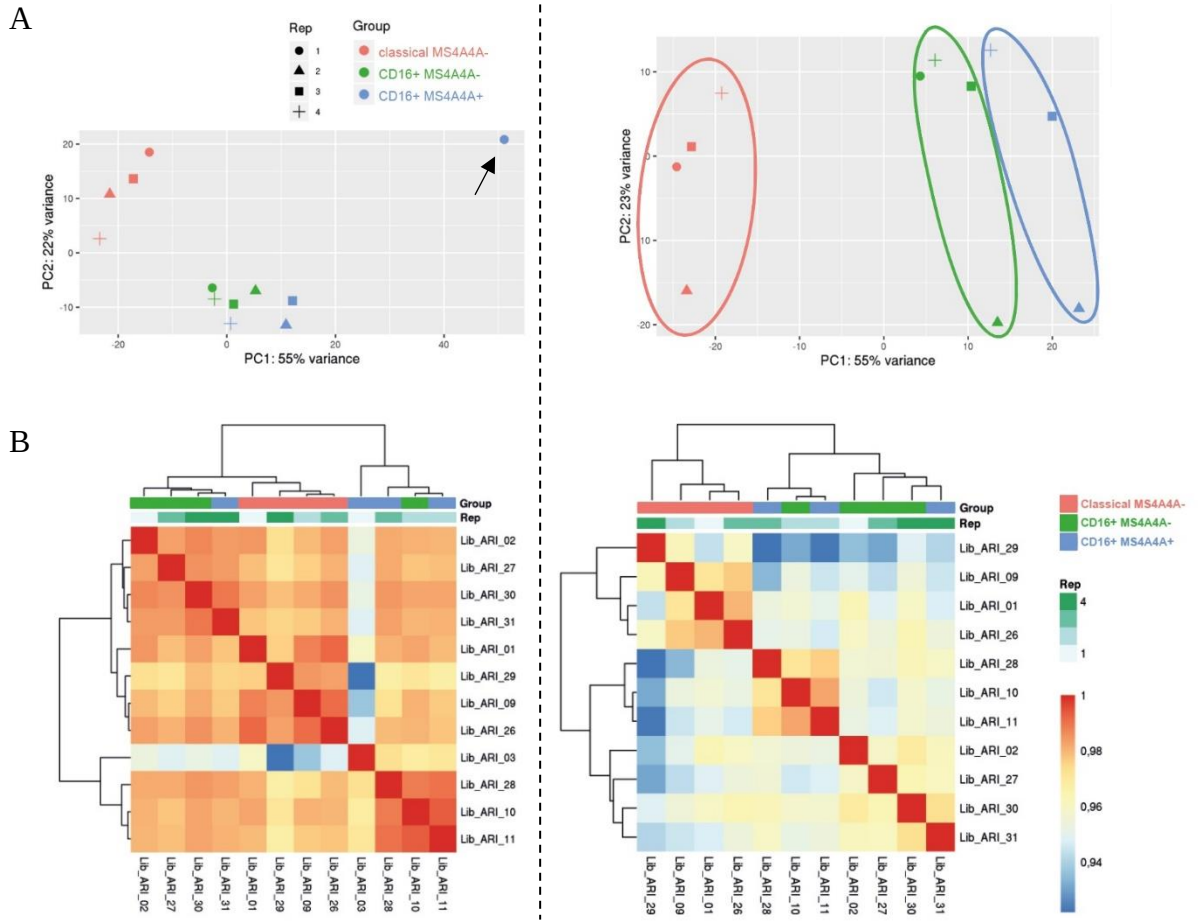

Figure 6.2. Bulk RNA-sequencing quality control. Gene expression profiles were subjected to (A left) principle component analysis visualized with t-SNE projection and (B left) Pearson's correlation analysis. Based on the results obtained, one sample (indicated by the arrow) has been excluded from data. The new data set was re-subjected to (A right) principal component analysis and (B right) Pearson's correlation analysis to confirmed Lib_ARI_03 as outlier. In A, shapes represent expression profiles of the different donors. The different monocyte subsets are circled and are represented by different colours as in legend. In B, Pearson's coefficient values are coloured coded from blue (lower) to red (higher); rows and columns are ordered by hierarchical clustering.

6.4.4 *DATA ANALYSIS*

An *ad hoc* design matrix was delineated so as to perform differential analyses. The glmQLFit model was adopted and p-values were adjusted with the Benjamini Hochberg correction.

Pathway analyses were performed with the IPA software (Qiagen *Ingenuity Pathway Analysis*, v01-13). Lists of differentially expressed genes ($pvalue_{adjusted} \leq 0.05$; $\log_2 FC \geq 0.5$) for each comparison were used for identification of significantly enriched pathways.

Pre-ranked GSEA differential analyses were performed on logFC (GSEA v.4.0.3).

6.4.5 *GENE CLUSTERING*

Considering the differential analyses previously performed (16n vs C, 16p vs C and 16p vs 16n), protein coding genes were selected ($pvalue_{adjusted} \leq 0.05$, $\log_2 FC \geq 1$). Only genes respecting the thresholds were taken into consideration, defining a list of selected genes. For the selected genes, CPM replicates values were averaged and a submatrix was obtained. Data were first log transformed and secondly were scaled by gene values. Genes were divided in 12 groups characterizing the possible behaviors a gene can have in three cell types.

6.5 GSE130157 dataset Analysis

Counts matrix of the public scRNAseq dataset from Griffiths et al. [222] was obtained from the Gene Expression Omnibus (GEO) database. Only data from time point C1 (baseline), C3 (reflecting treatment with only chemotherapy) and C5 (reflecting treatment with chemotherapy and immunotherapy) were considered. Preliminary filtering, data integration and marker analyses were performed as for our scRNAseq dataset (considering 1,000 as variable genes). A matrix of 16,657 genes per 55,293 cells was obtained.

As first approach, cell clustering was set out with Louvain Algorithm (FindClusters) function), choosing the value of 0.6 for the resolution. Then *SingleR* R package (v.1.0.6) was used to annotate clusters. Only cells computationally annotated as monocytes were selected for further analyses. Computational annotation is not accurate in distinguishing among DC, progenitors and monocytes. For this reason, computationally predicted monocytes were additionally checked considering lineage markers (as defined above). After markers checking, DC and progenitors were discarded.

In order to classify monocytes from Griffiths et al. dataset on the bases of the classification we set up a machine learning model. The model was developed using the caret R package, considering a polynomial Kernel support vector machine.

The healthy monocyte dataset was divided randomly in two parts: one training set (80% of the healthy monocyte dataset) and one test set (20%). 161 features were selected in order to train the model; features were obtained as the intersection of monocyte marker genes (previously defined in the HD dataset) and variable genes in the tumor dataset. The quality of the model was evaluated considering sensitivity, specificity and accuracy. It was tested in order to avoid overfitting typical error in machine learning developmental model. Cross validation (tenfold) was performed. After accurate evaluations, the model trained in the healthy monocyte dataset was applied in the tumour dataset and monocyte cells (from the GP dataset) were classified considering features patterns. In this way, we were able to recognize the defined clusters of the healthy dataset in the tumour immune dataset.

The "new" defined clusters of the tumour dataset were analyzed considering the frequency among the samples.

7 RESULTS

7.1 Single-cell analysis of human circulating mononuclear cells

Monocytes consist of different subsets with distinct developmental and functional properties. The most credited classification is based on the CD14 and CD16 markers and defines classical monocytes ($CD14^{++}CD16^{-}$), non-classical monocytes ($CD14^{++}CD16^{+}$) and an intermediate population ($CD14^{lo}CD16^{hi}$) [42]. However, current monocyte classification might mask a possible inter-cellular heterogeneity in terms of phenotype and, consequently, in terms of function within these subsets, even though an exact task-division among the different subsets has not been defined yet. To investigate the heterogeneity of blood monocyte populations, we performed a scRNA-seq analysis on circulating mononuclear cells from five healthy donors. PBMCs were isolated by density gradient and FACS sorted as live $CD45^{+}$, HLA-DR^{+}, lineage negative cells (Lin: CD3, CD19 and CD56 cells) (**Figure 7.1**). It's obvious that by adopting this gating strategy, we also considered other non-monocyte cell types, such as dendritic (DCs) and natural killer (NK) cells. In fact, we preferred to include non-monocyte populations, which we could have easily recognized after annotation, instead of being more stringent in the gating strategy, thus possibly loosing unknown monocyte subsets.

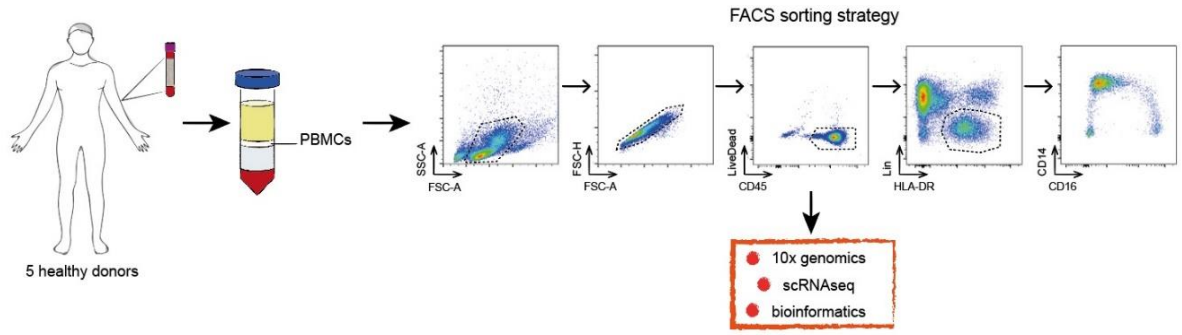

Figure 7.1. Illustration of the experimental workflow and gaiting strategy adopted for the scRNAseq. Blood samples were collected from 5 healthy donors and PBMCs were isolated by Lympholyte density gradient. Live lineage-HLA-DR^{+} cells were FACS-sorted and load for 10X Genomics platform based scRNA-seq. Lin: CD3, CD19 and CD56 cells.

We then obtained the transcriptomes of individual cells by performing droplet-based 10X Genomics' scRNA-seq. In total, we sequenced 35.635 cells. After quality control and filtering, we obtained 26.474 cells, with a median of 2.270 genes and a median of 65.897 reads detected per cells (**Table 7.1**).

	Estimated Number of Cells	Mean Reads per Cell	Median Genes per Cell	Total Genes Detected
s01	7.746	64.048	2.293	22.673
s02	7.186	68.804	2.270	22.707
s03	7.785	65.220	2.270	22.668
s04	5.932	65.897	2.156	21.686
s05	6.986	71.024	2.342	22.970

Table 7.1. Number of recovered cells calculated by Cell Ranger™ Analysis Pipelines and relative number of reads and genes after each step of quality control filtering. s01-05, sample 01-05 (each sample corresponds to one donor).

Unsupervised clustering identified 20 distinct cell populations that were annotated according to significant expression of canonical gene signatures (Errore. L'origine riferimento non è stata trovata. and Errore. L'origine riferimento non è stata trovata. in Materials and Methods). We identified 8 clusters of monocytes (c0, c1, c2, c3, c6, c7, c12 and c13), 6 clusters of dendritic cells (c5, c8, c15, c16, c18 and c19), NK cells (c4, c9 and c10), B cells (c17) and immature precursors (c11 and c14) (**Figure 7.2**). We next sought to better delineate the populations identified. Out of the whole monocytes, 5 clusters were classical (c0, c1, c2, c7, c12) based on expression, among others, of *CD14* and *VCAN*, and 2 clusters (c3, c13) were non-classical, expressing *FCGR3A* and *CSF1R* (**Figure 7.3**). One cluster (c6) was annotated as intermediate, presenting mid-levels of *CD14* and *FCGR3A* compared to the classical and non-classical monocytes, as well as a general signature resembling intermediate monocytes described in the literature [103] (**Figure 7.3**). Both myeloid and plasmacytoid DC populations were present. Myeloid DCs (clusters c5, c15 and c19) expressed high levels of HLA- genes (**Figure 7.3**). Based on increased expression of *CD1C*, *FCER1A* and *CLEC10A*, cluster 5 and cluster 19 were annotated as conventional DC2, while c15 expressed the highest levels of *CLEC9A* and *CADM1*, discriminative markers of myeloid cDC1 [223] (**Figure 7.3A-B**). C8 and c16, showing expression of *IL3RA/CD123*, *CLEC4C* and *NRP1*, were recognized as plasmacytoid DCs [223] (**Figure 7.3A-B**). Finally, we observed a small population of *AXL*-expressing pre-DCs with a profile generally similar to pDCs (c18) (**Figure 7.3A-B**). Among the NK cells, we identified two clusters ascribing to $CD56^{neg}$ or contaminating $CD56^{dim}$ NK cells (c10 and c4), given the exclusion of $CD56^{+}$ cells during the gating strategy adopted for the scRNAseq (**Figure 7.1**) and their expression of CD16 (**Figure 7.3**) [224], and one population of NKT cells (c9) (**Figure 7.3C**). The latter was identified based on its expression of typical NK markers such as lytic granule genes (*GZMA*, *GZMH*, *GZMM*, *NKG7* and *PRF1*)

and *CD3D*, *CD3E* and *CD3G* (Figure 7.3A-B). Two small clusters representing 1% and 0.6% of the total population (c11 and c14, respectively) showed different sets of immature precursor myeloid genes, such as *CD34*, *GATA1*, *GATA2* and *SOX4*, allowing annotation as common myeloid progenitors (**Figure 7.2B** and **Figure 7.3A** and **C**). Finally, the small cluster 17 expressed high levels of *MS4A1* (CD20) and was thus confirmed as population of contaminating B cells (**Figure 7.3A** and **C**).

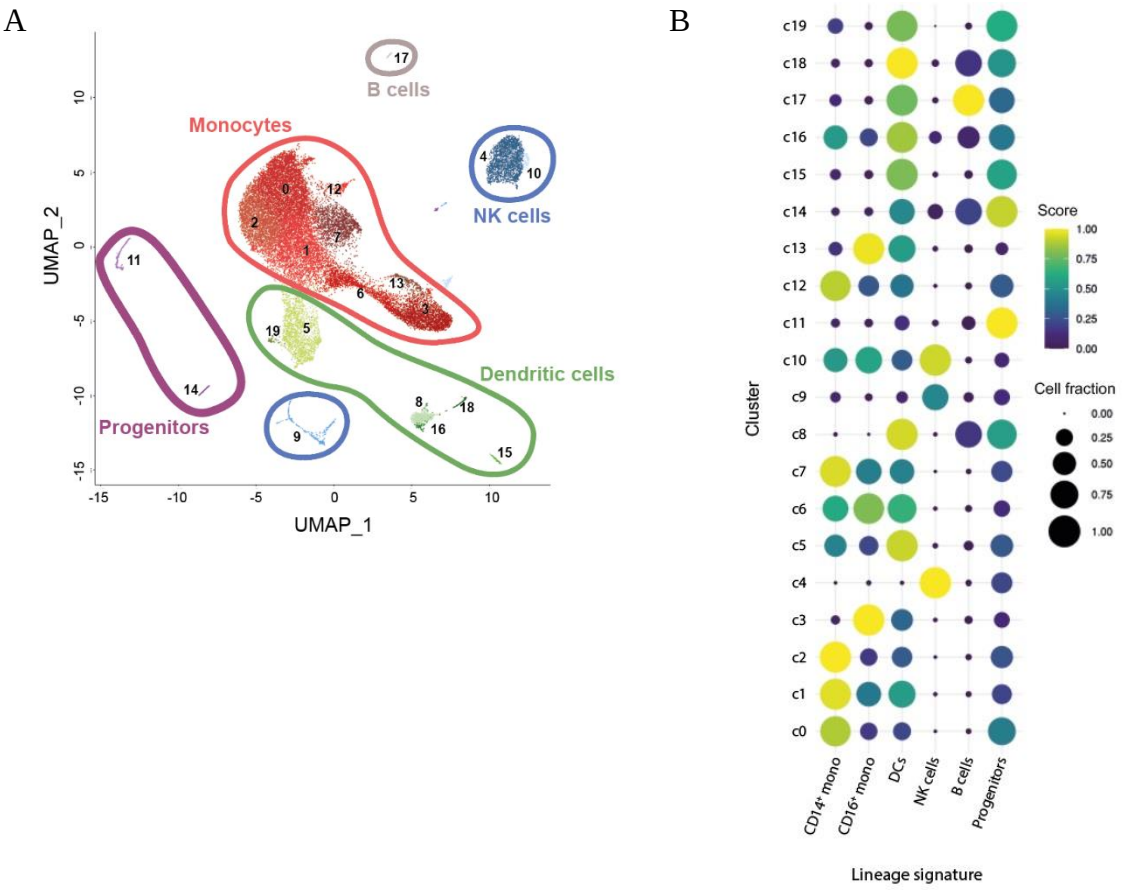

Figure 7.2. Single-cell RNA sequencing of healthy peripheral blood HLA-DR⁺ cells identified 20 cell clusters belonging to 5 distinct cell lineages. (A) UMAP projection of CD45⁺Lin⁻HLA-DR⁺ cells (n = 26,474) showing 20 clusters belonging to 5 major immune cell subsets. Clusters are numbered according to their size, from the largest (cluster 0) to the smallest (cluster 19). Each dot represents an individual cell. (B) Dot-plot showing annotated immune cells by lineage signatures (genes belonging to each signature are listed in *Errore. L'origine riferimento non è stata trovata.Errore. L'origine riferimento non è stata trovata.* ***in Material and Methods). SsGSEA-score based signature expression is coloured-coded from blue (low) to yellow (high); circle size indicates the fraction of cells expressing the signature. CD14⁺ mono indicates classical CD14⁺ monocytes; CD16⁺ mono, non-classical CD16⁺ monocytes; DCs, dendritic cells; NK cells, natural killer cells.***

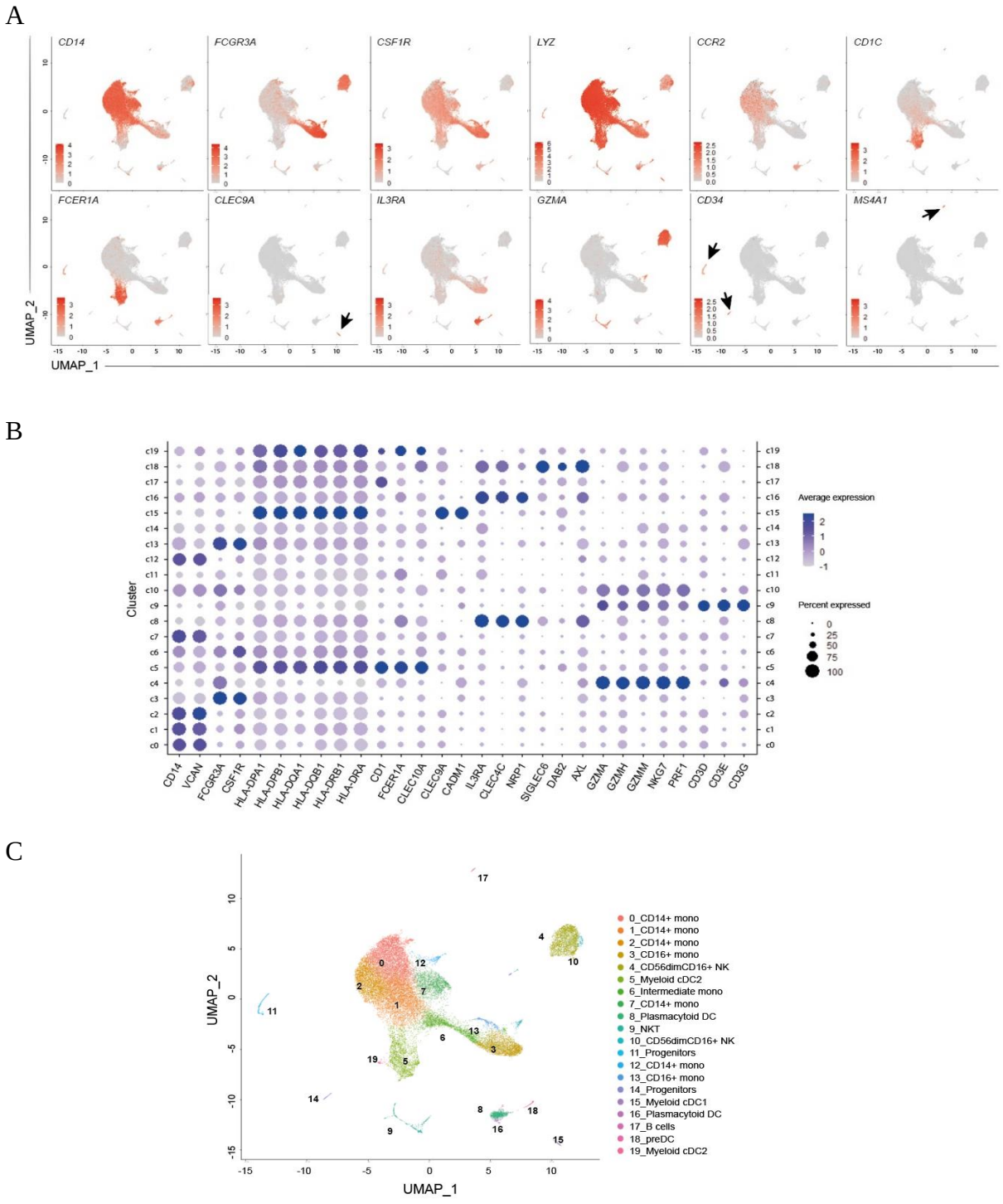

Figure 7.3. Manual cell cluster annotation after unsupervised clustering the scRNA-seq data. (A) Feature plot showing the expression of key genes used for manual cell cluster annotation. Gene expression is coloured-coded from grey (low) to red (high). (B) Dot-plot showing the expression of key genes adopted for manual cell cluster annotation. Gene expression is coloured-coded from grey (lower) to blue (higher); circle size indicates the fraction of cells expressing the gene. (C) UMAP projection of $CD45^{+}Lin^{-}HLA^{-}DR^{+}$ cells (n = 26,474) showing 20 clusters individually annotated. Clusters are numbered according to their size, from the largest (cluster 0) to the smallest (cluster 19). Each dot represents an individual cell.

Importantly, cells from all five donors contributed to every cell type, indicating that clustering was donor-independent, as confirmed by the significant reproducibility among biological replicates (**Figure 7.4**). Indeed, Pearson's correlation coefficients between the average expression of genes in each cell in each donor ranged from 0.98 to 0.99.

Once identified all distinct mononuclear cells we focused on monocytes.

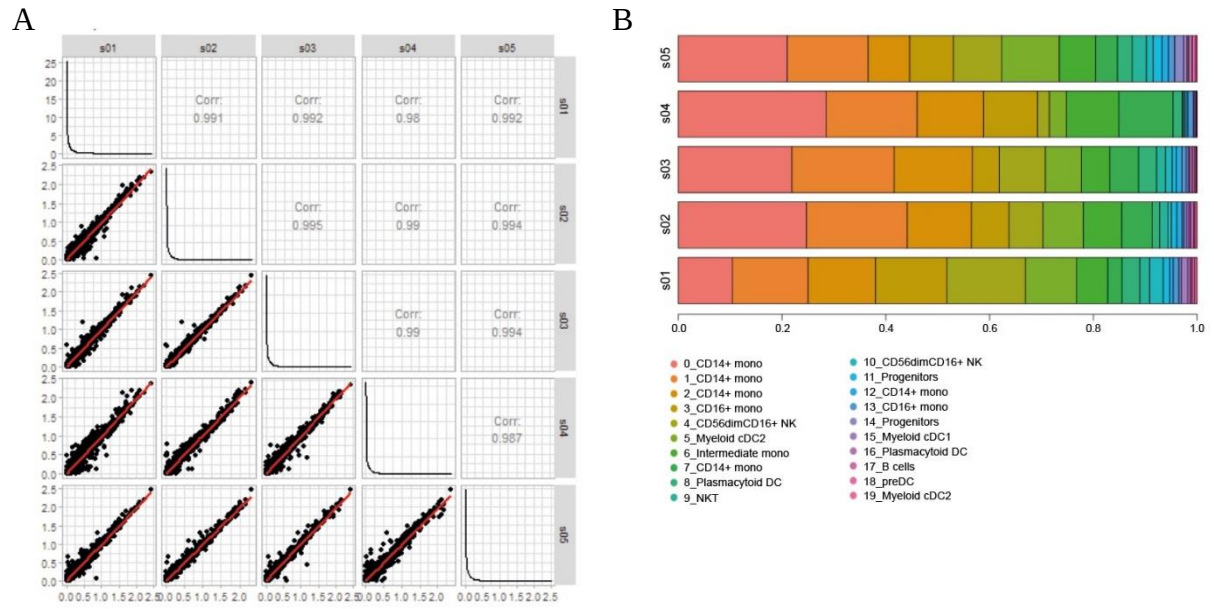

Figure 7.4. Under steady state, number and frequency of human peripheral blood HLA-DR$^+$ cells populations are analogous in all 5 healthy donors. (A) Scatter plot matrix representing Pearson's correlation coefficients of gene expression values in each cell between pairwise donors (s01-05). Rows and columns represent samples. Abscissa and ordinate axes show the logarithmic gene expression. Each dot represents a gene. (B) Bar plot showing the fraction, from 0 to 1, of each of the 20 identified cell clusters per donor (s01-05). Clusters are coloured according to cluster designation.

7.2 Circulating monocytes present distinct profiles in homeostatic conditions

The coexistence of distinct circulating monocyte subsets in homeostasis suggests that they may be dedicated to executing different tasks. In order to gain insights into their functional specialization, we better characterized their transcriptomic features by applying the single sample Gene Set Enrichment Analysis (ssGSEA) of the Hallmark gene sets to each cell. Some pathways were almost equally enriched within clusters belonging to the same major population: genes involved in angiogenesis, cell adhesion and cell-matrix interactions were upregulated in

the clusters of classical monocytes, while the Notch signalling pathway was enriched in non-classical cells (**Figure 7.5**).

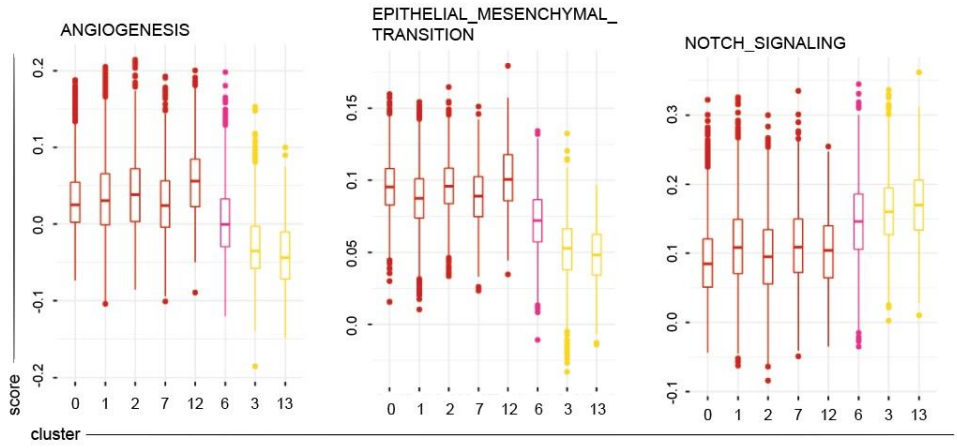

Figure 7.5. Pathways found equally enriched in clusters belonging to the same monocyte macro-group (classical and non-classical monocytes). Boxplot showing the normalized enrichment score (ssGSEA) of selected Hallmark signatures. All Hallmark scores were taken into consideration in normalizing values. Colour code: dark red, classical monocytes; pink, intermediate monocytes; yellow, non-classical monocytes.

Conversely, some pathways were selectively enriched in distinct subpopulations, regardless which macro-category they belonged to. Indeed, cells in cluster 0, compared to other classical monocyte clusters, had lower activation of pathways related to adipogenesis, fatty-acid metabolism, complement system and oxidative phosphorylation. The same pathways were slightly upregulated in non-classical cells from c13 compared to the ones from c3 (**Figure 7.6**). Notably, many genes involved in response to alpha and gamma interferons were selectively upregulated in cluster 7 and 13 (**Figure 7.6**). Overall, these results are consistent with the large body of evidence representing the classical and the non-classical monocytes as two distinct populations [223], but also provide evidence of functional differences within each of the two groups, suggesting that monocyte populations with distinct functional profiles coexist in homeostasis. We therefore addressed to deepen our understanding of the heterogeneity within each macro-group.

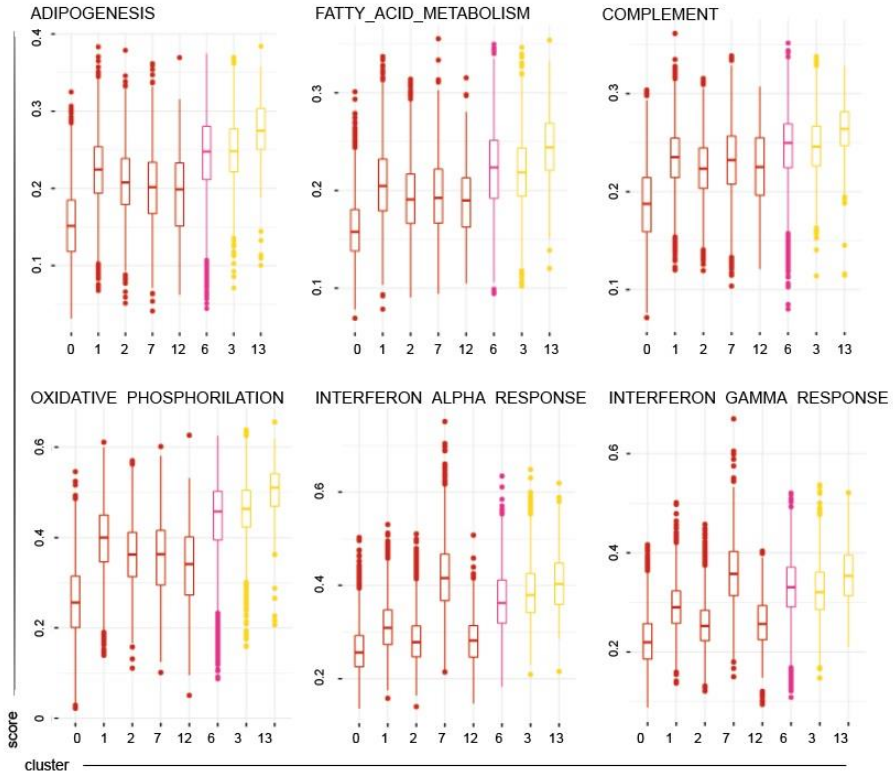

Figure 7.6. Pathways found differentially enriched in clusters belonging to the same monocyte macro-group (classical and non-classical monocytes). Boxplot showing the normalized enrichment score (ssGSEA) of selected Hallmark signatures. All Hallmark scores were taken into consideration in normalizing values. Colour code: dark red, classical monocytes; pink, intermediate monocytes; yellow, non-classical monocytes.

The subsets of classical monocytes c0, c1 and c2 were the most abundant monocyte subtypes, comprising 28.5%, 23.5% and 16.8% of the total monocyte population, respectively. They all shared a similar transcriptomic profile, with high levels of the most conventional classical genes, including the pattern recognition receptors *CD14*, *VCAN* and the chemokine receptor *CCR2* (**Figure 7.3A** and **Figure 7.7**).

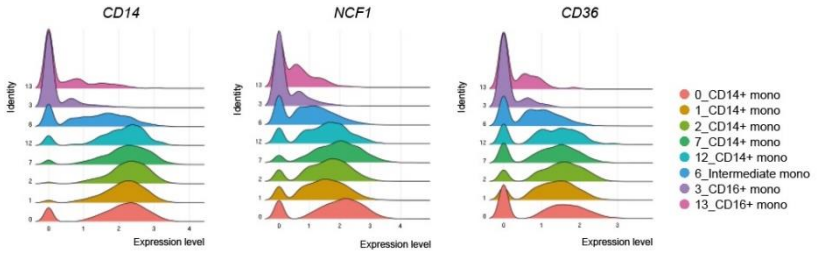

Figure 7.7. Ridge plot showing the expression levels of typical genes highly expressed in classical monocytes. Only monocyte subsets are shown and clusters are coloured according to cluster designation.

In our dataset, clusters c0 and c2 were strictly related, as appears from the Pearson's correlation analysis (**Figure 7.8**).

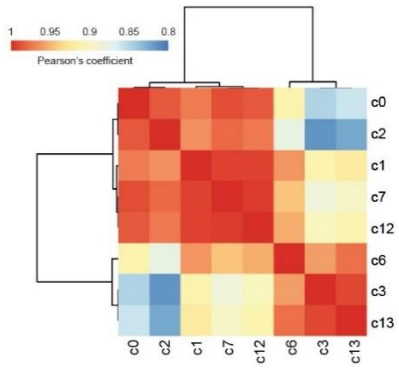

Figure 7.8. Heatmap representing Person's correlation between 8 subtypes of monocytes. Pearson's coefficient values are coloured coded from blue (lower) to red (higher). Rows and columns are ordered by hierarchical clustering.

Looking at the top 5 discriminative genes, both c0 and c2 emerged as the cell subsets that expressed the highest levels of proinflammatory genes *S100A8*, *S100A9* and *S100A12*, (**Figure 7.9A**). Emerging studies, both in mouse and humans, have classified a classical monocyte population expressing common neutrophilic markers, such as the S100A proteins, as "neutrophil-like monocytes" (NeuMo) [43, 44, 225]. Differential expression analysis (one monocyte cluster vs all the other monocyte cells) revealed higher expression of proinflammatory *CXCL8* and *TREM1* and of the transcript regulators *DUSP6*, *KLF6* and *FOSB* in c0 (**Figure 7.9B**). Moreover, consistent with the up-regulation of the arachidonate 5-lipoxygenase-activating gene (*ALOX5AP*), differential expressed genes (DEGs) analysis showed a significant enrichment of the leukotriene synthesis pathway. Instead, in c2 we found higher levels of genes involved in cell migration (*SELL* and *VCAN*), as well as of pro-inflammatory and antimicrobial *RETN*, *PADI4* and the lysozyme gene *LYZ*. Accordingly, pathways involved in the cellular defence against pathogens were up-regulated (**Figure 7.9B and C**). Cluster 1 exhibited a functional activation phenotype and pro-inflammatory features as well. Indeed, among its top-five cluster marker genes, we identified *NFKBIA*, which exerts an autoregulatory loop that sustains a positive regulation of NF-kB activity [226], interleukin 1β (*IL1B*), and both the chemokine *CCL3* (MIP-1-alpha) and *CCL3L1* (**Figure 7.9A**). Moreover, c1 significantly upregulated the TNF-α signalling pathway, displaying high levels of the TNF Alpha Induced Protein 3 (*TNFAIP3*) and *NFKBIA* (**Figure 7.9B** and **C**). Overall, these observations suggest that the three major clusters of classical monocytes display distinct inflammatory programs and activation states.

A

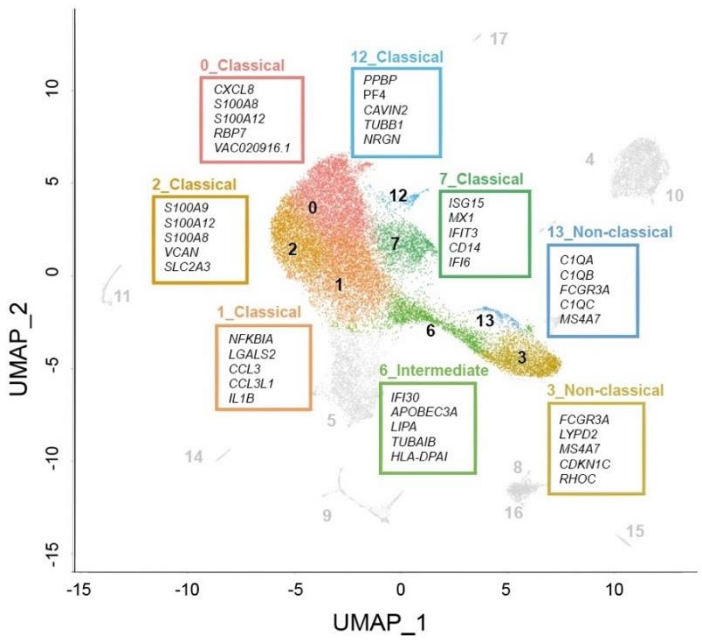
0_Classical
CXCL8
S100A8
S100A12
RBP7
VAC020916.1
12_Classical
PPBP
PF4
CAVIN2
TUBB1
NRGN
2_Classical
S100A9
S100A12
S100A8
VCAN
SLC2A3
7_Classical
ISG15
MX1
IFIT3
CD14
IFI6
13_Non-classical
C1QA
C1QB
FCGR3A
C1QC
MS4A7
1_Classical
NFKBIA
LGALS2
CCL3
CCL3L1
IL1B
6_Intermediate
IFI30
APOBEC3A
LIPA
TUBAIB
HLA-DPAI
3_Non-classical
FCGR3A
LYPD2
MS4A7
CDKN1C
RHOC
UMAP_2
UMAP_1

B

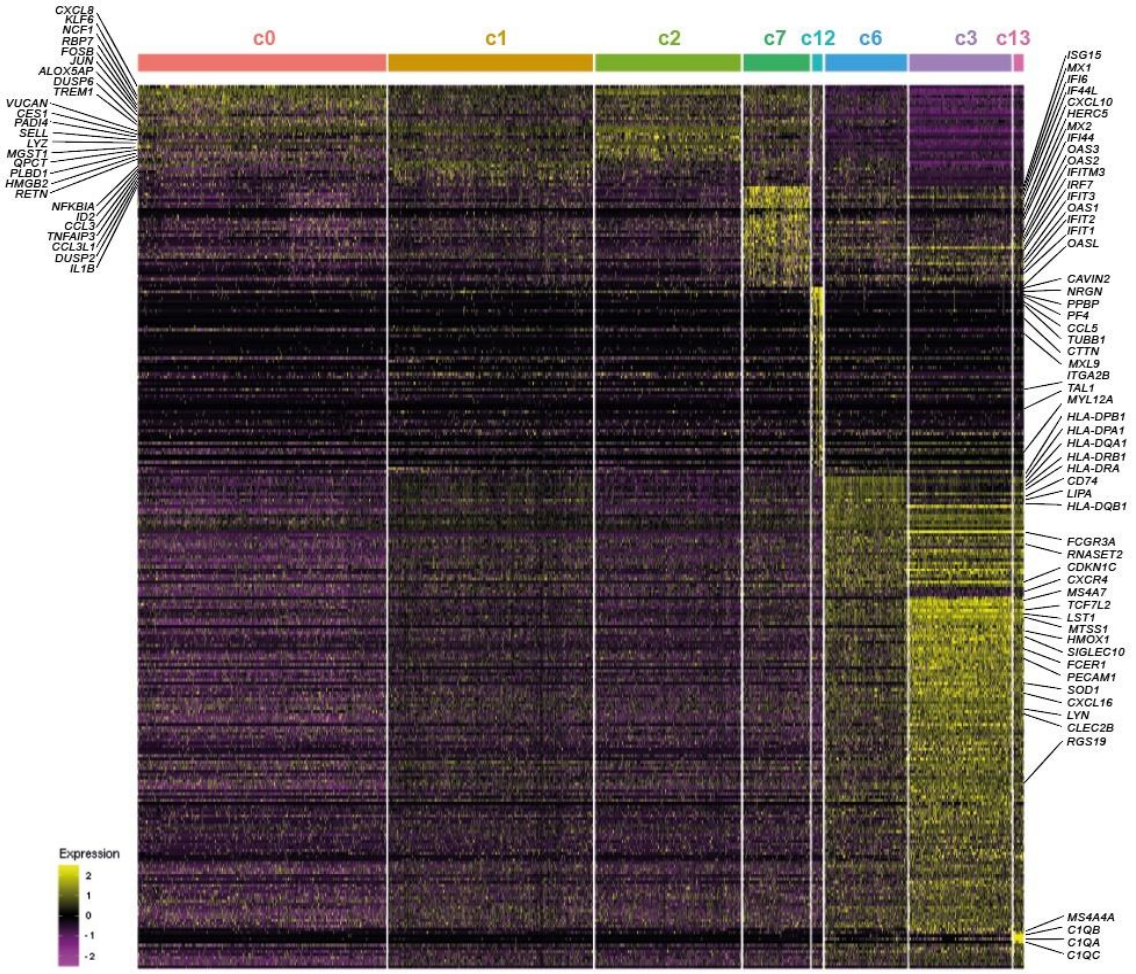
c0
c1
c2
c7
c12
c6
c3
c13
CXCL8
KLF6
NCF1
RBP7
FOSB
JUN
ALOX5AP
DUSP6
TREM1
VUCAN
CES1
PADI4
SELL
LYZ
MGST1
QPCT
PLBD1
HMGB2
RETN
NFKBIA
ID2
CCL3
TNFAIP3
CCL3L1
DUSP2
IL1B
ISG15
MX1
IFI6
IF44L
CXCL10
HERC5
MX2
IFI44
OAS3
OAS2
IFITM3
IRF7
IFIT3
OAS1
IFIT2
IFIT1
OASL
CAVIN2
NRGN
PPBP
PF4
CCL5
TUBB1
CTTN
MYL9
ITGA2B
TAL1
MYL12A
HLA-DPB1
HLA-DPA1
HLA-DQA1
HLA-DRB1
HLA-DRA
CD74
LIPA
HLA-DQB1
FCGR3A
RNASET2
CDKN1C
CXCR4
MS4A7
TCF7L2
LST1
MTSS1
HMOX1
SIGLEC10
FCER1
PECAM1
SOD1
CXCL16
LYN
CLEC2B
RGS19
MS4A4A
C1QB
C1QA
C1QC
Expression
2
1
0
-1
-2

C

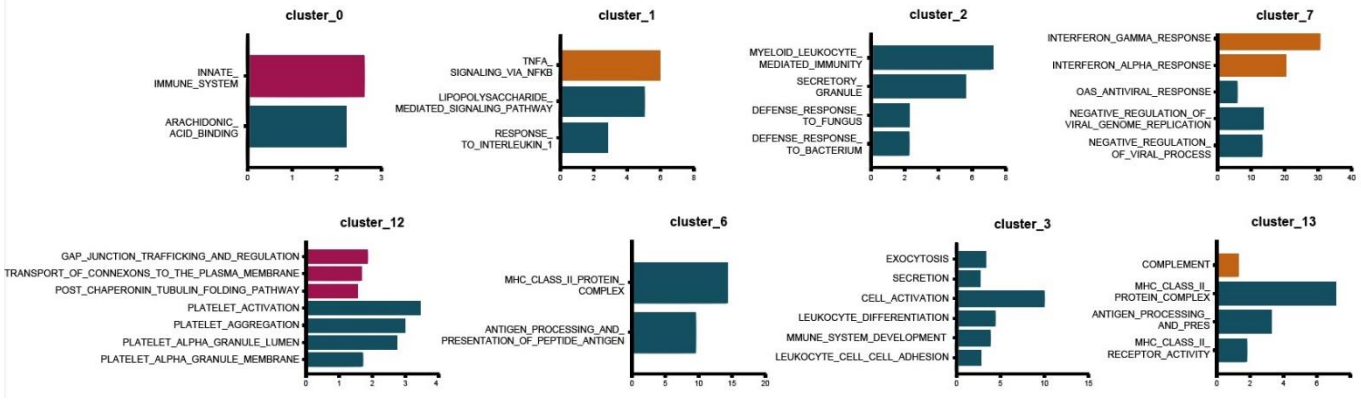

Figure 7.9. Characterization of transcriptional heterogeneity among human circulating monocytes. (A) Same UMAP projection as in Figure 7.3C, highlighting only monocyte clusters (c0, c1, c2, c3, c6, c7, c12 and c13). Up to five cluster marker genes are listed in boxes next to each cluster. Cluster marker genes are defined as in Material and Methods. (B) Single cell gene expression heatmap showing significant differentially expressing genes ($pvalue_{adj} \leq 0.05, pct1 \geq 0.1, pct2 \geq 0.1, log_2 FC \geq 0.5$) among monocyte cell subsets. Selected gene names are labelled; gene expression is coloured coded from purple (lower) to yellow (higher); gene expression level is scaled by row. (C) Key pathways enriched in individual populations of monocytes. HALLMARK (orange), GO (blue) and REACTOME (violet) pathway analysis of differentially expressed genes (one cluster of monocyte vs all the other monocyte cells). Only upregulated genes were considered. $-log\_10(pvalue)$ is shown in the x axis; values greater than 1.3 are significant.

Clusters c7 and c12 (7.7% and 1.2% of all monocytes, respectively) were less represented among the classical monocytes. Despite the fact that they expressed typical markers of classical monocytes, such as *NCF1*, a crucial component of the NADPH oxidase complex, and the scavenger receptor *CD36* (**Figure 7.7**), they both displayed strong characteristic transcriptional profiles, highlighting specific functional properties of these subpopulations. Cells in c7 significantly expressed high levels of antiviral genes, including *ISG15*, *MX1* and *IFIT3*, the top-three upregulated genes of the cluster, whereas the profile of c12 was associated with cellular motility and migration (*TUBB1*, *CCL5*, *CD9*) (**Figure 7.9A** and **B**). A robust profile of cells with anti-viral activity was confirmed in c7 by the differential expression analysis; thus, various interferon-induced proteins, such as *CXCL10*, *HERC5* and proteins belonging to the IFIT, IFI and OAS family, were upregulated in this cluster (**Figure 7.9B**). Accordingly, DEGs analysis showed enrichment of IFNα and IFNγ responses and defence response against viruses (**Figure 7.9C**). Instead, cluster c12 showed upregulation of pathways related to intracellular cytoskeleton reorganization and trafficking processes, as suggested by the elevated expression of *MYL9*, *MYL12* and tubulin genes (**Figure 7.9B** and **C**). Interestingly,

the top-two genes characteristic of this cluster were platelet related genes: the pro-platelet basic protein (*PPBP*) and the platelet factor 4 (*PF4*) (**Figure 7.9A**). Moreover, different platelet associated DEGs and pathways were significantly upregulated, corroborating the idea that c12 may correspond to circulating monocyte-platelet aggregates (MPA) (**Figure 7.9B** and **C**) [227, 228].

Non-classical monocytes clustered into two distinct groups: the majority of cells were included into c3, while a small number contributed to c13 (11.7% and 1.1% of the entire monocyte population, respectively). These two clusters were found to share almost the same transcriptome profile, showing high levels of genes associated with cell activation (*LST1*, *LYN*, *IFITM3*, *SIGLEC10*, *SOD1*, *RPS19*) and regulation of the cell cycle (*MTSS1*, *CDKN1C*) (**Figure 7.9A-C** and **Figure 7.10**).

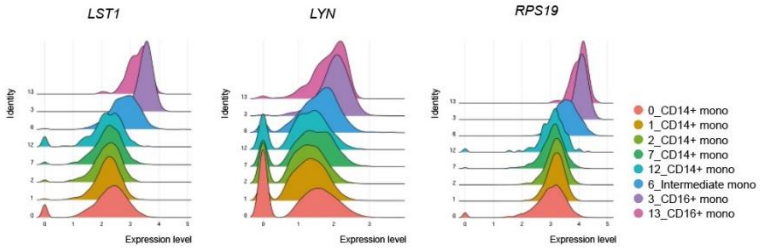

Figure 7.10. Ridge plot showing the expression levels of typical genes highly expressed in non-classical monocytes. Only monocyte subsets are shown and clusters are coloured according to cluster designation.

Involvement of non-classical monocytes in complement-mediated phagocytosis as well as in the pathway of the complement system has been reported [66, 100]. Notably, in our dataset, the complement genes *C1QA*, *C1QB* and *C1QC* were exclusively expressed by cells in c13 and the DEGs analysis confirmed the enrichment of complement pathway in this cluster (**Figure 7.9A-C**), demonstrating that this $CD16^{+}$ population was more specialized for complement activation. To better characterize the identity of c3 and c13 and find discriminative genes between the closely related non-classical clusters, we performed a differentially expression analysis, selectively between these two monocyte populations. As expected, we didn't find many differentially expressed genes. However, we interestingly observed higher levels of HLA genes in cluster 13, as confirmed by the major histocompatibility class II antigen presentation pathway enrichment in this subset (**Figure 7.11** and **Figure 7.9C**). Instead, we found cluster 3 enriched in genes involved in cell motility and chemotaxis (*ANXA1*, *ANXA2*, *RHOC*, *PECAM*).

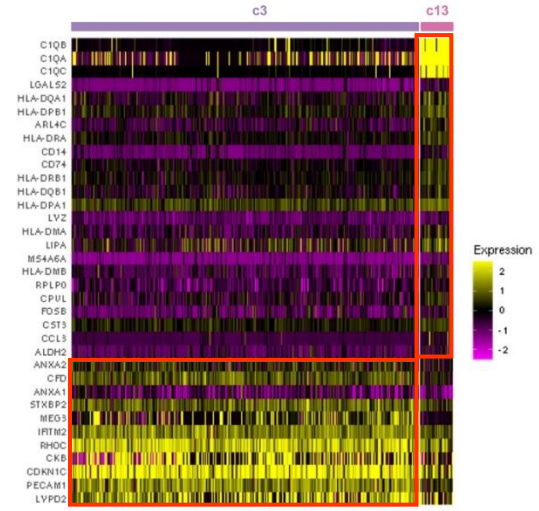

Figure 7.11. Single cell gene expression heatmap showing significant differentially expressing genes ($pvalue_{adj} \leq 0.05, pct1 \geq 0.1, pct2 \geq 0.1, |log_2 FC| \geq 0.5$) ***among non-classical monocyte cell subsets (c3 and c13). Gene expression is coloured coded from purple (lower) to yellow (higher); gene expression level is scaled by row.***

Finally, cluster 6 comprised 9.5% of the total monocytes. As reported previously, the intermediate monocytes were strongly characterized by high levels of HLA genes, and the consequent enrichment of antigen presentation pathways (**Figure 7.9B** and **C**) [66].

Taken together, the transcriptional profile of monocyte populations in human blood at single-cell level suggests a profound heterogeneity, whereby distinct populations are programmed to exert specific functions.

7.3 Trajectory reconstruction of monocyte populations

Many studies have demonstrated that classical monocytes are able to give rise to the non-classical population in mice [14, 74, 229, 230]. Recently, the same program has been shown also in humans [98], even though the hypothesis that some $CD14^{+}CD16^{-}$ cells can arise following another rout of development cannot be excluded [42]. Since we found several subsets of monocytes in our data set, we asked whether their developmental paths were connected and how. To this aim, Single-cell Trajectories Reconstruction, Exploration And Mapping (STREAM) analysis was performed. This tool allows capturing the transcriptional trajectory among subsets, grouping cells that share most of the transcriptional program in states. Then,

the states are aligned along an artificial pseudotime, thus helping understand how closely the subsets are related. We decided to carry out the investigation on myeloid progenitors, most likely precursors of our subsets of interest, monocytes and dendritic cells. DCs were included in the analysis because their closed relation with monocytes in terms of development. Indeed, as previously discussed in paragraph 4.1.2, both these lineages originate from the same monocyte/DC progenitor (MDP) and monocytes, during inflammation, can differentiate into dendritic cells, originating monocyte-derived DCs (moDCs). The analysis uncovered five cellular trajectories, as shown in **Figure 7.12**.

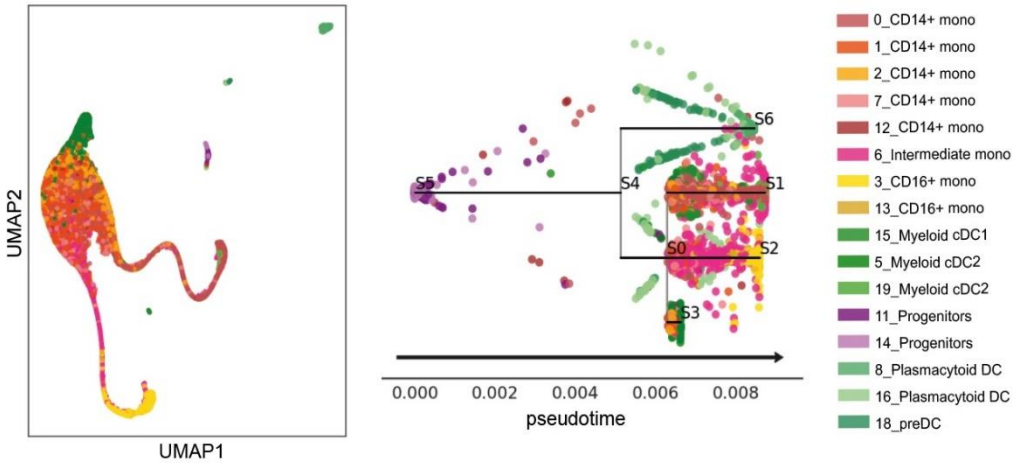

Figure 7.12. UMAP (left) and subway map plot (right) visualization of inferred developmental trajectory of myeloid progenitors, monocytes and DCs by STREAM. Cells are coloured according to the cluster of origin as shown in the legend.

Starting from myeloid progenitors, cells bifurcated into plasmacytoid dendritic cell lineage (branch S4-S6) and a branch that further separated into three sub-branches: classical monocytes (belonging to c1, c2, c7, c12) and cDC2 (from c5) primarily localized into node S0 and branch S0-S3. Branch S0-S1 mainly consisted of classical monocytes from c0, cDC1 and cDC2s from c19. Finally, branch S0-S2 identified a clear directional progress from the intermediate to the non-classical cells (**Figure 7.12** and **Figure 7.13**). This outcome is partially consistent with evidence reported in the literature. Certainly, plasmacytoid DCs are easily discernible from the other DCs and from monocytes, and thus clearly separated from other clusters, while higher is the transcriptomic similarity of cDCs with monocytes [223, 231]. Moreover, the consequential distribution and progression of classical, intermediate and non-classical monocytes along the pseudotime trajectory, as well as the cell distribution within the UMAP projection (

Figure 7.13 and **Figure 7.12**), are in line with new evidence suggesting a sequential transition from intermediate and non-classical monocytes in humans [98].

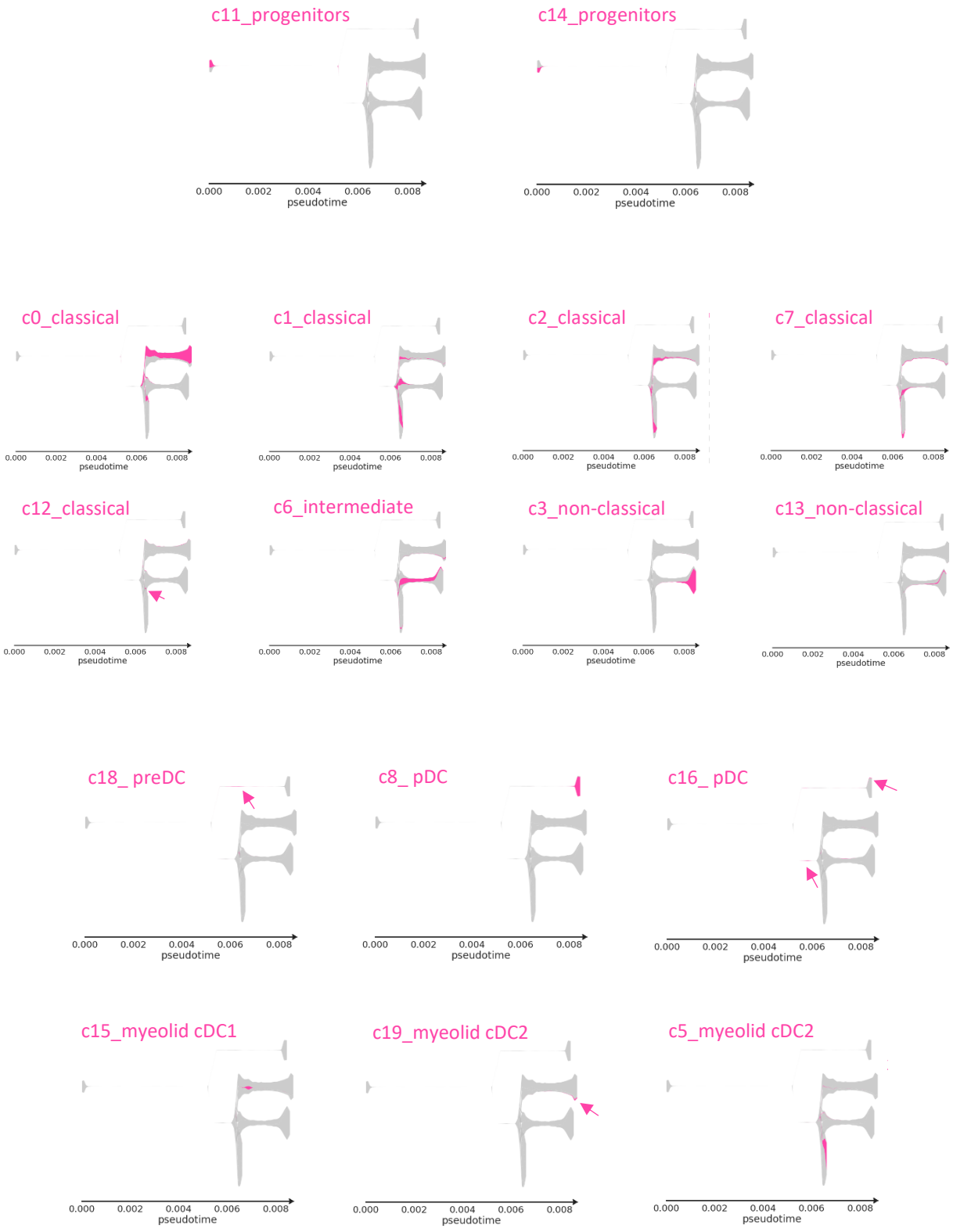

Figure 7.13. Stream plots visualization of inferred developmental trajectory of myeloid progenitors, monocytes and DCs by STREAM. Each plot show in pink one single cluster from the scRNA-seq.

Interestingly, focusing on $CD14^{+}CD16^{-}$ monocytes, we found a clear separation between the branch mainly composed of cells from c0 and all the other classical monocytes. Furthermore, while branch S0-S1 progressed along the pseudotime projection, the shorter branch S0-S3 did not. This scheme could suggest that cells belonging to cluster 0 are in an active state of transition and maturation. Previous results showing many functional pathways downregulated in c0 compared to all the other clusters of classical monocytes (**Figure 7.6**) possibly support this idea. To further investigate this hypothesis, we looked at gene expression of transition markers, genes whose mRNA values correlate with the pseudotime. As shown in **Figure 7.14**, among the genes more expressed in cells located at the endpoint of the branch considered, we found ferritin heavy/light chain (*FTH1*/*FTL*), crucial molecule in the iron retention metabolism and involved in the response to stimuli and pro-inflammatory responses in monocytes/macrophages [232-234], inflammatory S100 proteins (*S100A8*, *S100A6*, *S100A4*) and *FOS*. It thus seems that monocytes in cluster 0 are evolving towards a pro-inflammatory state.

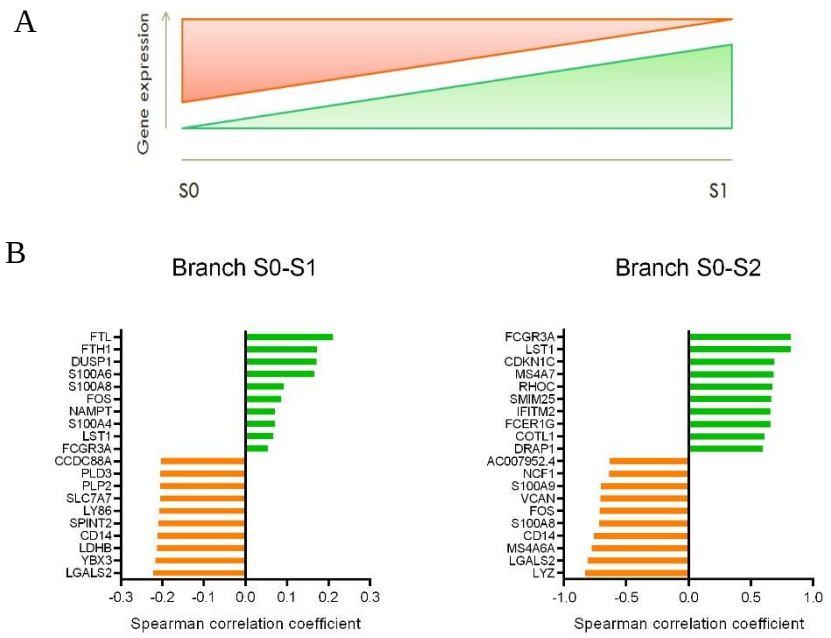

Figure 7.14. Identification of transition markers along branches S0-S1 and S0-S2 of the inferred developmental trajectory of myeloid progenitors, monocytes and DCs by STREAM. (A) As schematized in the figure, transition markers are genes expressed by cells between two nodes of the trajectory (in the example, S0 and S1), whose mRNA value positively (green) or negatively (red) correlates with the pseudotime. (B) Bar plot shows the top-20 transition markers significantly most correlated with the pseudotime calculated in branch S0-S1 (left), containing classical monocytes from cluster 0, or branch S0-S2 (right), containing intermediate and non-classical monocytes from c6, c3 and c13. 10 genes positively and 10 genes negatively correlated are shown.

Finally, transition markers of branch S0-S2 confirmed our previous observation that describes a progressive transition from classical to non-classical monocytes, given that typical genes of $CD14^+$ monocytes, like *LYZ*, *S100A8*, *S100A9*, *NCF1* and *VCAN*, were enriched near the node S0 and progressively decreased along the branch, while genes characteristic of $CD14^-$ monocytes, such as *FCGR3A*, *LST1* and *CDKN1C*, followed the opposite trend (**Figure 7.14**).

Collectively, STREAM analysis reconstructed the general cell lineage hierarchy of myeloid progenitors, circulating DCs and monocytes, even though we weren't able to discriminate the rout of differentiation of all classical monocytes. More in-depth analyses into the developmental relationship between monocytes subtypes are still needed to better characterize their connection, and hence to understand their responses in steady-state homeostasis and inflammation. Notwithstanding, such kind of analyses are not easily performed on human settings and more commonly take advantage of fate-mapping approaches in preclinical models.

7.4 MS4A gene family in human monocytes

Membrane-Spanning 4-domain subfamily A (MS4A) protein family represents a new emerging set of proteins structurally related to conventional tetraspanins. Some of these tetraspanin-like molecules have been reported by us and others as highly expressed in alternative activated macrophages [212, 213, 215]. In particular, in a previous study performed in our laboratory, it has been reported the expression of MS4A4A, MS4A6A and MS4A7 in tumour-associated macrophages, both in human and murine tumours, and it has been shown that they are involved in the formation of lipid raft-associated signalling complexes in macrophages [213]. Moreover, genome-wide association studies have shown a correlation between single nucleotide polymorphism variants within the *MS4A/MS4A6A* locus and the late-onset Alzheimer's disease and the cutaneous systemic sclerosis [235, 236].

Given the emerging role of MS4A proteins in macrophages, we decided to investigate this gene family also in monocytes, their cellular precursors. We thus first evaluated the expression of the MS4A genes in our dataset and found three genes expressed in myeloid cells: *MS4A4A* and *MS4A7* were mainly expressed by non-classical monocytes, while variable levels of

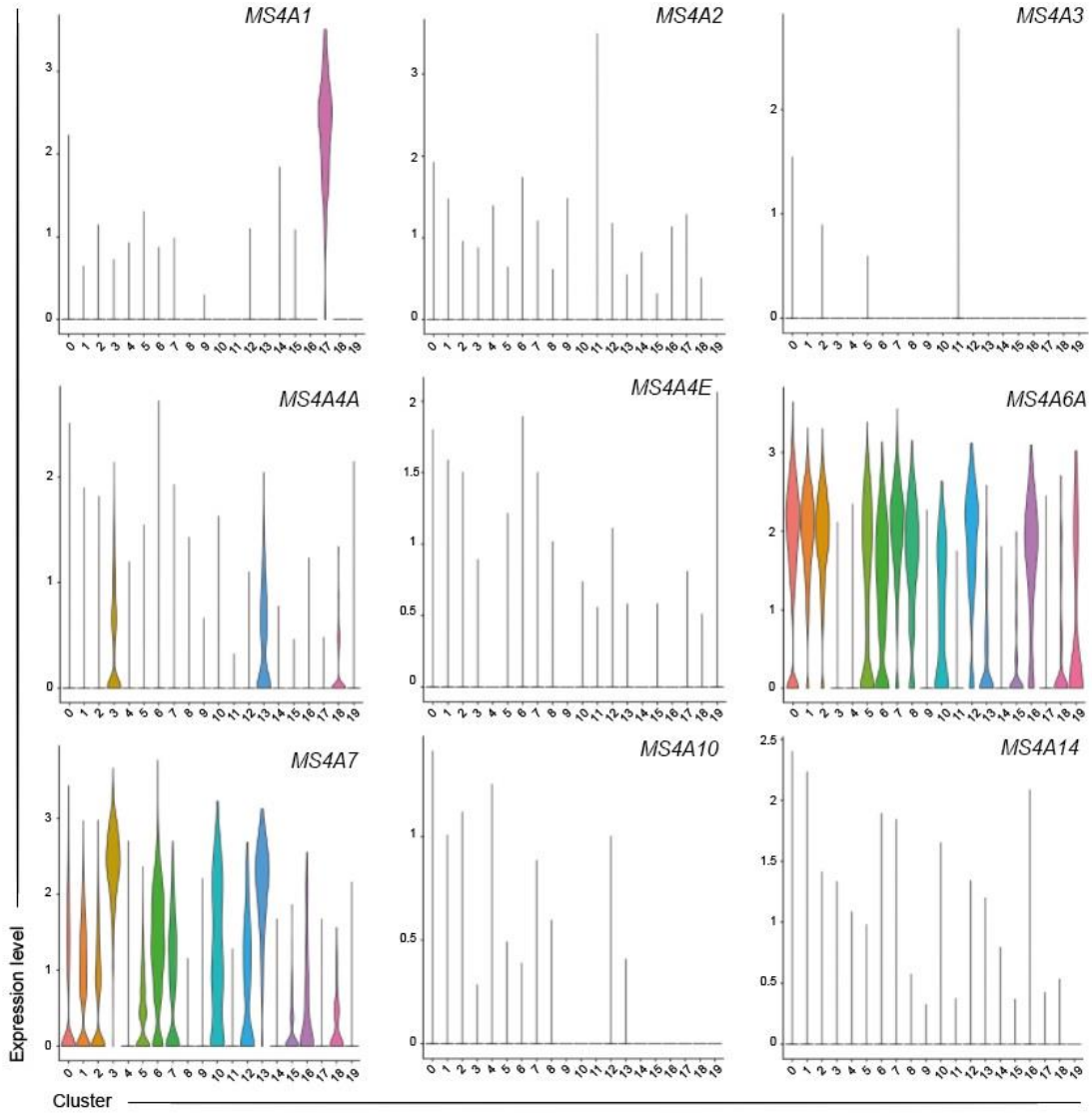

Figure 7.15. Expression distribution (violin plot) showing normalized expression levels of MS4A genes in human circulating HLA-DR$^+$ cell populations. CD14$^+$ mono (c0, c1, c2, c7, c12); CD16$^+$ mono (c3, c13); intermediate mono (c6); myeloid DCs (c5, c15, c19); plasmacytoid DCs (c8, c16); preDCs (c18); NK cells (c4, 10); NKT cells (c9); myeloid progenitors (c11, c14); B cells (c17).

MS4A7 expression were also found in intermediate and classical monocytes, as well as in dendritic cells. Finally, *MS4A6A* was highly expressed by cDC2, pDCs and both CD14$^+$CD16$^-$ and CD14$^+$CD16$^+$ monocytes (**Figure 7.15**). To finer depict the gene expression pattern described above, we computed a Pearson's correlation analysis of the three molecules in each population. This information may be helpful to capture the cross-regulation of the members of this family and in future studies aimed at analysing their function. In monocytes, we observed a strong negative linear correlation between *MS4A6A* and *MS4A7* mRNA expression (r=0.959). Similarly, *MS4A4A* and *MS4A6A* were linearly negatively correlated (r=0.981), while *MS4A7* appeared to be positively correlated with *MS4A4A* (r=0.974). As regarded dendritic cells, we

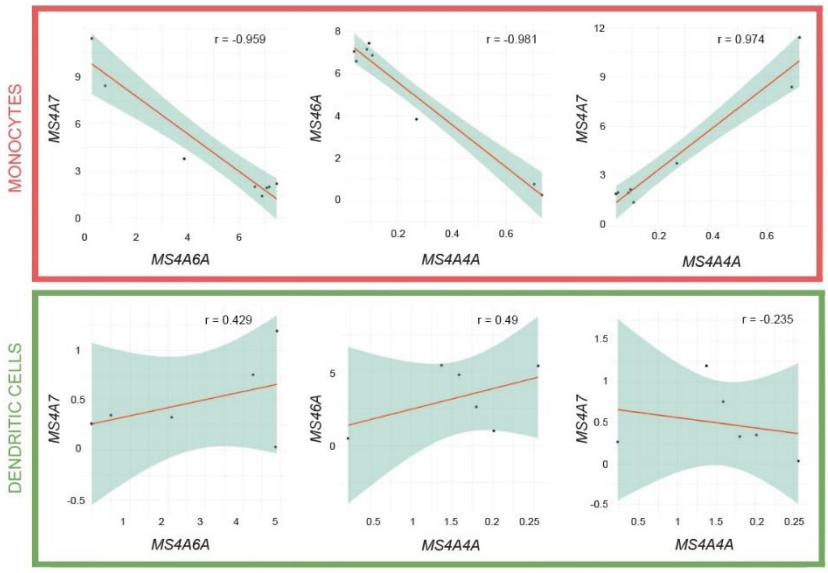

Figure 7.16. Scatter plot showing Pearson's correlation between MS4A4A, MS4A6A and MS4A7 genes in monocytes and dendritic cells. All Pearson's correlation coefficients, reported in the graph, are significant (P = <0.05).

obtained weak correlation between genes, with opposite results compared to what detected in monocytes: positive correlation between *MS4A6A* and *MS4A7* (r=0.429), positive correlation between *MS4A4A* and *MS4A6A* (r=0.490), and negative correlation between *MS4A6A* and *MS4A7* (r=0.235) (**Figure 7.16**). Overall, the three molecules under examination showed inverse expression patterns in monocytes and in dendritic cells. Moreover, we observed a distinct trend in *MS4A4A*, *MS4A6A* and *MS4A7* expression in monocytes compared to our previous data on in macrophages. Indeed, as mentioned, in macrophages the three MS4A proteins are co-expressed and associate at the level of the plasma membrane forming clusters [213]. Conversely, the expression of *MS4A4A* transcript in monocytes is almost restricted to the non-classical population (c3 and c13), *MS4A7* is enriched in $CD16^{+}$ monocytes, while *MS4A6A* was expressed, for the most part, by the classical subtype. To validate these observations, we interrogated The Human Cell Atlas public Immune System gene expression database, which confirmed our results (**Figure 7.17**).

As already discussed previously, circulating monocytes are critical contributors to the pool of resident tissue macrophages. However, the precisely measure for such contribution, both under steady state and during inflammation, is still an area of intense investigation. A recent fate-mapping study, aiming to develop a mouse model to estimate the contribution of monocytes to RTMs and discern monocytes from DCs, identified *Ms4a3*, belonging to the

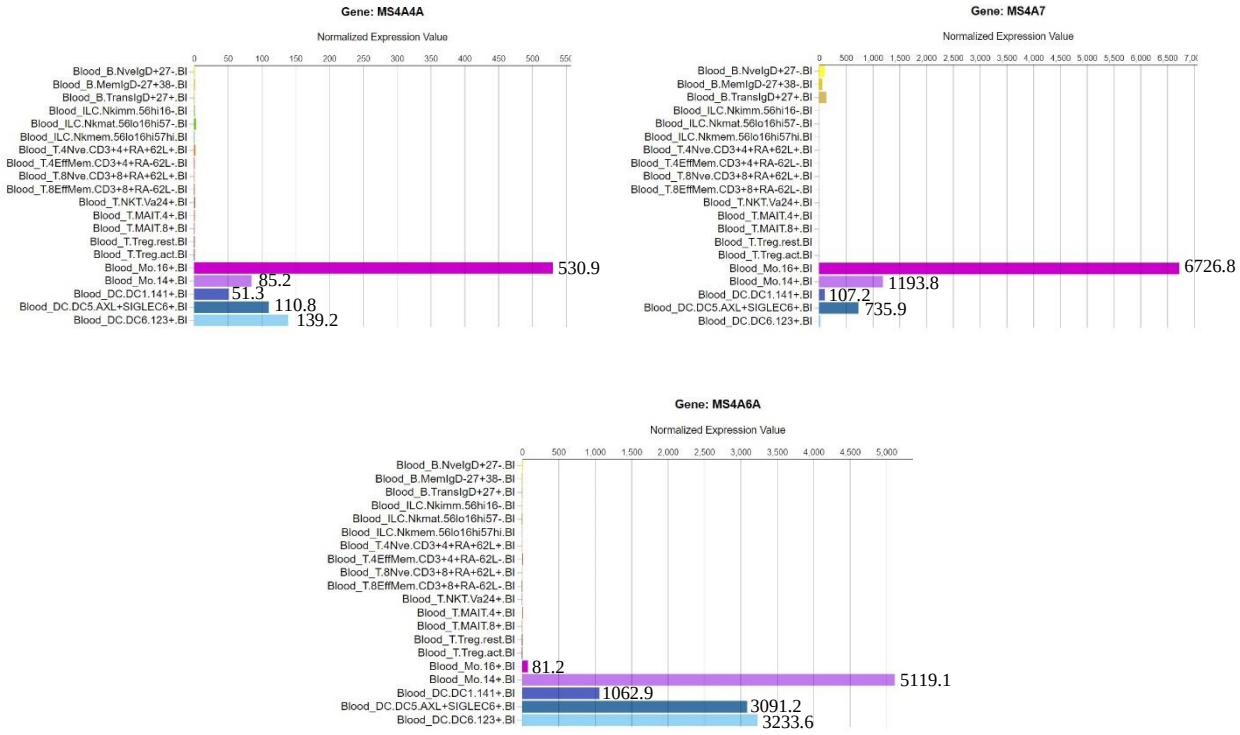

Figure 7.17. Transcription level of MS4A4A, MS4A6A and MS4A7 in human blood cells. MS4A4A, MS4A6A and MS4A7 transcript levels in human blood cell types based on the Human Cell Atlas, Immune System. CD16+ monocytes (Mo. 16^{+}) were sorted as HLA-DR^{+}CD16^{hi}CD14^{lo} PBMCs; CD14^{+} monocytes (Mo. CD14^{+}) were sorted as HLA^{-}DR^{+}CD16^{hi}CD14^{lo} PBMCs.

membrane-spanning 4A gene family, as a specific gene to track the GMP and the cMoP precursors in mice [68]. Given our previous results, we thus asked whether *MS4A4A, MS4A6A* and *MS4A7A* may be suitable as blood markers for the commitment to monocytes or dendritic cells in humans. We thus came back to the STREAM analysis of trajectories, focusing now on the MS4A gene family members, and found that *MS4A6A* was highly expressed by cells present in node S0 and gradually decreased along each myeloid branch following the pseudo-time trajectory. Conversely, *MS4A7* and *MS4A4A* upregulation within the intermediate and non-classical monocytes progressively increases along branch S0-S2 in the trajectory (**Figure 7.18**). Also, within the transition markers of the trajectory branch composed of intermediate and non-classical monocytes (S0-S2), we identified *MS4A6A* as gene whose expression was inversely correlated with the pseudotime, and *MS4A7* in the top genes progressively upregulated following the trajectory (**Figure 7.14**).

Collectively, this data suggests *MS4A4A* as marker for the commitment to circulating non-classical monocytes in humans.

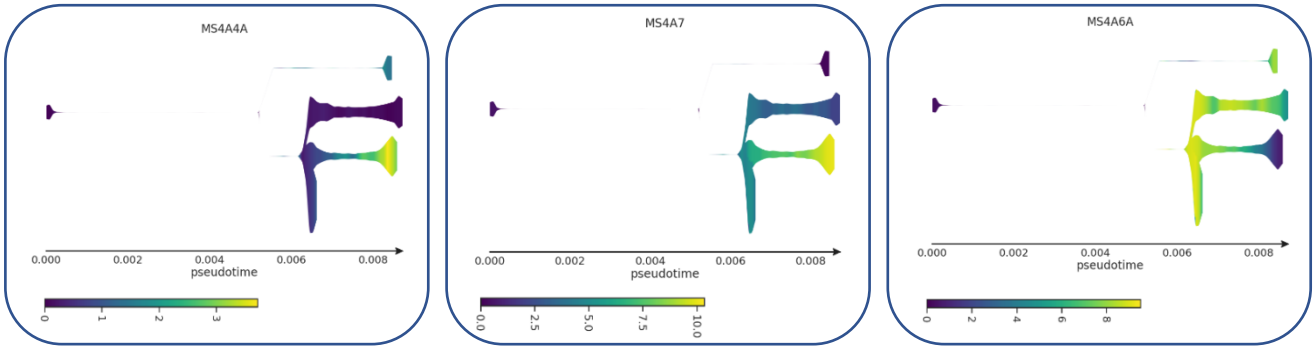

Figure 7.18. Stream plot showing the expression of myeloid MS4A genes along the same inferred developmental trajectory as in Figure 7.13. Gene expression is coloured code from blue (lower) to yellow (higher).

7.5 Focus on MS4A4A in human monocytes

This second part is focused on MS4A4A, one of the molecules that we found potentially valuable as a marker of non-classical and, as mentioned, molecule of interest in the group.

7.5.1 *MS4A4A PROTEIN IS EXPRESSED BY A FRACTION OF CD16$^+$ MONOCYTES*

Preliminary data from our laboratory suggests that MS4A4A interacts with a restricted set of molecular partners. Specifically, based on a yeast two-hybrid assay performed on RNA extracted from human monocyte-derived macrophages treated for 24h with Dexamethasone, relevant interactors resulted Dectin-1, as mentioned, but also the FcR signal transduced FcεRIγ chain, indicating a potential role of MS4A4A for FcγR signalling (*unpublished data*). Given the selective expression of MS4A4A gene in the CD16$^+$ non-classical population in monocytes, we decided to gain insight on the relevance/role of MS4A4A in this subset.

When investigated at the protein level by flow cytometry, only a fraction of CD16$^+$ monocytes stained positive for MS4A4A, whereas all the other monocyte subtypes (the classicals, most of the intermediates and a portion of non-classicals) were negative (**Figure 7.19**). MS4A4A expression pattern in non-classical monocytes was, therefore, consistent with mRNA levels detected in cluster 3 and cluster 13, albeit, compared to our transcriptomic data, MS4A4A was detected also by 15% on average of intermediate monocytes (**Figure 7.19B**). This divergent observation could be explained by the difficulty in dissecting the intermediate

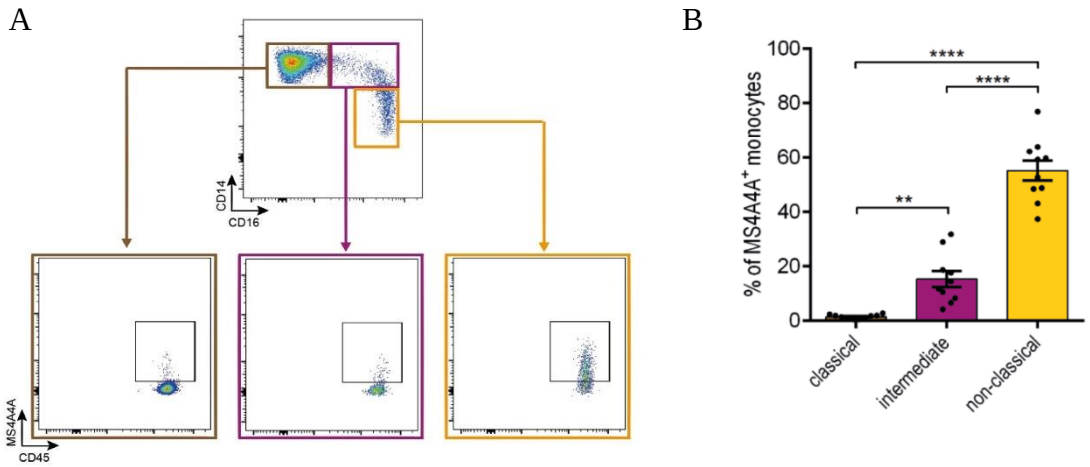

Figure 7.19. Frequency of MS4A4A in classical, intermediate and non-classical monocyte subsets of healthy donors. (A) Representative flow cytometry dot plot of MS4A4A expression in circulating human monocytes. (B) Percentage of MS4A4A^{pos} cells in circulating monocytes of healthy donors (N=10). Data plotted as mean±SEM (*P<0.05; **P<0.01; ***P<0.001; one-way ANOVA test).

and non-classical monocytes by FACS based only on the levels of CD14 and CD16, as confirmed by the numerous research efforts focused on the identification of new markers to overcome this issue [17-19].

Recently, SLAN has been proposed as a marker for human non-classical monocytes [19]. Given that SLAN$^+$ cells constitute a subset of CD16$^+$ monocytes, we asked whether MS4A4A$^+$ and SLAN$^+$ circulating monocytes represent the same cell subtype. Flow cytometry analysis showed that, even though both MS4A4A$^+$ and SLAN$^+$ monocytes localize within the non-classical monocyte gate, they do not constitute the same cell population: indeed, we detected cells expressing only MS4A4A or SLAN, as well as cells double positive for these two markers (**Figure 7.20**).

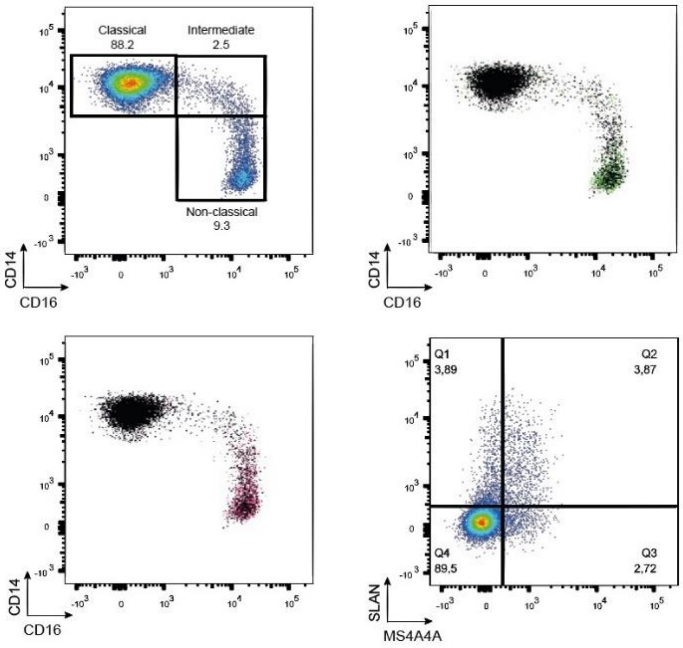

Figure 7.20. MS4A4A and SLAN expression in human monocytes. FACS Representative flow cytometry dot plot of frequency of classical, intermediate and non-classical (top left), SLAN distribution (top right) and MS4A4A distribution (bottom left) in human monocytes according to the expression of CD14 and CD16. Representative flow cytometry frequency of MS4A4A$^-$SLAN$^+$, MS4A4A$^+$SLAN$^+$, MS4A4A$^+$SLAN$^-$, and MS4A4A$^-$SLAN$^-$ cells is shown (bottom right).

Since morphology of human phagocytes is a peculiar feature exploited to classify them, we performed a cytospin of sorted cells to capture potential differences. However, no evident differences in terms of morphology were recorded between MS4A4A positive and MS4A4A negative cells (**Figure 7.21**).

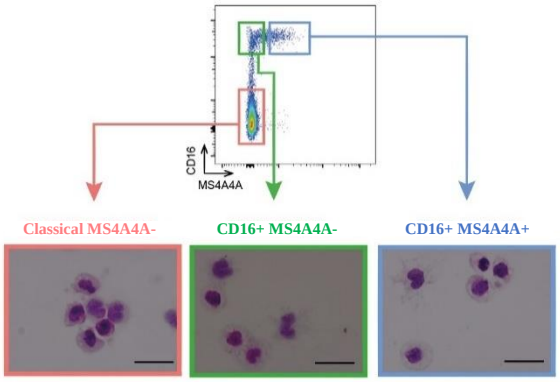

Figure 7.21. Representative CD16$^-$MS4A4A$^-$, CD16$^+$MS4A4A$^-$ and CD16$^+$MS4A4$^+$ circulating monocytes sorted from one healthy donor, cytospun and stained whith Hematoxylin and Eosin (scale bar = 200 µm).

7.5.2 *TRANSCRIPTOMIC ANALYSIS OF MS4A4A POSITIVE MONOCYTES*

To get insights into the molecular programs linking monocyte MS4A4A expression to their function, we decided to carry out bulk RNA-sequencing on the three major monocyte populations previously identified based on MS4A4A expression: $CD16^{-}MS4A4A^{-}$ (classical $MS4A4A^{-}$, C), $CD16^{+}MS4A4A^{-}$ (16n) and $CD16^{+}MS4A4A^{+}$ (16p) monocytes (**Figure 7.22**).

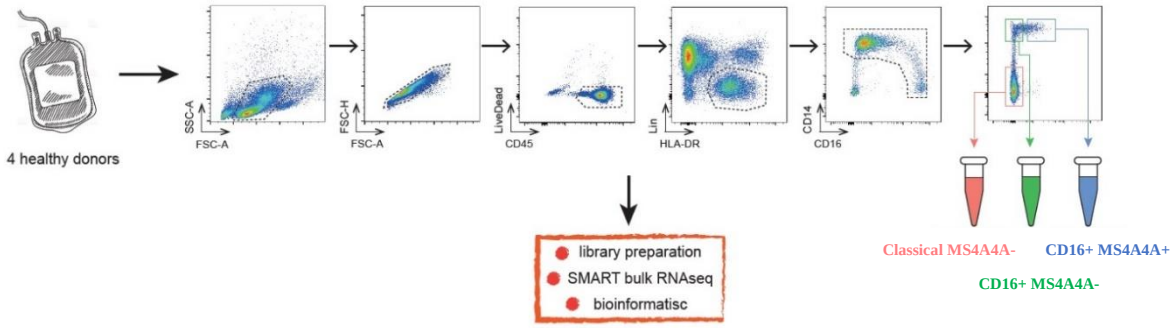

Figure 7.22. Illustration of the experimental workflow and gaiting strategy adopted for the bulk RNA sequencing. Blood samples were collected from 4 healthy donors and PBMCs were isolated by Lympholyte density gradient. Live monocytes were FACS-sorted, cells were lysed and the RNA extracted for SMART seq data.

The gene expression Principal Component Analysis (PCA) pointed out the degree of association between monocyte populations, showing that $CD16^{+}MS4A4A^{+}$ and $CD16^{+}MS4A4A^{-}$ cells were most closely related, whereas the classical $MS4A4A^{-}$ and $CD16^{+}MS4A4A^{+}$ were most distantly clustered (**Figure 7.23**). To address cell heterogeneity among populations expressing different levels of MS4A4A in an unsupervised and unbiased manner, we calculated the differentially expressed genes in the dataset. 1,316 genes were found significantly differentially expressed in $CD16^{+}MS4A4A^{+}$ versus classical $MS4A4A^{-}$, 611 DEGs between $CD16^{+}MS4A4A^{-}$ versus classical $MS4A4A^{-}$. Only 31 DEGs were detected between $CD16^{+}MS4A4A^{-}$ and $CD16^{+}MS4A4A^{+}$, and surprisingly, among them, we found some genes typical of natural killer cells, such as granzyme B and granulysin (**Figure 7.23B**), leading us to consider the presence of a small proportion of contaminating $CD16^{+}CD56^{-}$ NK cells within the non-classical MS4A4A-negative monocytes. These results indicate that the two major monocyte populations distinguished by the traditional marker CD16 are clearly transcriptionally distinct, confirming the consolidated data reported in literature and in our single-cell analysis. On the other hand, the very high transcriptional diversity between MS4A4A positive cells and classical monocytes strongly suggested that MS4A4A could identify a subset of $CD16^{+}$ non-classical monocytes possessing a more mature phenotype

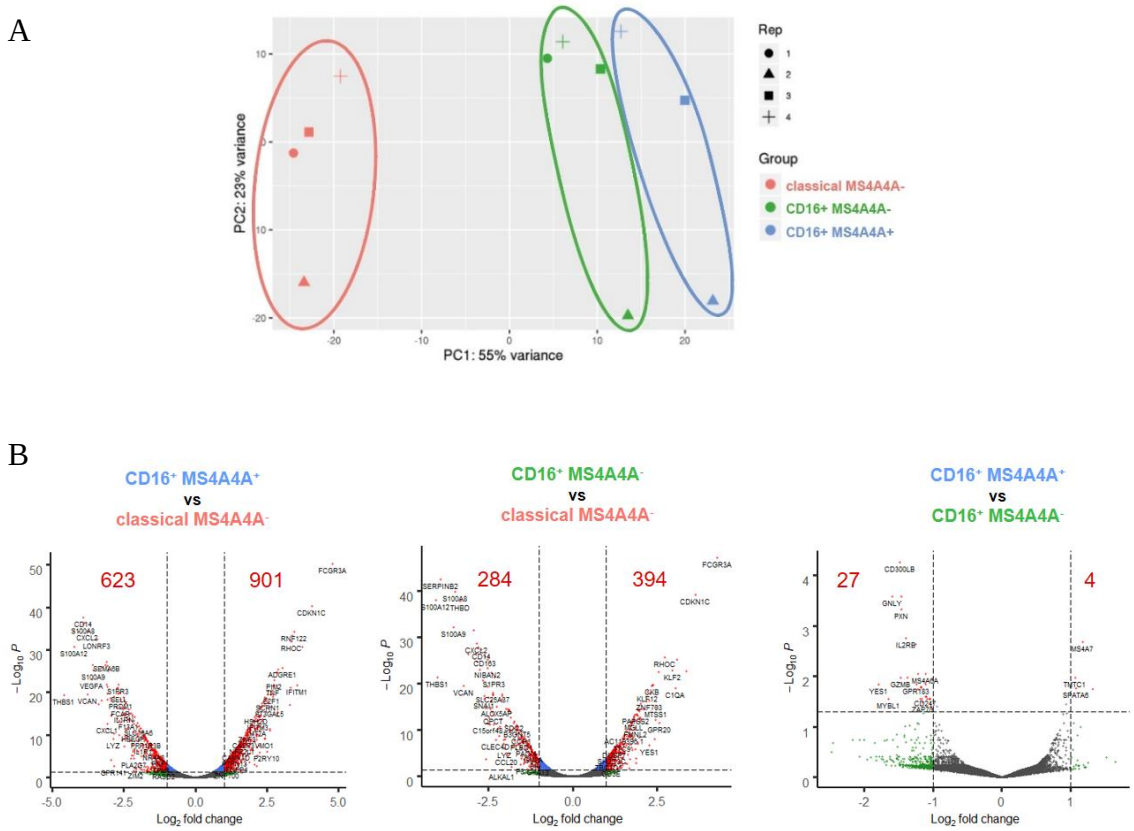

Figure 7.23. CD16$^+$MS4A4A$^-$ and CD16$^+$MS4A4A$^+$ monocytes are closely related. (A) Principle Component Analysis (PCA) visualized with t-SNE projection of bulk RNA-seq data. Shapes represent expression profiles of the different donors. The different monocyte subsets are circled and are represented by different colours as in legend. (B) Volcano plot of the expression profile of the classical MS4A4A-, CD16+MS4A4A- and CD16+MS4A4A+ monocyte populations sorted from 5 healthy donors. Horizontal dashed lines show –Log10 adjusted P value 1.3 (corresponding to FDR 0.05); vertical dashed lines show |log2 fold change| = 1).

compared to MS4A4A negative CD16$^+$ cells. This hypothesis was supported by the higher expression of genes like *CD14*, *CCR1*, *CCL3* and *HLA-DQA1* in CD16$^+$MS4A4A$^-$ monocytes, and the upregulation in CD16$^+$MS4A4A$^+$ cells of genes whose transcription level was reported to be increased in the non-classical monocytes, such as *SOD1*, *TMTC1* and the creatine kinase B (*CKB*) [237] (**Figure 7.24**). Notably, among the differentially expressed genes between MS4A4A-positive and MS4A4A-negative populations, we found the tetraspanin-like molecules *MS4A7* and *MS4A6A* (**Figure 7.24**), corroborating our previous findings and reinforcing our proposal of nominating these molecules as markers of monocyte lineage differentiation.

To better characterize our monocyte populations, we created a list of differentially expressed genes for at least one of the possible comparisons between 2 groups (**Figure 7.25A-B**). When genes were clustered, MS4A4A positive monocytes were definitely confirmed the most mature subset of $CD16^+$ cells, expressing genes typical of classical monocytes at the lower levels, and

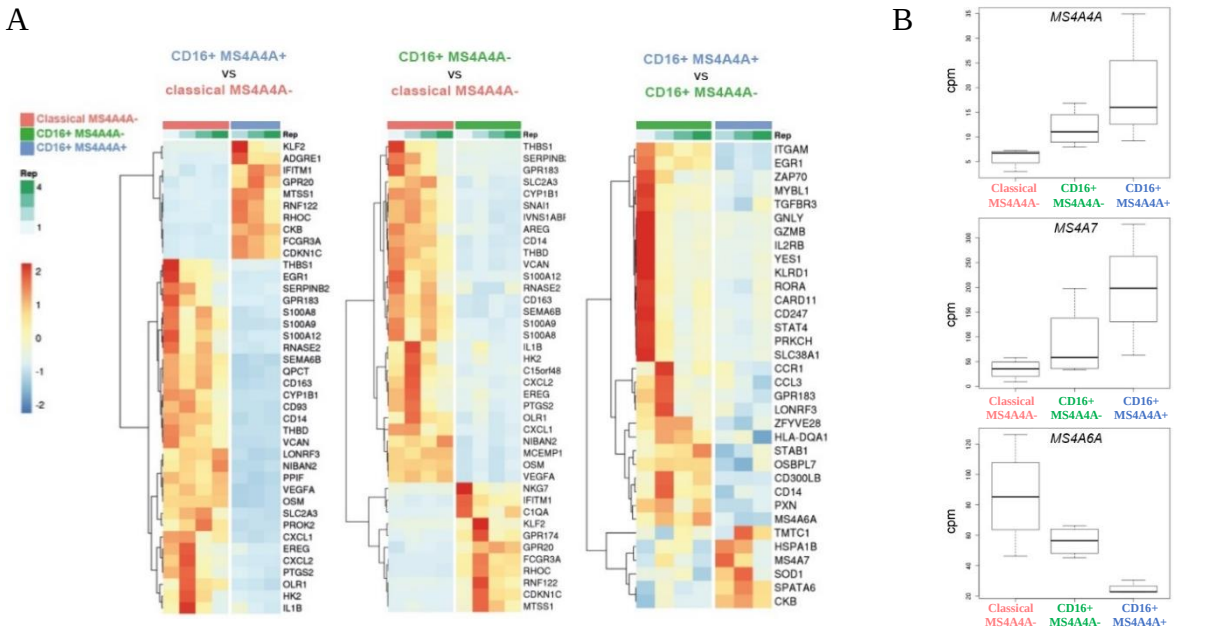

Figure 7.24. Gene expression profile from human circulating monocytes shows MS4A4A as marker of non-classical monocytes. (A) Heatmap representing the top differentially expressed genes (FDR < 0.05; \|log2 fold change\| > 1) in classical versus $CD16^+MS4A^{neg}$, classical versus $CD16^+MS4A4A^{pos}$ and $CD16^+MS4A4A^{neg}$ versus $CD16^+MS4A4A^{pos}$ monocytes comparisons. Gene expression is coloured coded from blue (lower) to red (higher); each column represent one healthy donor as indicated in the legend (rep=biological replicate); gene expression level is scaled by row. (B) Boxplot showing the gene expression of MS4A4A, MS4A6A and MS4A7 genes within the three monocyte populations of the bulk RNA-seq. Gene expression measured as Count Per Million (CPM) mapped reads.

genes characteristic of non-classical monocytes at the higher levels (**Figure 7.25C**).

In particular, genes involved in the response to bacteria, inflammation, angiogenesis, chemotaxis and coagulation were up-regulated in classical monocytes compared with $MS4A4A^+$ non-classical ones. Conversely, genes implicated in the response to viruses and stress, cell adhesion, cell cycle and FcR-mediated phagocytosis were most highly expressed by cells expressing MS4A4A (**Figure 7.25C**). Instead, $CD16^+MS4A4A^-$ monocytes represented a subset of cells with intermediate phenotype. Finally, the very small cluster of up-regulated genes related to natural killer cells observed within this population (**Figure 7.25C**), confirmed the presence of some contaminating CD16 positive NK cells. In further experiments, the inclusion of additional markers such as CD57 [238].

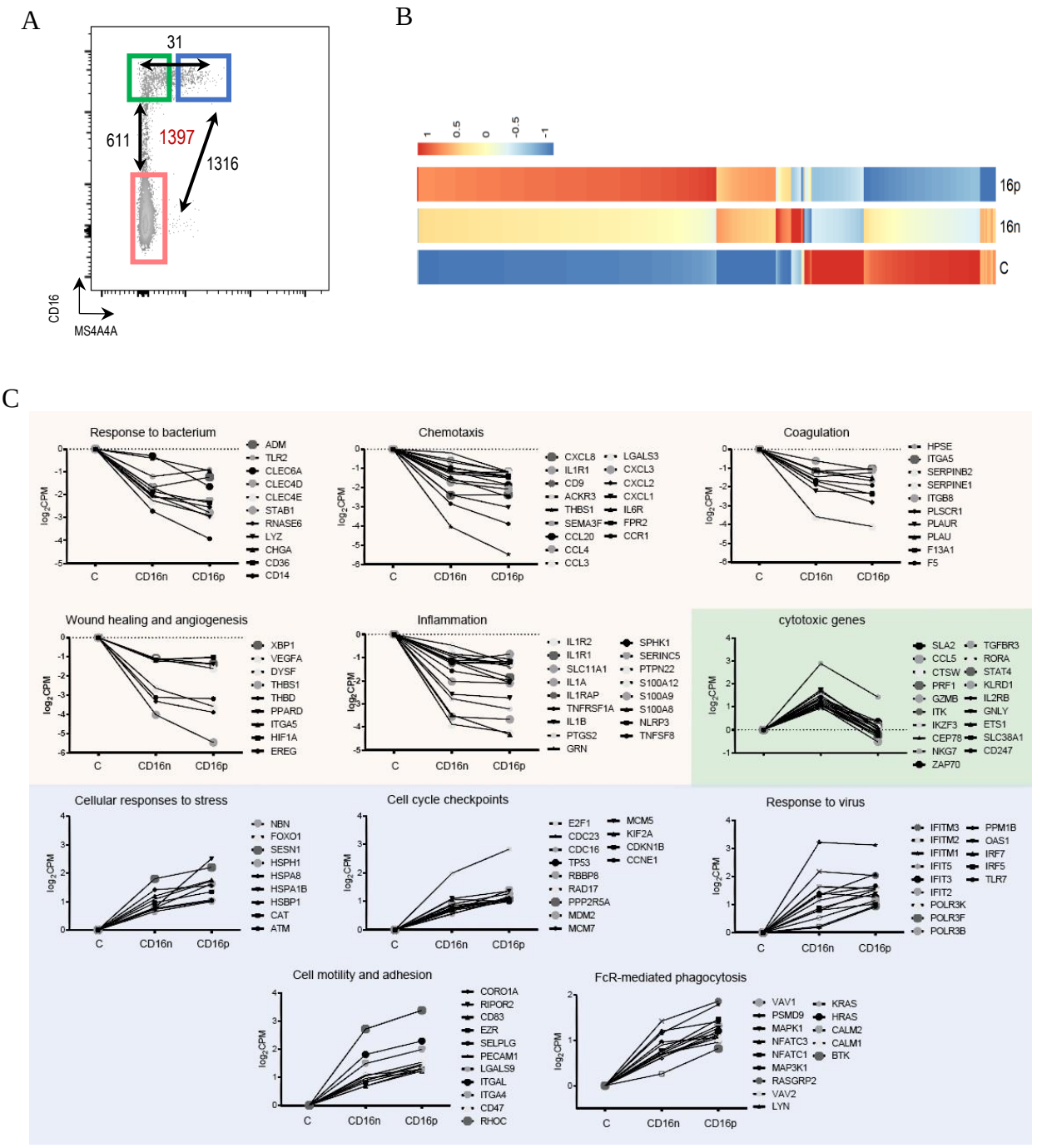

Figure 7.25. Clustering of differentially expressed genes and their expression in each monocyte subset. (A) Transcriptomic analysis of CD16-MS4A4A- [C], CD16+MS4A4A- [16n] and CD16+MS4A4A+ [16p] monocytes revealed 1,397 differentially expressed genes (FDR < 0.05; |log2 fold change| > 1) for at least one of the possible comparisons between 2 subsets. Number of genes found in each comparison (represented by black arrows) is shown. (B) Heatmap showing the clustering of the DEGs found as in [A]. Gene expression is coloured coded from blue (lower) to red (higher); gene expression level is scaled by column. (C) Representative genes enriched in CD16-MS4A4A- (C, pink square), CD16+MS4A4A- (CD16n, green square) and CD16+MS4A4A+ (CD16p, blue square) monocytes grouped according to their functional category. Gene expression measured as Counts Per Million (CPM) mapped reads and shown as the log2CPM value normalized to the classical subset.

We then performed the Ingenuity Pathway Analysis (IPA). Interestingly, among the pathways upregulated in MS4A4A positive monocytes compared to classical cells (but not found when comparing the $CD16^{+}MS4A4A^{-}$ and classical subtypes), we identified the Fc Epsilon Receptor 1 signalling pathway (**Figure 7.26**).

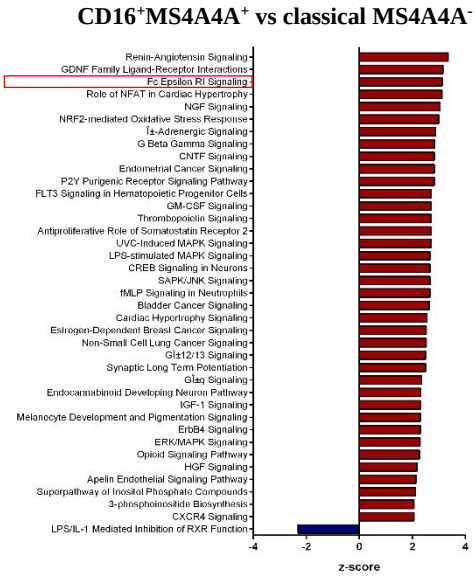

Figure 7.26. Bar graph showing pathways enriched in $CD16^{+}MS4A4A^{+}$ or classical $MS4A4A^{-}$ monocyte populations resulted from IPA analysis. Pathways positive regulated with a with a z-score ≥ 2 (red) and pathways negative regulated with a z-score ≤ –2 (blue) are shown.

This finding was surprising, given that, to our knowledge, expression of the FcεR and activation of its pathway have never been reported specifically in non-classical monocytes.

We thus decided to better examine this aspect. To this aim, we first selected all the molecular signatures related to FcεR and FcγR signalling pathways listed in the Molecular Signature Database (MSigDB) and found 5 signatures related to the FcεR and 8 signatures related to the FcγR (**Figure 7.27A**). Because of the overlap between the two receptor signalling transductions [239], we compared all the signatures and identified the genes listed exclusively in one of the two pathways or present in to both of them. When visualized as heatmaps in the three groups of monocytes sorted for the bulk RNA sequencing, a general enhancement was found in MS4A4A positive monocytes (**Figure 7.27B**). Finally, ssGSEA applied to the non-classical monocyte subpopulations confirmed a significantly enrichment of both the Fcγ and the Fcε receptors signalling pathways in $MS4A4A^{+}$ cells (**Figure 7.27C**).

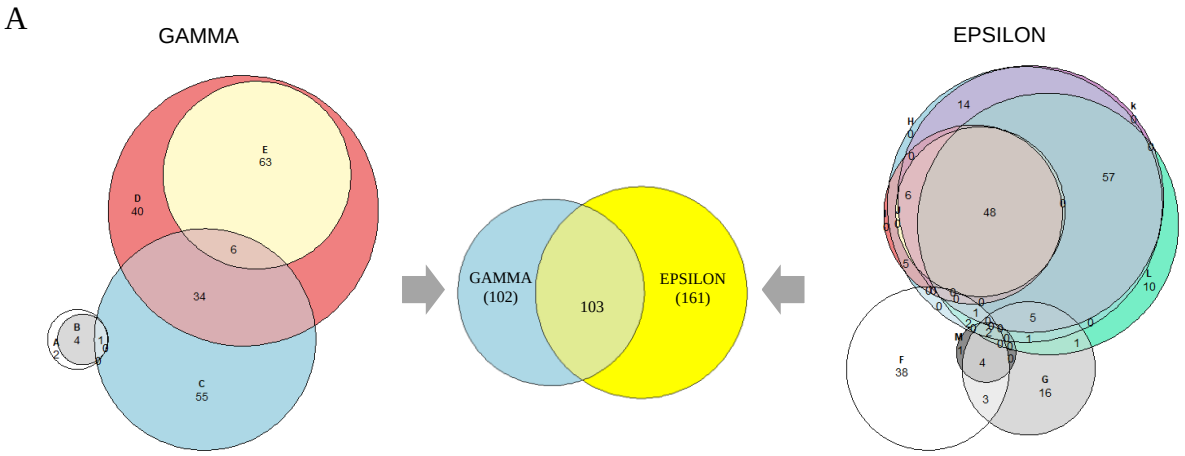

A. GO_REGULATION_OF_FC_GAMMA_RECEPTOR_SIGNALING_PATHWAY_INVOLVED_IN_PHAGOCYTOSIS (7)
B. GO_POSITIVE_REGULATION_OF_FC_GAMMA_RECEPTOR_SIGNALING_PATHWAY_INVOLVED_IN_PHAGOCYTOSIS (5)
C. KEGG_FC_GAMMA_R_MEDIATED_PHAGOCYTOSIS (96)
D. REACTOME_FCGAMMA_RECEPTOR_FCGR_DEPENDENT_PHAGOCYTOSIS (143)
E. REACTOME_FCGR_ACTIVATION (69)
F. KEGG_FC_EPSILON_RI_SIGNALING_PATHWAY (79)
G. PID_FCER1_PATHWAY (60)
H. REACTOME_FC_EPSILON_RECEPTOR_FCERI_SIGNALING (186)
I. REACTOME_FCERI_MEDIATED_CAPLUS2_MOBILIZATION (863)
J. REACTOME_FCERI_MEDIATED_MAPK_ACTIVATION (87)
K. REACTOME_FCERI_MEDIATED_NF_KB_ACTIVATION (136)
L. GO_FC_EPSILON_RECEPTOR_SIGNALING_PATHWAY (168)
M. BIOCARTA_FCER1_ PATHWAY (39)

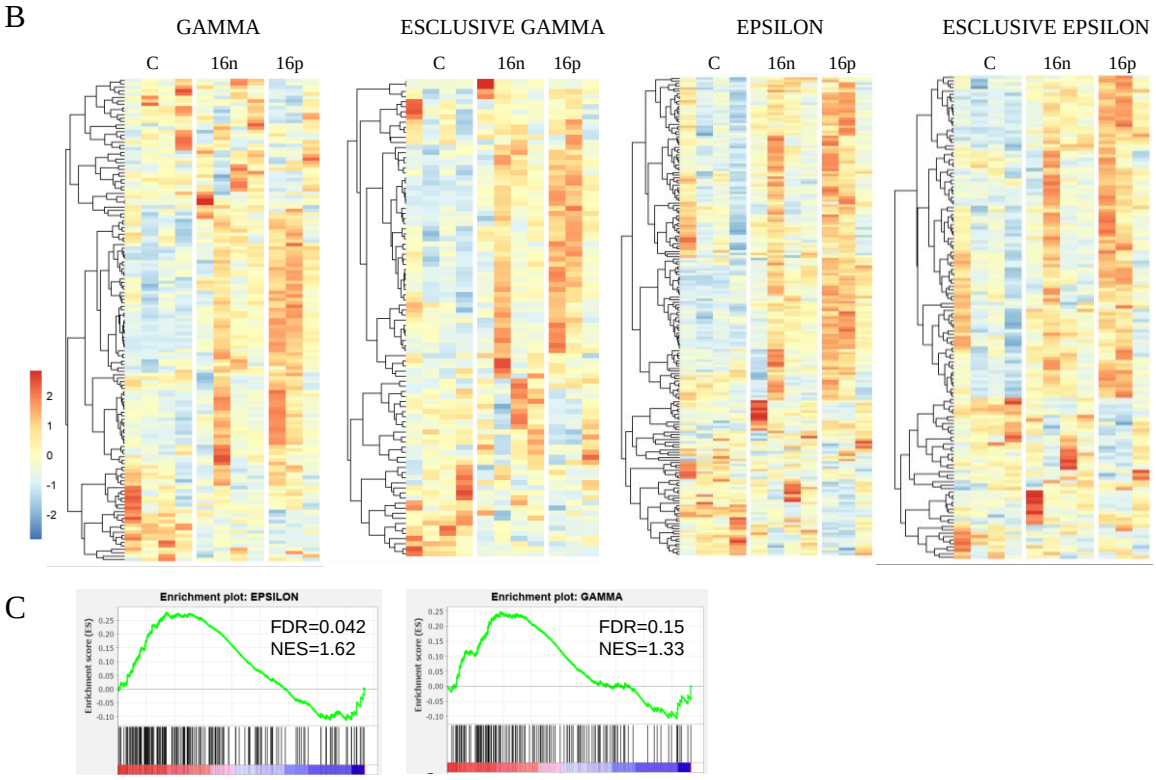

Figure 7.27. Gene and pathway analysis related to FCγR and FCεR signalling in human MS4A4A positive monocytes. (A) Venn-diagrams of genes belonging to the FCγR (left) and FCεR (right) related molecular signatures of the Molecular Signature Database. (B) Heatmaps representing genes related to FCγR and FCεR signalling selected as in [A] in the human monocyte subtypes of bulk RNA-seq: CD16-MS4A4A- [C], CD16+MS4A4A- [16n] and CD16+MS4A4A+ [16p] monocytes. Each column represents one healthy donor; gene expression is coloured coded from blue (lower) to red (higher); gene expression level is scaled by row.

(C) GSEA results showing FcγR and FCεR signalling pathways as significantly enriched biological processes in CD16+MS4A4A+ compared to CD16+MS4A4A- human monocyte populations. The green curve represents the enrichment score, showing the measure to which the genes are overrepresented at the top or bottom of a ranked list of genes. Vertical black bars indicate the position in the ranked list of each gene, belonging to the gene set. Genes positioned in the red and blue sides are up-regulated and down-regulated, respectively, in MS4A4A-positive monocytes compared with MS4A4A-negative ones. FDR and normalized enrichment score (NES) are shown.

Further analyses are still ongoing to clarify FcRs expression in distinct monocyte subsets and to assess the functional role of MS4A proteins in FcRs signalling in human monocytes. Preliminary data at the protein level showed different expression of CD64, CD32, CD89 and CD23 along the monocyte subtypes (***Figure 7.28***).

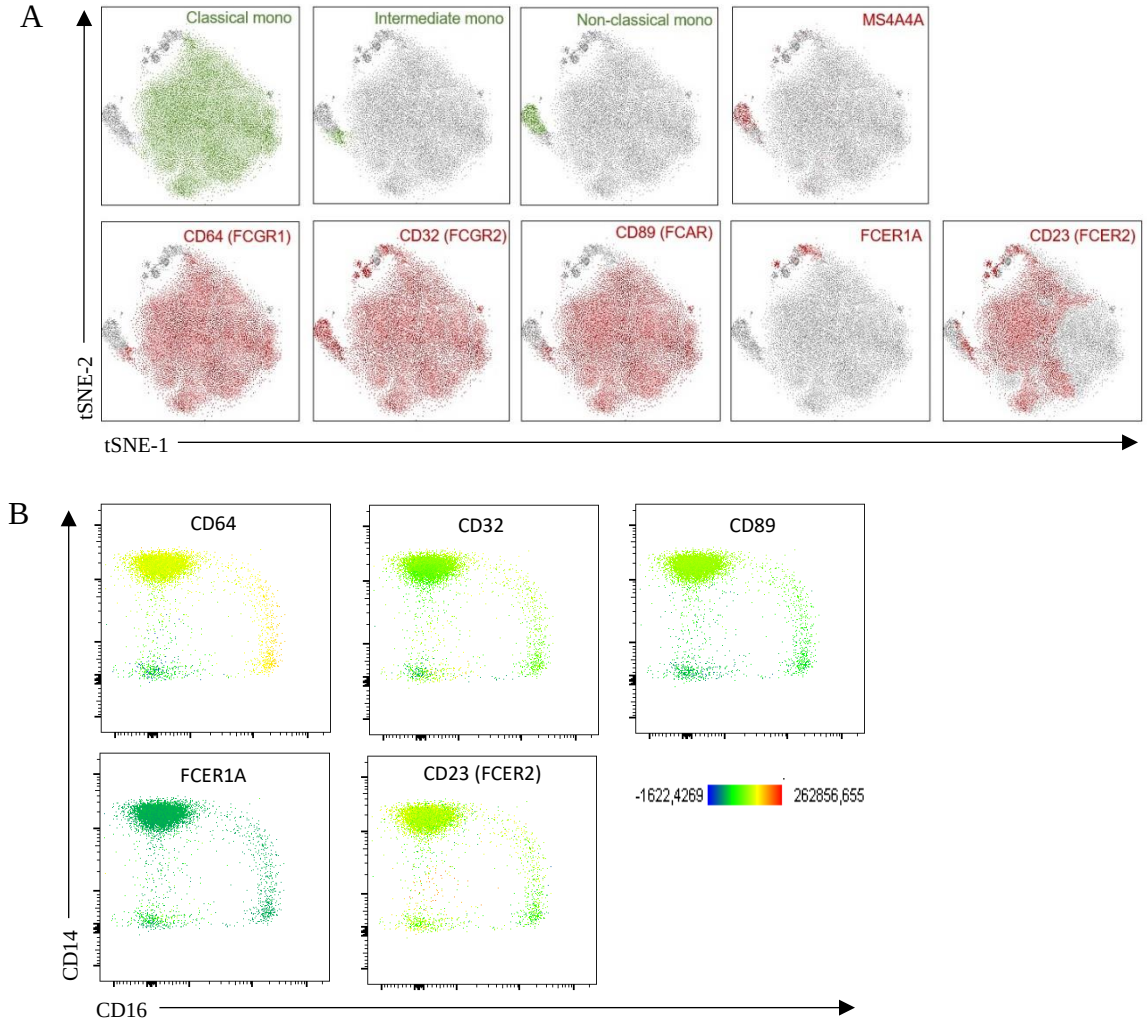

Figure 7.28. Flow cytometry analysis of FcRs expression in human monocytes from healthy donor (N=1). (A) t-SNE graphs showing the spatial distribution of MS4A4A and FcRs in CD45+Lin-HLA-DR+ cells. (B) Expression of FcRs is visualized on CD45+Lin-HLA-DR+. Mean fluorescence intensity is coloured coded, from blue (lower) to red (higher).

7.6 A preliminary translation to pathology setting: i.e. relevance of monocyte diversity in pathology

It is well established that in pathological conditions, including tumours, monocytes are recruited into tissues where they reinforce and acquire new effector functions as well as regulatory properties, but an exact task-division among the different subsets has not been defined yet. This is a critical open question for tumour biology, as Fc receptors expressed by monocytes/macrophages are exploited in cancer immunotherapy to design therapeutic antibodies eliciting antibody-dependent cellular phagocytosis (ADCP) and antibody-dependent cellular cytotoxicity (ADCC) of cancer cells [141, 240]. Moreover, recent work has suggested that the frequency of different peripheral blood immune populations can offer a non-invasive indicator of immunotherapy responsiveness [241].

To investigate phenotype changes and dynamics of the circulating monocyte subpopulations previously characterized in homeostatic conditions, in response to targeted antibody-mediated therapies, we inspected a published scRNA-seq dataset from Griffiths et al. [222]. This study showed how the immune cell phenotypes in peripheral blood reflect into a tumour-immune activity in the early phases of cancer therapy. Specifically, it comprises data from PBMCs collected from 13 advanced (stage 3/4) gastrointestinal (GI) cancer patients (phase I clinical trial, NCT02268825) at 3 time points of treatment: before treatment (C1), after two cycles of only modified FOLFOX6 (mFOLFOX6) chemotherapy (C3), and after two cycles of treatment with both mFOLFOX6 chemotherapy and anti-PD-1 immunotherapy (**Figure 7.29A**). What we aimed at was to superimpose the transcriptional signature of monocytes on the published dataset, localize "our" monocytes and test their response to anticancer strategies.

To enable a more precise comparison between our data of peripheral blood monocytes from healthy donors and the data from GI cancer patients (hereinafter referred as "GP dataset"), we re-analysed all the dataset following the same strategy we used in our scRNA-seq (hereinafter referred as "HD dataset"). After quality control and filtering, we obtained 55,293 cells. Unsupervised clustering identified 25 distinct cell populations (**Figure 7.29B**). In the first instance, SingleR was used to computationally annotate clusters. We thus identified 3 clusters of B cells (c8, c9, c22), 3 clusters of $CD4^+$ T cells (c2, c6, c20), 5 clusters of $CD8^+$ T cells (c3, c5, c1, c17, c23), 4 clusters of NK cells (c1, c12, c16, c21) and 10 clusters of monocytes (c0, c4, c7, c10, c11, c14, c15, c18, c19, c24) (**Figure 7.29B**). This allowed us to reject lymphocytes and NK cells in the first election round, and thus to focus our attention on the 21,209 cells computationally predicted as monocytes. We next sought to manual revise the identity of this

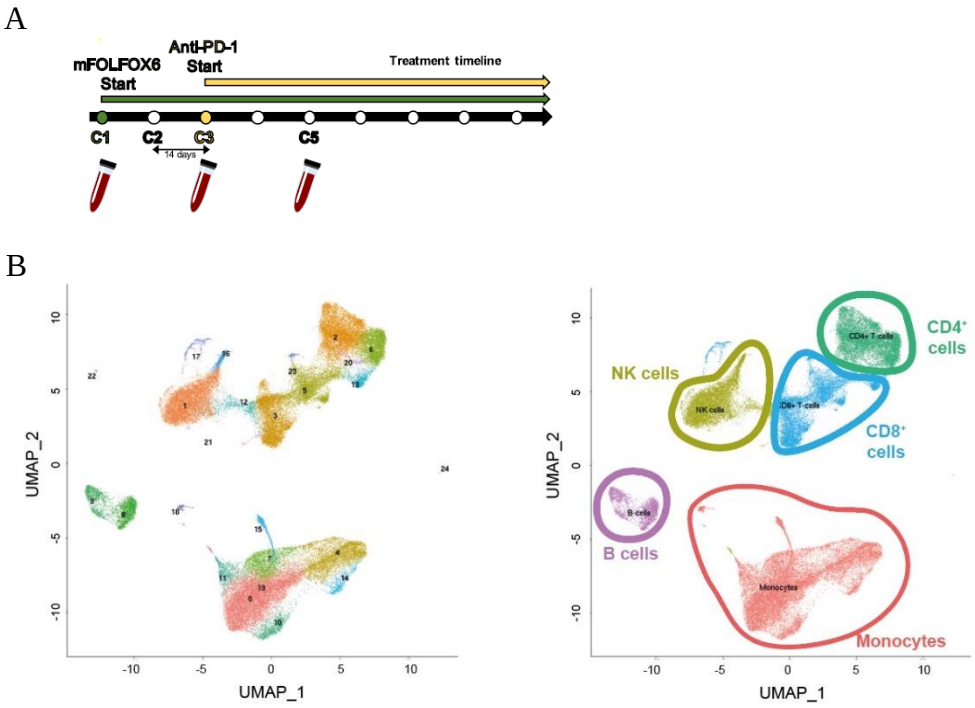

Figure 7.29. Single-cell RNA sequencing of PBMCs from 13 advance gastrointestinal cancer patients at 3 time points of the treatment identified 5 distinct cell lineages. (A) Schematic illustration of the clinical trial treatment strategy adopted in the study of Griffiths and colleagues (Mod. from Griffiths et al., PNAS, 2020). Advanced GI patients received mFOLFOX6 chemotherapy at the beginning of the trial for 2 cycles (14 days per cycles). From cycle 3 through 12, they received the combination of mFOLFOX6 and anti-PD-1 immunotherapy. Blood samples were collected at C1 (cycle 1, baseline), C3 (cycle 3) and C5 (cycle 5). PBMCs were isolated and frozen. Single cell RNA sequencing was performed on the cryopreserved PBMCs samples using 10X Genomics technology and sequenced on an Illumina HiSEq. (B) UMAP projection of GI pts PBMCs (n = 55,293) showing 25 clusters (left) belonging to 5 major immune cell subsets (right). Clusters are numbered according to their size, from the largest (cluster 0) to the smallest (cluster 24). Each dot represents an individual cell.

computationally predicted population, in order to check the probable presence of cell contaminants, such as dendritic cells. To this aim, lineage gene signatures previously used in the HD dataset were adopted. Out of the whole computationally cells predicted as monocytes, 5 clusters showed a phenotype typical of classical monocytes (c0, c7, c10, c11, c19) and 2 clusters were recognized as non-classicals (c4, c14). This approach did not allow us to identify a distinct cluster of intermediate monocytes, probably because the cluster resolution value we chose during this step, aimed at distinguish monocytes from other cell types, was too high. Two clusters were recognized as cDC1 and cDC2 (c24 and c15, respectively) and finally cluster 19 was composed by cells with an intermediate phenotype of preDC and pDC (**Figure 7.30**). This second step of "manual" annotation led us to specifically select monocytes, our immune cell

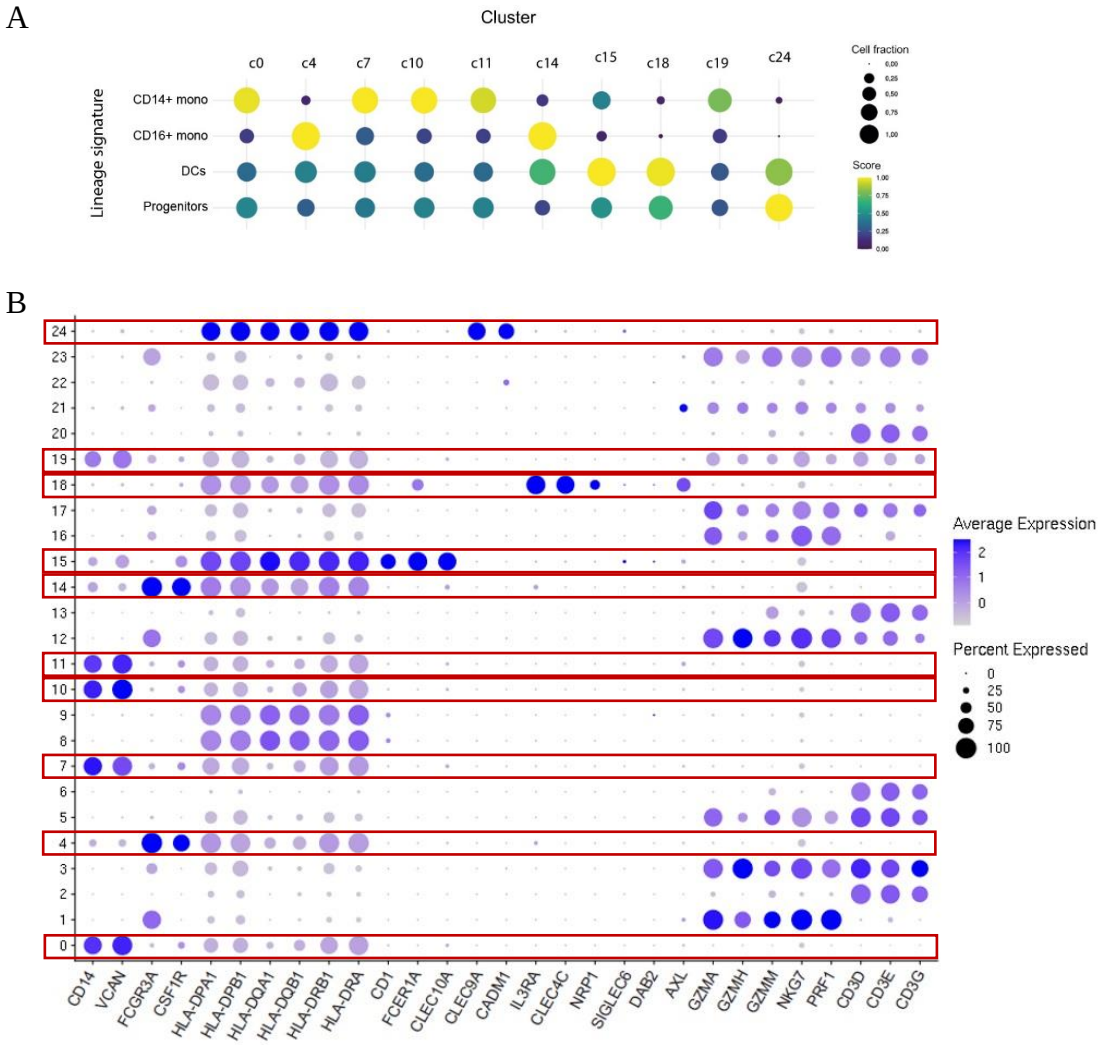

Figure 7.30. Reviewed cell cluster annotation of the computationally predicted monocyte population of the GP dataset. Dot-plots showing the expression of (A) lineage signatures (genes belonging to each signature are listed in Material and Methods) and (B) key genes adopted for manual cell cluster annotation. Gene expression is coloured coded from grey (lower) to blue (higher); circle size indicates the fraction of cells expressing the gene. CD14$^+$ mono indicates classical CD14$^+$ monocytes; CD16$^+$ mono, non-classical CD16$^+$ monocytes; DCs, dendritic cells. Clusters belonging to the computationally predicted monocyte population are highlighted (red squares).

population of interest. Finally, we had to classify cells based on monocyte subtypes we of our HD dataset, therefore, a third and final step of clustering was performed, taking in consideration only cells selected as described above. This operation was carried out by the definition of a machine learning model with high accuracy, sensitivity and specificity (see Material and Methods section). We were thus able to recognize all the circulating monocyte subtypes identified in healthy donors in the blood of cancer patients (**Figure 7.31**), indicating that these subpopulations are generally conserved in steady-state and in disease, at least in gastrointestinal

cancer patients. Yet, we observed an overlap between classical monocytes from cluster 0 and cluster 2, making a clear division between them a difficult task. It is indeed not surprising, given the already established close similarity of these two pro-inflammatory cell subtypes in homeostatic conditions.

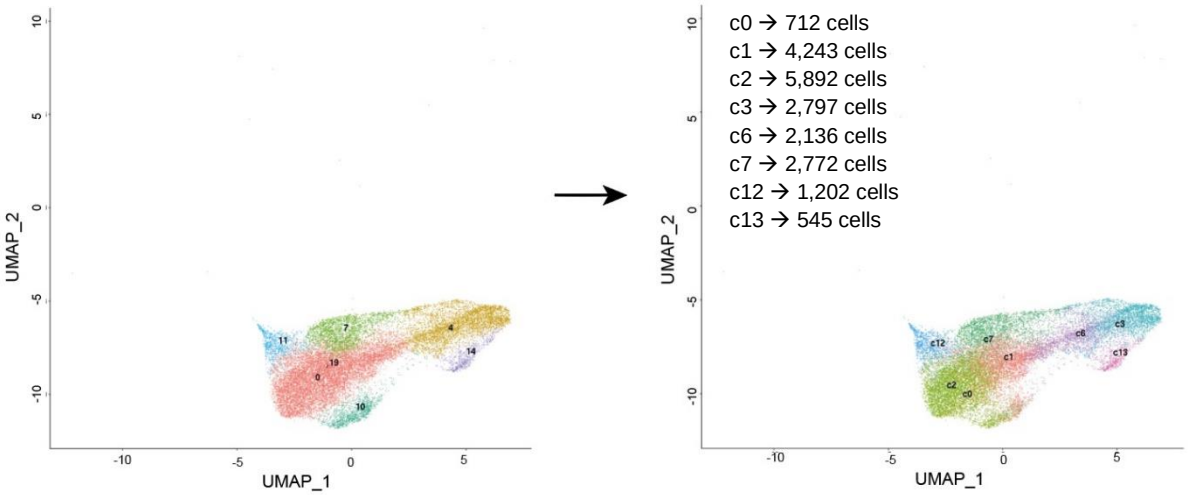

Figure 7.31. Recognition of monocyte subpopulations previously characterized in the blood of healthy donors in the circulation of advanced GI cancer patients. (A) UMAP projections of unsupervised clustering on GI pts PBMCs. Clusters are numbered according to their size, from the largest (cluster 0) to the smallest (cluster 24). Only cells manually annotated as monocytes are shown (n = 20,292). Each dot represents an individual cell. (B) UMAP projection of the same monocyte population as in [A] clustered using a machine learning model developed to identify the subtypes of monocytes previously characterized in homeostatic conditions. Clusters are numbered according to the matched cluster of the HD dataset.

To investigate if patient responsiveness to chemotherapy or immunotherapy was associated with variations in the numerousness of selected immune cell subtypes, we analysed the frequency of monocyte populations in the GP dataset within the three different time points, comparing responders and non-responders. Overall, the cell frequency was not greatly altered during chemotherapy treatment, both in responders and in non-responders (Figure 7.32).

Conversely, after two cycles of anti-PD-1 treatment, there was an increase in the number of classical monocytes characterized by the expression of high levels of IFN-related genes (cluster 7) (**Figure 7.32**). Interestingly, such cellular expansion was specific to responders (Figure 7.32). These preliminary results provide motivation for deepen the role of monocyte subpopulations in patient response to immunotherapy. Further investigations are ongoing and will require an intense effort in retrieving samples from patients undergoing immunotherapy.

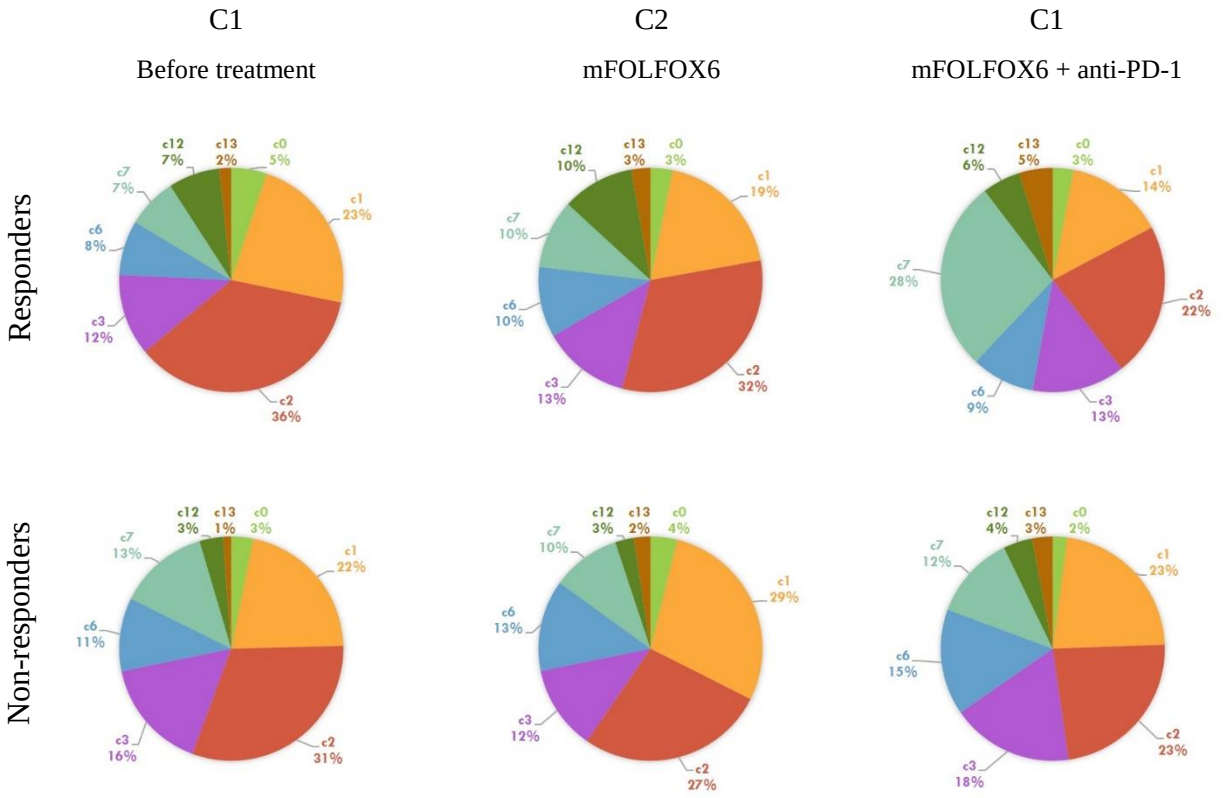

Figure 7.32. Monocyte from cluster 7 are enriched in GI patients after immunotherapy. Pie-chart showing the frequency of monocyte subpopulations in advance gastrointestinal cancer patients. Cell frequency was examined in responders (upper panel) and non-responders (lower panel) patients at three time points: before treatment, after two cycles of chemotherapy and after two cycles of chemotherapy combined with immunotherapy.

8 DISCUSSION

This thesis summarizes the key findings and results of my PhD project. The rationale of this study stems on the strong interest of our laboratory in understanding the monocyte/macrophage biology and on the emerging diversity of these cells, for which a clear evidence of functional role has not been unequivocally defined. In particular, in this work we focused our attention on the biology of monocytes.

In the setting of immune responses, monocytes represent versatile cells capable to rapidly react to environmental signals and stimuli. They are fundamental orchestrators of acute and chronic inflammation and take part in the pathogenesis and progression of several diseases, including cardiovascular, respiratory, autoimmune and disorders, as well as cancer [103]. Until now, the involvement of monocytes in pathological states has been mainly related to their role as source of functional tissue resident macrophages and monocyte-derived dendritic cells. And the same can be said for physiological conditions. However, growing evidence has shed light on the unique property of monocytes to act as both effector and precursor cells, and have led to a paradigm shift of our understanding on the biology of these cells, both in homeostasis and disease. Moreover, recent works adopting single-cell technologies have started to dissect the complexity of such myeloid plasticity and brought to light the variety of mononuclear phagocytes in several conditions [32, 153, 222]. Nevertheless, despite this new wide-ranging body of literature showing the great heterogeneity of monocytes, the most credited classification of circulating monocytic cells remain the one proposed in 2010 based on the CD14 and CD16 markers [12]. Even though this monocyte division into classical ($CD14^{++}CD16^{-}$), intermediate ($CD14^{++}CD16^{+}$) and non-classical ($CD14^{low}CD16^{high}$) monocytes depicts the general task [66], current monocyte classification emerges as inappropriate, inasmuch it might mask a possible inter-cellular heterogeneity in terms of phenotype and function. To overcome the remarkable lack of consensus on monocyte subset identity and interrelationship, in this work I took advantage of single cell RNA sequencing technology to investigate the heterogeneity of human circulating monocytes and their complexity in steady state. We thus performed scRNA-seq on $CD45^{+}$, HLA-DR^{+}, lin^{-} (Lin: CD3, CD19 and CD56 cells) PBMCs from healthy donors. We have thought a lot about the possibility to restrict the gating strategy and sort only monocytes, but we preferred to keep some contaminant cells (e.g. DCs or NK cells), rather than losing some rare monocyte populations. Our clustering approach allowed the identification of 20 clusters, spanning, not

surprisingly, monocytes, dendritic cells, natural killer cells, $CD34^+$ precursors and B cells. Eight clusters were annotated as monocytes. Differential expression of *CD14* and *FCGR3A* (CD16) were capable to distinguish the classical from intermediate and non-classical monocytes. In particular, classicals were composed of 5 distinct populations, of which three (c0, c1, c2) were the most frequent and close related. In general, the three major clusters of classical monocytes displayed distinct inflammatory programs and activation states but, even their general similarity, we found transcriptomic differences that possibly explain why these subsets do not cluster all together. Interestingly though, c0 and c2 had a transcriptional profile similar to the one of neutrophil-like monocytes, i.e. a population of monocytes expressing common neutrophilic markers. The biology of these cells has been assessed in few studies and they were reported to arise from GMP progenitors (which also produce neutrophils) and to express several granule enzymes, suggesting that they could be specialized in direct pathogen killing [43]. Also, given that their production is boosted by selective stimuli (e.g. LSP but not CpG), it has been inferred that NeuMo could play a role during specific inflammatory settings taking part to the emergency monopoiesis process [43]. Moreover, NeuMo expressing markers of classical monocytes were recently found as tumour infiltrating myeloid cell type in non-small cell lung cancer patients [225]. Interestingly, this population was distinct from the only other cluster of classical monocytes found in the study. Overall, our data is in line with previous finding and offers new indications about human NeuMo. Indeed, to the best of our knowledge, this is the first time that two distinct populations of NeuMo were reported in humans. Given the increased expression of genes associated to cellular motility in c2 compared to c0, and considering that these are circulating monocytes in a healthy environment, it is possible to hypothesize that these two clusters differentially interact with the endothelium, suggesting a sort of sub-specialization, or that they could be monocytes captured at two different time points of their life. This second possibility is sustained by the downregulation of different pathways related to immune responses and cellular metabolism observed in c0 and by our finding from trajectories analysis discussed below. The other two classical clusters (c7 and c12) were very interesting and seemed fairly specialized monocytes. Particularly, cluster 7 showed a strong signature enriched in IFN-genes and caught our attention, as a potential population of cells ready to respond to a viral infection. In our future plans, we would like to analyse the fate of this subset in Covid patients. The last classical cluster had a profile enriched in platelet genes, therefore suggesting that these cells could be monocyte-platelet aggregates. We could test whether this population is somewhat affected in patients suffering of venous thrombosis.

Two clusters were annotated as non-classical, and they presented an extremely similar profile, except for a group of genes related to the complement family that was particularly expressed in c13, with a consequent enrichment in complement pathway in this cluster. Involvement of non-classical monocytes in complement-mediated phagocytosis as well as in the pathway of the complement system has been reported [66, 100]. This could represent a population of non-classical monocytes specialized in this important task. Finally, c6, corresponding to $CD14^{+}CD16^{+}$ subset, was found enriched in HLA genes, in line with the robust literature describing intermediate monocytes as cells involved in antigen processing and presentation [18, 66, 242].

The presence of two populations of precursors allowed us to investigate developmental trajectories. Tracing the origin of immune cells is a critical point not easy to disentangle in human studies. Commonly, fate-mapping studies performed in preclinical models are suitable to answer questions related to ontogeny. The prevailing hypothesis is that classical monocytes give rise to the non-classical population. This has been shown in mice [14, 74] and more recently in humans [98]. Notwithstanding, some subsets could arise following another rout of development [243]. We addressed whether the developmental paths of monocyte populations were connected and how, by analysing the transcriptional trajectory and taking advantage of the presence of DCs (whose origin is strictly linked to the one of monocytes) and $CD34^{+}$ cells. Two notable facts emerged from this analysis. The first was the consequential distribution and progression of classical, intermediate and non-classical monocytes along the pseudotime trajectory, confirming the consensus view of a sequential transition from $CD14^{++}CD16^{+}$ and $CD14^{low}CD16^{high}$ monocytes in humans [98]. The second was the separation between c0 and the other clusters of classical monocytes, suggesting that cells in this cluster are evolving towards a new state of maturation. However, we weren't able to discriminate the rout of differentiation of all classical monocytes. In general, such kind of analyses are not easily performed on human settings, as mentioned. Moreover, the small number of $CD34^{+}$ myeloid progenitors found in our dataset and the consequent large gap between them and the mature monocytes may have masked developmental bifurcation points between distinct monocyte subtypes.

Different single cell analyses have been conducted to dissect the heterogeneity of myeloid cells. Nevertheless, until now, circulating monocytes are still not fully characterized. In the study from Villani et al., which has been considered a reference paper in the field, 6 subsets of DCs and 4 subsets of monocytes were identified in human blood under physiological conditions [32]. However, subsequent analyses of the same dataset suggested a misclassification of Villani

et al.'s clusters, probably due to the experimental strategy, where DCs and monocytes were sorted and analysed separately [33, 34, 244]. Other studies, using the approach of high-dimensional flow cytometry, highlighted the great heterogeneity among monocytes [28, 245]. Yet, the limitation of these analyses is that the markers used for the classification and description of the cell subsets are chosen *a priori*. Also Dutertre and colleagues have studied human peripheral mononuclear cells during homeostatic conditions [34]. However, the focus of this study was on DCs, which were extensively characterized. Indeed, even though 13 clusters of monocytes were identified by a High-Dimensional Single-Cell Protein Expression Pipeline (while, by using scRNA-seq, only the canonical 3 clusters of classical, intermediate and non-classical were detected), the authors only partially studied their diversity, but rather used it to clearly define the cDC2s identity. Overall, the results collected from this first part of our study provide a new framework for analysing human monocytes both in health and pathology. Certainly, more accurate functional analyses are needed to better characterize the 8 subsets of monocytes we have identified.

As mentioned, this project arises from the desire to elucidate aspects of monocyte/macrophage biology still controversial in literature. Previous studies from our laboratory have given significant contribution in the characterization of different biological aspects of alternatively activated and tumour-associated macrophages. Our group and others have recently reported on the upregulation of the tetraspanin-like protein MS4A4A in TAMs [214-217], its interaction with the β-glucan receptor Dectin-1 and its role in Dectin-1 signaling and relative NK-cell anti-tumor activities [213]. MS4A4A belong to the Membrane-Spanning 4-domain subfamily A (MS4A) protein family, which represents a new emerging set of proteins (at least 18 members in humans) structurally related to conventional tetraspanins, each with an expression profile restricted to specific cell types [182]. MS4A4A was found to be expressed also in different normal human tissue, such as lung, colon and skin. Of note, its expression was restricted to a subset of tissue resident macrophages $CD163^{pos}$, while lung pDCs, colon DCs and Langerhans's cells did not express MS4A4A [213]. Moreover, studies aiming at clarifying the connection between different polymorphisms from MS4A locus with late-onset Alzheimer's disease risk have shown the expression of MS4A4A restricted to microglia in the brain [208]. It is well established that monocytes represent an important source for tissue macrophages both in health and disease, but the exact task-division among the various monocyte subsets in this process is not fully understood. Recent studies have shown a different contribution of distinct monocyte populations in originating tissue Mφ, depending on the

district and the context [90, 119]. However this aspect remains to be elucidated and could have major clinical implications. Translated to our research interest, the question was whether there was a population of monocytes preferentially originating MS4A4A^{+} macrophages. Given that other MS4A proteins have been reported to be expressed in hematopoietic cells, the investigation was extended to all the MS4A family members. We confirmed *MS4A4A* expression restricted to the monocytic-lineage. Different degrees of *MS4A7* and *MS4A6A* expression were detected in distinct clusters of both monocytes and DCs. Overall, our results lead us to speculate about the possibility to elect expression of *MS4A4A* as marker for the commitment to circulating non-classical monocytes in humans. Of note, MS4A7 has been suggested as ontogeny marker for brain macrophages, since, both in brain macrophage transplantation mouse models and in the brain from cases of Alzheimer's and severe cerebrovascular disease, its expression was selective in HSC-derived Mφ but not in YS-derived Mφ neither in microglia (Bennett, 2018). Moreover, in mice, Ms4a3, another gene of the MS4A family, has been identified as specific marker expressed by GMP progenitors [68]. Collectively, this evidence raises the interesting possibility that *MS4A4A*, *MS4A6A* and *MS4A7* genes, irrespective of their significance, could serve as biomarkers of distinct monocyte and DC subsets recruited in injured tissues during pathological conditions, such as neurodegenerative diseases and cancer. This would have significant applications to our understanding of the immune contexture in pathology and, in a therapeutic perspective, could open to the possibility of the development of new therapies targeting monocytes/macrophages. As mention, MS4A4A has been coupled with the scavenger receptor CD163, the pattern recognition receptor Dectin-1 and arginase-1 [213, 218]. Our evidence of MS4A4A protein expression in a subpopulation of non-classical patrolling monocytes suggest a specific immune functional properties of these cells. Following this hypothesis, we characterized the transcriptome of CD16^{-}MS4A4A^{-}, CD16^{+}MS4A4A^{-} and CD16^{+}MS4A4A^{+} monocyte populations and found MS4A4A positive cells, within the non-classical population, displayed a more mature phenotype. Moreover, we observed a significant enrichment of the FcγR and FcεR pathways in MS4A4A^{pos} subset of CD16^{pos} monocytes, in line with preliminary data showing the interaction of MS4A4A with the FcR signal transduced FcεRIγ chain, indicating a potential role of MS4A4A for FcR signalling (*unpublished data*). A recent study have demonstrated that MS4A4A function in mast cell degranulation through FcεRI, promoting FcεRI-PLCγ1 complex interaction with signaling molecules in lipid rafts and favoring IgE-dependent store-operated Ca2+ entry (SOCE) [221]. It is therefore possible to speculate that MS4A4A could amplify FcRs cell surface expression and augment signals transduced through

Fc receptors also in monocytes, in the similar way as MS4A2 in basophils and mast cells [246]. It will be interesting in the future to deepen our understanding of MS4A4A contribution in FcRs function. We are already planning to clarify the expression and distribution of Fc-receptors on human monocyte subsets, reinforcing our very preliminary flow cytometry data.

Many studies have addressed the question of whether the frequency and phenotype of peripheral blood immune cells is altered in cancer patients compared to healthy donors. This information could lead to the identification of new predictive/prognostic biomarkers. Moreover, concerning monocytes, these studies could unravel specific functional subtypes recruited within tumour lesions and functioning as mediators of critical relevance in the mechanism of action of therapeutic antibodies. Melanoma patients responding to treated with ipilimumab, an anti-CTLA-4 monoclonal antibody, displayed higher percentages and absolute counts of circulating non-classical monocytes compared to healthy donors [244]. Interestingly, *ex vivo* experiments demonstrated the selective capability of CD14 non-classical $CD14^{+}CD16^{++}$ monocytes to mediate ADCC-mediated lysis of regulatory T cells (Treg) [244]. Moreover, a recent study showed that, in patients with stage IV melanoma, the frequency of $CD14^{+}CD16^{-}$HLA-DR^{hi} monocytes before anti-PD-1 immunotherapy is a strong predictor of progression-free and overall survival in response to the therapy [238].

Along this line, we inspected a published scRNA-seq dataset from Griffiths et al. [221] and confirmed the presence of the 8 subtypes of monocytes we previously identified in homeostasis also in advanced gastrointestinal cancer patients. However, classical monocytes from c0 and c2 showed a degree of overlap, possibly suggesting a fully maturation of c0 in patients compared to healthy donors. Furthermore, we observed the expansion of classical monocytes from cluster 7 (the one enriched in IFN-related genes and in pathways related to antiviral responses) after the combination of chemo- and anti-PD-1 immuno-therapy selectively in responders patients. These data are in line with the observation from Griffiths et al. of an up-regulation of IFN stimulation genes in monocytes from responder patients after start of anti-PD-1 therapy. Our analysis suggests that, among all monocytes, c7 could represent the specific subset involved in the response to immunotherapy. More in depth investigations could disclose mechanisms involved in the role of this monocyte population in immunotherapy-dependent anti-tumour functions.

9 BIBLIOGRAPHY

1. van Furth, R., et al., *The mononuclear phagocyte system: a new classification of macrophages, monocytes, and their precursor cells.* Bull World Health Organ, 1972. **46**(6): p. 845-52.
2. Butenko, S., et al., *Transcriptomic Analysis of Monocyte-Derived Non-Phagocytic Macrophages Favors a Role in Limiting Tissue Repair and Fibrosis.* Front Immunol, 2020. **11**: p. 405.
3. Ehrlich and Paul, *Methodologische Beitr€age zur Physiologie und Pathologie der verschiedenen Formen der Leukocyten*. 1880: Z. Klin. Med. p. 553–560.
4. Jung, S., et al., *Analysis of fractalkine receptor CX(3)CR1 function by targeted deletion and green fluorescent protein reporter gene insertion.* Mol Cell Biol, 2000. **20**(11): p. 4106-14.
5. Passlick, B., D. Flieger, and H.W. Ziegler-Heitbrock, *Identification and characterization of a novel monocyte subpopulation in human peripheral blood.* Blood, 1989. **74**(7): p. 2527-34.
6. Geissmann, F., S. Jung, and D.R. Littman, *Blood monocytes consist of two principal subsets with distinct migratory properties.* Immunity, 2003. **19**(1): p. 71-82.
7. Akiyama, Y., et al., *Characterization of a human blood monocyte subset with low peroxidase activity.* J Clin Invest, 1983. **72**(3): p. 1093-105.
8. Cros, J., et al., *Human CD14dim monocytes patrol and sense nucleic acids and viruses via TLR7 and TLR8 receptors.* Immunity, 2010. **33**(3): p. 375-86.
9. Ancuta, P., et al., *Transcriptional profiling reveals developmental relationship and distinct biological functions of CD16+ and CD16- monocyte subsets.* BMC Genomics, 2009. **10**: p. 403.
10. Grage-Griebenow, E., et al., *Identification of a novel dendritic cell-like subset of CD64(+) / CD16(+) blood monocytes.* Eur J Immunol, 2001. **31**(1): p. 48-56.
11. Skrzeczyńska-Moncznik, J., et al., *Peripheral blood CD14high CD16+ monocytes are main producers of IL-10.* Scand J Immunol, 2008. **67**(2): p. 152-9.
12. Ziegler-Heitbrock, L., et al., *Nomenclature of monocytes and dendritic cells in blood.* Blood, 2010. **116**(16): p. e74-80.
13. Mildner, A., et al., *Genomic Characterization of Murine Monocytes Reveals C/EBPβ Transcription Factor Dependence of Ly6C.* Immunity, 2017. **46**(5): p. 849-862.e7.
14. Sunderkötter, C., et al., *Subpopulations of mouse blood monocytes differ in maturation stage and inflammatory response.* J Immunol, 2004. **172**(7): p. 4410-7.
15. Briseño, C.G., et al., *Distinct Transcriptional Programs Control Cross-Priming in Classical and Monocyte-Derived Dendritic Cells.* Cell Rep, 2016. **15**(11): p. 2462-74.
16. Wong, K.L., et al., *The three human monocyte subsets: implications for health and disease.* Immunol Res, 2012. **53**(1-3): p. 41-57.
17. Thomas, G.D., et al., *Human Blood Monocyte Subsets: A New Gating Strategy Defined Using Cell Surface Markers Identified by Mass Cytometry.* Arterioscler Thromb Vasc Biol, 2017. **37**(8): p. 1548-1558.
18. Ong, S.M., et al., *A Novel, Five-Marker Alternative to CD16-CD14 Gating to Identify the Three Human Monocyte Subsets.* Front Immunol, 2019. **10**: p. 1761.
19. Hofer, T.P., et al., *6-Sulfo LacNAc (Slan) as a Marker for Non-classical Monocytes.* Front Immunol, 2019. **10**: p. 2052.
20. Schäkel, K., et al., *6-Sulfo LacNAc, a novel carbohydrate modification of PSGL-1, defines an inflammatory type of human dendritic cells.* Immunity, 2002. **17**(3): p. 289-301.
21. Schäkel, K., et al., *A novel dendritic cell population in human blood: one-step immunomagnetic isolation by a specific mAb (M-DC8) and in vitro priming of cytotoxic T lymphocytes.* Eur J Immunol, 1998. **28**(12): p. 4084-93.
22. Schäkel, K., et al., *M-DC8+ leukocytes--a novel human dendritic cell population.* Pathobiology, 1999. **67**(5-6): p. 287-90.
23. de Baey, A., et al., *Phenotype and function of human dendritic cells derived from M-DC8(+) monocytes.* Eur J Immunol, 2001. **31**(6): p. 1646-55.

24. Siedlar, M., et al., *The M-DC8-positive leukocytes are a subpopulation of the CD14+ CD16+ monocytes.* Immunobiology, 2000. **202**(1): p. 11-7.
25. Hofer, T.P., et al., *slan-defined subsets of CD16-positive monocytes: impact of granulomatous inflammation and M-CSF receptor mutation.* Blood, 2015. **126**(24): p. 2601-10.
26. van Leeuwen-Kerkhoff, N., et al., *Transcriptional profiling reveals functional dichotomy between human slan.* J Leukoc Biol, 2017. **102**(4): p. 1055-1068.
27. Roussel, M., et al., *Mass cytometry deep phenotyping of human mononuclear phagocytes and myeloid-derived suppressor cells from human blood and bone marrow.* J Leukoc Biol, 2017. **102**(2): p. 437-447.
28. Hamers, A.A.J., et al., *Human Monocyte Heterogeneity as Revealed by High-Dimensional Mass Cytometry.* Arterioscler Thromb Vasc Biol, 2019. **39**(1): p. 25-36.
29. Murdoch, C., et al., *Expression of Tie-2 by human monocytes and their responses to angiopoietin-2.* J Immunol, 2007. **178**(11): p. 7405-11.
30. Venneri, M.A., et al., *Identification of proangiogenic TIE2-expressing monocytes (TEMs) in human peripheral blood and cancer.* Blood, 2007. **109**(12): p. 5276-85.
31. De Palma, M., et al., *Tie2 identifies a hematopoietic lineage of proangiogenic monocytes required for tumor vessel formation and a mesenchymal population of pericyte progenitors.* Cancer Cell, 2005. **8**(3): p. 211-26.
32. Villani, A.C., et al., *Single-cell RNA-seq reveals new types of human blood dendritic cells, monocytes, and progenitors.* Science, 2017. **356**(6335).
33. Calzetti, F., et al., *Human dendritic cell subset 4 (DC4) correlates to a subset of CD14$^{dim/2}$ CD16^{++} monocytes*. J Allergy Immunol, 2018: 141:2276-9
34. Dutertre, C.A., et al., *Single-Cell Analysis of Human Mononuclear Phagocytes Reveals Subset-Defining Markers and Identifies Circulating Inflammatory Dendritic Cells.* Immunity, 2019. **51**(3): p. 573-589.e8.
35. Hoeffel, G., et al., *C-Myb(+) erythro-myeloid progenitor-derived fetal monocytes give rise to adult tissue-resident macrophages.* Immunity, 2015. **42**(4): p. 665-78.
36. Hoeffel, G. and F. Ginhoux, *Fetal monocytes and the origins of tissue-resident macrophages.* Cell Immunol, 2018. **330**: p. 5-15.
37. Li, Z., et al., *Adult Connective Tissue-Resident Mast Cells Originate from Late Erythro-Myeloid Progenitors.* Immunity, 2018. **49**(4): p. 640-653.e5.
38. Gomez Perdiguero, E., et al., *Tissue-resident macrophages originate from yolk-sac-derived erythro-myeloid progenitors.* Nature, 2015. **518**(7540): p. 547-51.
39. McGrath, K.E., et al., *Distinct Sources of Hematopoietic Progenitors Emerge before HSCs and Provide Functional Blood Cells in the Mammalian Embryo.* Cell Rep, 2015. **11**(12): p. 1892-904.
40. Hoeffel, G., et al., *Adult Langerhans cells derive predominantly from embryonic fetal liver monocytes with a minor contribution of yolk sac-derived macrophages.* J Exp Med, 2012. **209**(6): p. 1167-81.
41. Khan, J.A., et al., *Fetal liver hematopoietic stem cell niches associate with portal vessels.* Science, 2016. **351**(6269): p. 176-80.
42. Guilliams, M., A. Mildner, and S. Yona, *Developmental and Functional Heterogeneity of Monocytes.* Immunity, 2018. **49**(4): p. 595-613.
43. Yáñez, A., et al., *Granulocyte-Monocyte Progenitors and Monocyte-Dendritic Cell Progenitors Independently Produce Functionally Distinct Monocytes.* Immunity, 2017. **47**(5): p. 890-902.e4.
44. Weinreb, C., et al., *Lineage tracing on transcriptional landscapes links state to fate during differentiation.* Science, 2020. **367**(6479).
45. Ikeda, N., et al., *Emergence of immunoregulatory Ym1.* Sci Immunol, 2018. **3**(28).
46. Rodriguez-Fraticelli, A.E., et al., *Clonal analysis of lineage fate in native haematopoiesis.* Nature, 2018. **553**(7687): p. 212-216.

47. Tusi, B.K., et al., *Population snapshots predict early haematopoietic and erythroid hierarchies.* Nature, 2018. **555**(7694): p. 54-60.
48. Friedman, A.D., *Transcriptional regulation of granulocyte and monocyte development.* Oncogene, 2002. **21**(21): p. 3377-90.
49. Lara-Astiaso, D., et al., *Immunogenetics. Chromatin state dynamics during blood formation.* Science, 2014. **345**(6199): p. 943-9.
50. Walsh, J.C., et al., *Cooperative and antagonistic interplay between PU.1 and GATA-2 in the specification of myeloid cell fates.* Immunity, 2002. **17**(5): p. 665-76.
51. Schönheit, J., et al., *PU.1 level-directed chromatin structure remodeling at the Irf8 gene drives dendritic cell commitment.* Cell Rep, 2013. **3**(5): p. 1617-28.
52. Kurotaki, D., et al., *IRF8 inhibits C/EBPα activity to restrain mononuclear phagocyte progenitors from differentiating into neutrophils.* Nat Commun, 2014. **5**: p. 4978.
53. Dickinson, R.E., et al., *Exome sequencing identifies GATA-2 mutation as the cause of dendritic cell, monocyte, B and NK lymphoid deficiency.* Blood, 2011. **118**(10): p. 2656-8.
54. Collin, M., R. Dickinson, and V. Bigley, *Haematopoietic and immune defects associated with GATA2 mutation.* Br J Haematol, 2015. **169**(2): p. 173-87.
55. Yáñez, A., et al., *IRF8 acts in lineage-committed rather than oligopotent progenitors to control neutrophil vs monocyte production.* Blood, 2015. **125**(9): p. 1452-9.
56. Alder, J.K., et al., *Kruppel-like factor 4 is essential for inflammatory monocyte differentiation in vivo.* J Immunol, 2008. **180**(8): p. 5645-52.
57. Dai, X.M., et al., *Targeted disruption of the mouse colony-stimulating factor 1 receptor gene results in osteopetrosis, mononuclear phagocyte deficiency, increased primitive progenitor cell frequencies, and reproductive defects.* Blood, 2002. **99**(1): p. 111-20.
58. Chong, S.Z., et al., *CXCR4 identifies transitional bone marrow premonocytes that replenish the mature monocyte pool for peripheral responses.* J Exp Med, 2016. **213**(11): p. 2293-2314.
59. Serbina, N.V. and E.G. Pamer, *Monocyte emigration from bone marrow during bacterial infection requires signals mediated by chemokine receptor CCR2.* Nat Immunol, 2006. **7**(3): p. 311-7.
60. Tsou, C.L., et al., *Critical roles for CCR2 and MCP-3 in monocyte mobilization from bone marrow and recruitment to inflammatory sites.* J Clin Invest, 2007. **117**(4): p. 902-9.
61. Jung, H., et al., *Localized CCR2 Activation in the Bone Marrow Niche Mobilizes Monocytes by Desensitizing CXCR4.* PLoS One, 2015. **10**(6): p. e0128387.
62. Shi, C., et al., *Bone marrow mesenchymal stem and progenitor cells induce monocyte emigration in response to circulating toll-like receptor ligands.* Immunity, 2011. **34**(4): p. 590-601.
63. Debien, E., et al., *S1PR5 is pivotal for the homeostasis of patrolling monocytes.* Eur J Immunol, 2013. **43**(6): p. 1667-75.
64. Teh, Y.C., et al., *Capturing the Fantastic Voyage of Monocytes Through Time and Space.* Front Immunol, 2019. **10**: p. 834.
65. Rua, R. and D.B. McGavern, *Elucidation of monocyte/macrophage dynamics and function by intravital imaging.* J Leukoc Biol, 2015. **98**(3): p. 319-32.
66. Wong, K.L., et al., *Gene expression profiling reveals the defining features of the classical, intermediate, and nonclassical human monocyte subsets.* Blood, 2011. **118**(5): p. e16-31.
67. Smedman, C., et al., *FluoroSpot Analysis of TLR-Activated Monocytes Reveals Several Distinct Cytokine-Secreting Subpopulations.* Scand J Immunol, 2012. **75**(2): p. 249-58.
68. Liu, Z., et al., *Fate Mapping via Ms4a3-Expression History Traces Monocyte-Derived Cells.* Cell, 2019. **178**(6): p. 1509-1525.e19.
69. Kotzin, J.J., et al., *The long non-coding RNA Morrbid regulates Bim and short-lived myeloid cell lifespan.* Nature, 2016. **537**(7619): p. 239-243.
70. Weber, C., et al., *Differential chemokine receptor expression and function in human monocyte subpopulations.* J Leukoc Biol, 2000. **67**(5): p. 699-704.

71. Varol, C., A. Mildner, and S. Jung, *Macrophages: development and tissue specialization.* Annu Rev Immunol, 2015. **33**: p. 643-75.
72. Ginhoux, F. and S. Jung, *Monocytes and macrophages: developmental pathways and tissue homeostasis.* Nat Rev Immunol, 2014. **14**(6): p. 392-404.
73. Naito, M., K. Takahashi, and S. Nishikawa, *Development, differentiation, and maturation of macrophages in the fetal mouse liver.* J Leukoc Biol, 1990. **48**(1): p. 27-37.
74. Yona, S., et al., *Fate mapping reveals origins and dynamics of monocytes and tissue macrophages under homeostasis.* Immunity, 2013. **38**(1): p. 79-91.
75. Guilliams, M., et al., *Alveolar macrophages develop from fetal monocytes that differentiate into long-lived cells in the first week of life via GM-CSF.* J Exp Med, 2013. **210**(10): p. 1977-92.
76. Schneider, C., et al., *Induction of the nuclear receptor PPAR-γ by the cytokine GM-CSF is critical for the differentiation of fetal monocytes into alveolar macrophages.* Nat Immunol, 2014. **15**(11): p. 1026-37.
77. Epelman, S., et al., *Embryonic and adult-derived resident cardiac macrophages are maintained through distinct mechanisms at steady state and during inflammation.* Immunity, 2014. **40**(1): p. 91-104.
78. Ginhoux, F., et al., *Fate mapping analysis reveals that adult microglia derive from primitive macrophages.* Science, 2010. **330**(6005): p. 841-5.
79. Bain, C.C., et al., *Resident and pro-inflammatory macrophages in the colon represent alternative context-dependent fates of the same Ly6Chi monocyte precursors.* Mucosal Immunol, 2013. **6**(3): p. 498-510.
80. Bain, C.C., et al., *Constant replenishment from circulating monocytes maintains the macrophage pool in the intestine of adult mice.* Nat Immunol, 2014. **15**(10): p. 929-937.
81. Tamoutounour, S., et al., *Origins and functional specialization of macrophages and of conventional and monocyte-derived dendritic cells in mouse skin.* Immunity, 2013. **39**(5): p. 925-38.
82. Molawi, K., et al., *Progressive replacement of embryo-derived cardiac macrophages with age.* J Exp Med, 2014. **211**(11): p. 2151-8.
83. Calderon, B., et al., *The pancreas anatomy conditions the origin and properties of resident macrophages.* J Exp Med, 2015. **212**(10): p. 1497-512.
84. Mossadegh-Keller, N., et al., *Developmental origin and maintenance of distinct testicular macrophage populations.* J Exp Med, 2017. **214**(10): p. 2829-2841.
85. Locati, M., G. Curtale, and A. Mantovani, *Diversity, Mechanisms, and Significance of Macrophage Plasticity.* Annu Rev Pathol, 2020. **15**: p. 123-147.
86. Chorro, L., et al., *Langerhans cell (LC) proliferation mediates neonatal development, homeostasis, and inflammation-associated expansion of the epidermal LC network.* J Exp Med, 2009. **206**(13): p. 3089-100.
87. Goldmann, T., et al., *Origin, fate and dynamics of macrophages at central nervous system interfaces.* Nat Immunol, 2016. **17**(7): p. 797-805.
88. Trzebanski, S. and S. Jung, *Plasticity of monocyte development and monocyte fates.* Immunol Lett, 2020. **227**: p. 66-78.
89. Shaw, T.N., et al., *Tissue-resident macrophages in the intestine are long lived and defined by Tim-4 and CD4 expression.* J Exp Med, 2018. **215**(6): p. 1507-1518.
90. Evren, E., *Distinct developmental pathways from blood monocytes generate human lung macrophage diversity.* 2021(54): p. 1-17.
91. Lavin, Y., et al., *Tissue-resident macrophage enhancer landscapes are shaped by the local microenvironment.* Cell, 2014. **159**(6): p. 1312-26.
92. Mass, E., et al., *Specification of tissue-resident macrophages during organogenesis.* Science, 2016. **353**(6304).
93. Olingy, C.E., H.Q. Dinh, and C.C. Hedrick, *Monocyte heterogeneity and functions in cancer.* J Leukoc Biol, 2019. **106**(2): p. 309-322.

94. Rodero, M.P., et al., *Immune surveillance of the lung by migrating tissue monocytes.* Elife, 2015. **4**: p. e07847.
95. Looney, M.R., et al., *Stabilized imaging of immune surveillance in the mouse lung.* Nat Methods, 2011. **8**(1): p. 91-6.
96. Swirski, F.K., et al., *Identification of splenic reservoir monocytes and their deployment to inflammatory sites.* Science, 2009. **325**(5940): p. 612-6.
97. Robbins, C.S., et al., *Extramedullary hematopoiesis generates Ly-6C(high) monocytes that infiltrate atherosclerotic lesions.* Circulation, 2012. **125**(2): p. 364-74.
98. Patel, A.A., et al., *The fate and lifespan of human monocyte subsets in steady state and systemic inflammation.* J Exp Med, 2017. **214**(7): p. 1913-1923.
99. Varol, C., et al., *Monocytes give rise to mucosal, but not splenic, conventional dendritic cells.* J Exp Med, 2007. **204**(1): p. 171-80.
100. Gren, S.T., et al., *A Single-Cell Gene-Expression Profile Reveals Inter-Cellular Heterogeneity within Human Monocyte Subsets.* PLoS One, 2015. **10**(12): p. e0144351.
101. Schmidl, C., et al., *Transcription and enhancer profiling in human monocyte subsets.* Blood, 2014. **123**(17): p. e90-9.
102. Prabhu, V.M., et al., *Monocyte Based Correlates of Immune Activation and Viremia in HIV-Infected Long-Term Non-Progressors.* Front Immunol, 2019. **10**: p. 2849.
103. Kapellos, T.S., et al., *Human Monocyte Subsets and Phenotypes in Major Chronic Inflammatory Diseases.* Front Immunol, 2019. **10**: p. 2035.
104. Gómez-Olarte, S., et al., *Intermediate Monocytes and Cytokine Production Associated With Severe Forms of Chagas Disease.* Front Immunol, 2019. **10**: p. 1671.
105. Landsman, L., et al., *CX3CR1 is required for monocyte homeostasis and atherogenesis by promoting cell survival.* Blood, 2009. **113**(4): p. 963-72.
106. White, G.E., et al., *Fractalkine promotes human monocyte survival via a reduction in oxidative stress.* Arterioscler Thromb Vasc Biol, 2014. **34**(12): p. 2554-62.
107. Hanna, R.N., et al., *The transcription factor NR4A1 (Nur77) controls bone marrow differentiation and the survival of Ly6C- monocytes.* Nat Immunol, 2011. **12**(8): p. 778-85.
108. Tamura, A., et al., *C/EBPβ is required for survival of Ly6C.* Blood, 2017. **130**(16): p. 1809-1818.
109. Narasimhan, P.B., et al., *Patrolling Monocytes Control NK Cell Expression of Activating and Stimulatory Receptors to Curtail Lung Metastases.* J Immunol, 2020. **204**(1): p. 192-198.
110. Carlin, L.M., et al., *Nr4a1-dependent Ly6C(low) monocytes monitor endothelial cells and orchestrate their disposal.* Cell, 2013. **153**(2): p. 362-75.
111. Auffray, C., et al., *Monitoring of blood vessels and tissues by a population of monocytes with patrolling behavior.* Science, 2007. **317**(5838): p. 666-70.
112. Franklin, R.A., et al., *The cellular and molecular origin of tumor-associated macrophages.* Science, 2014. **344**(6186): p. 921-5.
113. Nourshargh, S. and R. Alon, *Leukocyte migration into inflamed tissues.* Immunity, 2014. **41**(5): p. 694-707.
114. Jenner, W., et al., *Characterisation of leukocytes in a human skin blister model of acute inflammation and resolution.* PLoS One, 2014. **9**(3): p. e89375.
115. Eguíluz-Gracia, I., et al., *Rapid recruitment of CD14(+) monocytes in experimentally induced allergic rhinitis in human subjects.* J Allergy Clin Immunol, 2016. **137**(6): p. 1872-1881.e12.
116. Jardine, L., et al., *Lipopolysaccharide inhalation recruits monocytes and dendritic cell subsets to the alveolar airspace.* Nat Commun, 2019. **10**(1): p. 1999.
117. Rodero, M.P., et al., *In vivo imaging reveals a pioneer wave of monocyte recruitment into mouse skin wounds.* PLoS One, 2014. **9**(10): p. e108212.
118. Jakubzick, C.V., G.J. Randolph, and P.M. Henson, *Monocyte differentiation and antigen-presenting functions.* Nat Rev Immunol, 2017. **17**(6): p. 349-362.
119. Serbina, N.V., et al., *TNF/iNOS-producing dendritic cells mediate innate immune defense against bacterial infection.* Immunity, 2003. **19**(1): p. 59-70.

120. Bosschaerts, T., et al., *Tip-DC development during parasitic infection is regulated by IL-10 and requires CCL2/CCR2, IFN-gamma and MyD88 signaling.* PLoS Pathog, 2010. **6**(8): p. e1001045.
121. Guilliams, M., et al., *IL-10 dampens TNF/inducible nitric oxide synthase-producing dendritic cell-mediated pathogenicity during parasitic infection.* J Immunol, 2009. **182**(2): p. 1107-18.
122. De Trez, C., et al., *iNOS-producing inflammatory dendritic cells constitute the major infected cell type during the chronic Leishmania major infection phase of C57BL/6 resistant mice.* PLoS Pathog, 2009. **5**(6): p. e1000494.
123. Lin, J.D., et al., *Single-cell analysis of fate-mapped macrophages reveals heterogeneity, including stem-like properties, during atherosclerosis progression and regression.* JCI Insight, 2019. **4**(4).
124. Saresella, M., et al., *A complex proinflammatory role for peripheral monocytes in Alzheimer's disease.* J Alzheimers Dis, 2014. **38**(2): p. 403-13.
125. Mildner, A., et al., *CCR2+Ly-6Chi monocytes are crucial for the effector phase of autoimmunity in the central nervous system.* Brain, 2009. **132**(Pt 9): p. 2487-500.
126. Shaked, I., et al., *Transcription factor Nr4a1 couples sympathetic and inflammatory cues in CNS-recruited macrophages to limit neuroinflammation.* Nat Immunol, 2015. **16**(12): p. 1228-34.
127. Ajami, B., et al., *Infiltrating monocytes trigger EAE progression, but do not contribute to the resident microglia pool.* Nat Neurosci, 2011. **14**(9): p. 1142-9.
128. Ajami, B. and L. Steinman, *Nonclassical monocytes: are they the next therapeutic targets in multiple sclerosis?* Immunol Cell Biol, 2018. **96**(2): p. 125-127.
129. Rodero, M.P. and K. Khosrotehrani, *Skin wound healing modulation by macrophages.* Int J Clin Exp Pathol, 2010. **3**(7): p. 643-53.
130. Rodero, M.P., et al., *Reduced Il17a expression distinguishes a Ly6c(lo)MHCII(hi) macrophage population promoting wound healing.* J Invest Dermatol, 2013. **133**(3): p. 783-792.
131. Askenase, M.H., et al., *Bone-Marrow-Resident NK Cells Prime Monocytes for Regulatory Function during Infection.* Immunity, 2015. **42**(6): p. 1130-42.
132. Quintar, A., et al., *Endothelial Protective Monocyte Patrolling in Large Arteries Intensified by Western Diet and Atherosclerosis.* Circ Res, 2017. **120**(11): p. 1789-1799.
133. Scott, M.K.D., et al., *Increased monocyte count as a cellular biomarker for poor outcomes in fibrotic diseases: a retrospective, multicentre cohort study.* Lancet Respir Med, 2019. **7**(6): p. 497-508.
134. Cornwell, W.D., et al., *Activation and polarization of circulating monocytes in severe chronic obstructive pulmonary disease.* BMC Pulm Med, 2018. **18**(1): p. 101.
135. Puchner, A., et al., *Non-classical monocytes as mediators of tissue destruction in arthritis.* Ann Rheum Dis, 2018. **77**(10): p. 1490-1497.
136. Gjelstrup, M.C., et al., *Subsets of activated monocytes and markers of inflammation in incipient and progressed multiple sclerosis.* Immunol Cell Biol, 2018. **96**(2): p. 160-174.
137. Bekkering, S., et al., *Innate immune cell activation and epigenetic remodeling in symptomatic and asymptomatic atherosclerosis in humans in vivo.* Atherosclerosis, 2016. **254**: p. 228-236.
138. Merad, M. and J.C. Martin, *Pathological inflammation in patients with COVID-19: a key role for monocytes and macrophages.* Nat Rev Immunol, 2020. **20**(6): p. 355-362.
139. Hanahan, D. and R.A. Weinberg, *Hallmarks of cancer: the next generation.* Cell, 2011. **144**(5): p. 646-74.
140. Allavena, P., et al., *The Yin-Yang of tumor-associated macrophages in neoplastic progression and immune surveillance.* Immunol Rev, 2008. **222**: p. 155-61.
141. Mantovani, A., et al., *Tumour-associated macrophages as treatment targets in oncology.* Nat Rev Clin Oncol, 2017. **14**(7): p. 399-416.
142. Cortese, N., et al., *Macrophages at the crossroads of anticancer strategies.* Front Biosci (Landmark Ed), 2019. **24**: p. 1271-1283.

143. Chun, E., et al., *CCL2 Promotes Colorectal Carcinogenesis by Enhancing Polymorphonuclear Myeloid-Derived Suppressor Cell Population and Function.* Cell Rep, 2015. **12**(2): p. 244-57.
144. Qian, B.Z., et al., *CCL2 recruits inflammatory monocytes to facilitate breast-tumour metastasis.* Nature, 2011. **475**(7355): p. 222-5.
145. Arwert, E.N., et al., *A Unidirectional Transition from Migratory to Perivascular Macrophage Is Required for Tumor Cell Intravasation.* Cell Rep, 2018. **23**(5): p. 1239-1248.
146. Loyher, P.L., et al., *Macrophages of distinct origins contribute to tumor development in the lung.* J Exp Med, 2018. **215**(10): p. 2536-2553.
147. Qian, B., et al., *A distinct macrophage population mediates metastatic breast cancer cell extravasation, establishment and growth.* PLoS One, 2009. **4**(8): p. e6562.
148. Lapenna, A., M. De Palma, and C.E. Lewis, *Perivascular macrophages in health and disease.* Nat Rev Immunol, 2018. **18**(11): p. 689-702.
149. Mazzieri, R., et al., *Targeting the ANG2/TIE2 axis inhibits tumor growth and metastasis by impairing angiogenesis and disabling rebounds of proangiogenic myeloid cells.* Cancer Cell, 2011. **19**(4): p. 512-26.
150. Singhal, S., et al., *Human tumor-associated monocytes/macrophages and their regulation of T cell responses in early-stage lung cancer.* Sci Transl Med, 2019. **11**(479).
151. Coffelt, S.B., et al., *Angiopoietin-2 regulates gene expression in TIE2-expressing monocytes and augments their inherent proangiogenic functions.* Cancer Res, 2010. **70**(13): p. 5270-80.
152. Shojaei, F., et al., *Tumor refractoriness to anti-VEGF treatment is mediated by CD11b+Gr1+ myeloid cells.* Nat Biotechnol, 2007. **25**(8): p. 911-20.
153. Cassetta, L., et al., *Human Tumor-Associated Macrophage and Monocyte Transcriptional Landscapes Reveal Cancer-Specific Reprogramming, Biomarkers, and Therapeutic Targets.* Cancer Cell, 2019. **35**(4): p. 588-602.e10.
154. Vermi, W., et al., s*lan+ Monocytes and Macrophages Mediate CD20-Dependent B-cell Lymphoma Elimination via ADCC and ADCP.* Cancer Res, 2018. **78**(13): p. 3544-3559.
155. Gordon, I.O. and R.S. Freedman, *Defective antitumor function of monocyte-derived macrophages from epithelial ovarian cancer patients.* Clin Cancer Res, 2006. **12**(5): p. 1515-24.
156. Griffith, T.S., et al., *Monocyte-mediated tumoricidal activity via the tumor necrosis factor-related cytokine, TRAIL.* J Exp Med, 1999. **189**(8): p. 1343-54.
157. Pellizzari, G., et al., *Harnessing Therapeutic IgE Antibodies to Re-educate Macrophages against Cancer.* Trends Mol Med, 2020. **26**(6): p. 615-626.
158. Karagiannis, S.N., et al., *IgE-antibody-dependent immunotherapy of solid tumors: cytotoxic and phagocytic mechanisms of eradication of ovarian cancer cells.* J Immunol, 2007. **179**(5): p. 2832-43.
159. Josephs, D.H., et al., *Anti-Folate Receptor-α IgE but not IgG Recruits Macrophages to Attack Tumors via TNFα/MCP-1 Signaling.* Cancer Res, 2017. **77**(5): p. 1127-1141.
160. Karagiannis, S.N., et al., *Activity of human monocytes in IgE antibody-dependent surveillance and killing of ovarian tumor cells.* Eur J Immunol, 2003. **33**(4): p. 1030-40.
161. Satoh, T., et al., *Identification of an atypical monocyte and committed progenitor involved in fibrosis.* Nature, 2017. **541**(7635): p. 96-101.
162. Baldridge, M.T., K.Y. King, and M.A. Goodell, *Inflammatory signals regulate hematopoietic stem cells.* Trends Immunol, 2011. **32**(2): p. 57-65.
163. Griseri, T., et al., *Dysregulated hematopoietic stem and progenitor cell activity promotes interleukin-23-driven chronic intestinal inflammation.* Immunity, 2012. **37**(6): p. 1116-29.
164. Nagai, Y., et al., *Toll-like receptors on hematopoietic progenitor cells stimulate innate immune system replenishment.* Immunity, 2006. **24**(6): p. 801-12.
165. Wolf, A.A., et al., *The Ontogeny of Monocyte Subsets.* Front Immunol, 2019. **10**: p. 1642.
166. Lessard, A.J., et al., *Triggering of NOD2 Receptor Converts Inflammatory Ly6C.* Cell Rep, 2017. **20**(8): p. 1830-1843.

167. Netea, M.G., et al., *Defining trained immunity and its role in health and disease.* Nat Rev Immunol, 2020. **20**(6): p. 375-388.
168. Arts, R.J.W., et al., *BCG Vaccination Protects against Experimental Viral Infection in Humans through the Induction of Cytokines Associated with Trained Immunity.* Cell Host Microbe, 2018. **23**(1): p. 89-100.e5.
169. Walk, J., et al., *Outcomes of controlled human malaria infection after BCG vaccination.* Nat Commun, 2019. **10**(1): p. 874.
170. Redelman-Sidi, G., M.S. Glickman, and B.H. Bochner, *The mechanism of action of BCG therapy for bladder cancer--a current perspective.* Nat Rev Urol, 2014. **11**(3): p. 153-62.
171. Stewart, J.H. and E.A. Levine, *Role of bacillus Calmette-Guérin in the treatment of advanced melanoma.* Expert Rev Anticancer Ther, 2011. **11**(11): p. 1671-6.
172. Powles, R.L., et al., *Maintenance of remission in acute myelogenous leukaemia by a mixture of B.C.G. and irradiated leukaemia cells.* Lancet, 1977. **2**(8048): p. 1107-10.
173. Villumsen, M., et al., *Risk of lymphoma and leukaemia after bacille Calmette-Guérin and smallpox vaccination: a Danish case-cohort study.* Vaccine, 2009. **27**(49): p. 6950-8.
174. Kaufmann, E., et al., *BCG Educates Hematopoietic Stem Cells to Generate Protective Innate Immunity against Tuberculosis.* Cell, 2018. **172**(1-2): p. 176-190.e19.
175. Machiels, B., et al., *A gammaherpesvirus provides protection against allergic asthma by inducing the replacement of resident alveolar macrophages with regulatory monocytes.* Nat Immunol, 2017. **18**(12): p. 1310-1320.
176. Yao, Y., et al., *Induction of Autonomous Memory Alveolar Macrophages Requires T Cell Help and Is Critical to Trained Immunity.* Cell, 2018. **175**(6): p. 1634-1650.e17.
177. Netea, M.G., L.A. Joosten, and J.W. van der Meer, *Adaptation and memory in innate immunity.* Semin Immunol, 2016. **28**(4): p. 317-8.
178. Hlavacek, W.S., et al., *The complexity of complexes in signal transduction.* Biotechnol Bioeng, 2003. **84**(7): p. 783-94.
179. Kummer, D., et al., *Tetraspanins: integrating cell surface receptors to functional microdomains in homeostasis and disease.* Med Microbiol Immunol, 2020.
180. Eon Kuek, L., et al., *The MS4A family: counting past 1, 2 and 3.* Immunol Cell Biol, 2016. **94**(1): p. 11-23.
181. Zuccolo, J., et al., *Phylogenetic analysis of the MS4A and TMEM176 gene families.* PLoS One, 2010. **5**(2): p. e9369.
182. Liang, Y. and T.F. Tedder, *Identification of a CD20-, FcepsilonRIbeta-, and HTm4-related gene family: sixteen new MS4A family members expressed in human and mouse.* Genomics, 2001. **72**(2): p. 119-27.
183. Ishibashi, K., et al., *Identification of a new multigene four-transmembrane family (MS4A) related to CD20, HTm4 and beta subunit of the high-affinity IgE receptor.* Gene, 2001. **264**(1): p. 87-93.
184. Hulett, M.D., et al., *Isolation, tissue distribution, and chromosomal localization of a novel testis-specific human four-transmembrane gene related to CD20 and FcepsilonRI-beta.* Biochem Biophys Res Commun, 2001. **280**(1): p. 374-9.
185. McAleese, S.M. and H.R. Miller, *Cloning and sequencing of the equine and ovine high-affinity IgE receptor beta-and gamma-chain cDNA.* Immunogenetics, 2003. **55**(2): p. 122-5.
186. Xu, Y., et al., *cDNA cloning and localization of Sp3111 (also called Ms4a14) in the rat testis.* Reproduction, 2014. **148**(1): p. 81-6.
187. Kano, R., et al., *Canine CD20 gene.* Vet Immunol Immunopathol, 2005. **108**(3-4): p. 265-8.
188. Liang, Y., et al., *Structural organization of the human MS4A gene cluster on Chromosome 11q12.* Immunogenetics, 2001. **53**(5): p. 357-68.
189. Hupp, K., et al., *Gene mapping of the three subunits of the high affinity FcR for IgE to mouse chromosomes 1 and 19.* J Immunol, 1989. **143**(11): p. 3787-91.

190. Tedder, T.F. and P. Engel, *CD20: a regulator of cell-cycle progression of B lymphocytes.* Immunol Today, 1994. **15**(9): p. 450-4.
191. Panizo, C., *Safety of subcutaneous administration of rituximab during the first-line treatment of patients with non-hodgkin lymphoma: the mabrella study.* 2016(128(22):2971).
192. Freeman, C.L. and L. Sehn, *Anti-CD20 Directed Therapy of B Cell Lymphomas: Are New Agents Really Better?* Curr Oncol Rep, 2018. **20**(12): p. 103.
193. Du, F.H., E.A. Mills, and Y. Mao-Draayer, *Next-generation anti-CD20 monoclonal antibodies in autoimmune disease treatment.* Auto Immun Highlights, 2017. **8**(1): p. 12.
194. Pavlasova, G. and M. Mraz, *The regulation and function of CD20: an "enigma" of B-cell biology and targeted therapy.* Haematologica, 2020. **105**(6): p. 1494-1506.
195. Kuijpers, T.W., et al., *CD20 deficiency in humans results in impaired T cell-independent antibody responses.* J Clin Invest, 2010. **120**(1): p. 214-22.
196. Uchida, J., et al., *Mouse CD20 expression and function.* Int Immunol, 2004. **16**(1): p. 119-29.
197. O'Keefe, T.L., et al., *Mice carrying a CD20 gene disruption.* Immunogenetics, 1998. **48**(2): p. 125-32.
198. Li, H., et al., *Store-operated cation entry mediated by CD20 in membrane rafts.* J Biol Chem, 2003. **278**(43): p. 42427-34.
199. Franke, A., et al., *Antibodies against CD20 or B-cell receptor induce similar transcription patterns in human lymphoma cell lines.* PLoS One, 2011. **6**(2): p. e16596.
200. Pavlasova, G., et al., *Rituximab primarily targets an intra-clonal BCR signaling proficient CLL subpopulation characterized by high CD20 levels.* Leukemia, 2018. **32**(9): p. 2028-2031.
201. Kraft, S. and J.P. Kinet, *New developments in FcepsilonRI regulation, function and inhibition.* Nat Rev Immunol, 2007. **7**(5): p. 365-78.
202. Kraft, S. and N. Novak, *Fc receptors as determinants of allergic reactions.* Trends Immunol, 2006. **27**(2): p. 88-95.
203. Donnadieu, E., et al., *Competing functions encoded in the allergy-associated F(c)epsilonRIbeta gene.* Immunity, 2003. **18**(5): p. 665-74.
204. Cruse, G., et al., *A novel FcεRIβ-chain truncation regulates human mast cell proliferation and survival.* FASEB J, 2010. **24**(10): p. 4047-57.
205. Ohtsubo-Yoshioka, M., et al., *Fc receptor beta chain deficiency exacerbates murine arthritis in the anti-type II collagen antibody-induced experimental model.* Mod Rheumatol, 2013. **23**(4): p. 804-10.
206. Deming, Y., et al., *The MS4A gene cluster is a key modulator of soluble TREM2 and Alzheimer's disease risk.* Sci Transl Med, 2019. **11**(505).
207. Hou, X.H., et al., *Genome-wide association study identifies Alzheimer's risk variant in MS4A6A influencing cerebrospinal fluid sTREM2 levels.* Neurobiol Aging, 2019. **84**: p. 241.e13-241.e20.
208. Schwabe, T., K. Srinivasan, and H. Rhinn, *Shifting paradigms: The central role of microglia in Alzheimer's disease.* Neurobiol Dis, 2020. **143**: p. 104962.
209. Ulland, T.K. and M. Colonna, *TREM2 - a key player in microglial biology and Alzheimer disease.* Nat Rev Neurol, 2018. **14**(11): p. 667-675.
210. Martinez, F.O., et al., *Macrophage activation and polarization.* Front Biosci, 2008. **13**: p. 453-61.
211. Murray, P.J., et al., *Macrophage activation and polarization: nomenclature and experimental guidelines.* Immunity, 2014. **41**(1): p. 14-20.
212. Martinez, F.O., et al., *Transcriptional profiling of the human monocyte-to-macrophage differentiation and polarization: new molecules and patterns of gene expression.* J Immunol, 2006. **177**(10): p. 7303-11.
213. Mattiola, I., et al., *The macrophage tetraspan MS4A4A enhances dectin-1-dependent NK cell-mediated resistance to metastasis.* Nat Immunol, 2019. **20**(8): p. 1012-1022.

214. Czimmerer, Z., et al., *Identification of novel markers of alternative activation and potential endogenous PPARγ ligand production mechanisms in human IL-4 stimulated differentiating macrophages.* Immunobiology, 2012. **217**(12): p. 1301-14.
215. Sanyal, R., et al., *MS4A4A: a novel cell surface marker for M2 macrophages and plasma cells.* Immunol Cell Biol, 2017. **95**(7): p. 611-619.
216. Wang, H., X. Wu, and Y. Chen, *Stromal-Immune Score-Based Gene Signature: A Prognosis Stratification Tool in Gastric Cancer.* Front Oncol, 2019. **9**: p. 1212.
217. Siemers, N.O., et al., *Genome-wide association analysis identifies genetic correlates of immune infiltrates in solid tumors.* PLoS One, 2017. **12**(7): p. e0179726.
218. Sui, Y. and W. Zeng, *MS4A4A Regulates Arginase 1 Induction during Macrophage Polarization and Lung Inflammation in Mice.* Eur J Immunol, 2020. **50**(10): p. 1602-1605.
219. Schmieder, A., et al., *Synergistic activation by p38MAPK and glucocorticoid signaling mediates induction of M2-like tumor-associated macrophages expressing the novel CD20 homolog MS4A8A.* Int J Cancer, 2011. **129**(1): p. 122-32.
220. Cruse, G., et al., *The CD20 homologue MS4A4 directs trafficking of KIT toward clathrin-independent endocytosis pathways and thus regulates receptor signaling and recycling.* Mol Biol Cell, 2015. **26**(9): p. 1711-27.
221. Arthur, G.K., et al., *The FcεRIß homologue, MS4A4A, promotes FcεRI signal transduction and store-operated Ca.* Cell Signal, 2020. **71**: p. 109617.
222. Griffiths, J.I., et al., *Circulating immune cell phenotype dynamics reflect the strength of tumor-immune cell interactions in patients during immunotherapy.* Proc Natl Acad Sci U S A, 2020. **117**(27): p. 16072-16082.
223. Collin, M. and V. Bigley, *Human dendritic cell subsets: an update.* Immunology, 2018. **154**(1): p. 3-20.
224. Björkström, N.K., H.G. Ljunggren, and J.K. Sandberg, *CD56 negative NK cells: origin, function, and role in chronic viral disease.* Trends Immunol, 2010. **31**(11): p. 401-6.
225. Zilionis, R., et al., *Single-Cell Transcriptomics of Human and Mouse Lung Cancers Reveals Conserved Myeloid Populations across Individuals and Species.* Immunity, 2019. **50**(5): p. 1317-1334.e10.
226. Ping, Z., et al., *Activation of NF-κB driven inflammatory programs in mesenchymal elements attenuates hematopoiesis in low-risk myelodysplastic syndromes.* Leukemia, 2019. **33**(2): p. 536-541.
227. Michelson, A.D., et al., *Circulating monocyte-platelet aggregates are a more sensitive marker of in vivo platelet activation than platelet surface P-selectin: studies in baboons, human coronary intervention, and human acute myocardial infarction.* Circulation, 2001. **104**(13): p. 1533-7.
228. Furman, M.I., et al., *Circulating monocyte-platelet aggregates are an early marker of acute myocardial infarction.* J Am Coll Cardiol, 2001. **38**(4): p. 1002-6.
229. Tacke, F., et al., *Immature monocytes acquire antigens from other cells in the bone marrow and present them to T cells after maturing in the periphery.* J Exp Med, 2006. **203**(3): p. 583-97.
230. Varol, D., et al., *Dicer Deficiency Differentially Impacts Microglia of the Developing and Adult Brain.* Immunity, 2017. **46**(6): p. 1030-1044.e8.
231. See, P., et al., *Mapping the human DC lineage through the integration of high-dimensional techniques.* Science, 2017. **356**(6342).
232. Zarjou, A., et al., *Ferritin Light Chain Confers Protection Against Sepsis-Induced Inflammation and Organ Injury.* Front Immunol, 2019. **10**: p. 131.
233. Mesquita, G., et al., *H-Ferritin is essential for macrophages' capacity to store or detoxify exogenously added iron.* Sci Rep, 2020. **10**(1): p. 3061.
234. Gaetano, C., L. Massimo, and M. Alberto, *Control of iron homeostasis as a key component of macrophage polarization.* Haematologica, 2010. **95**(11): p. 1801-3.

235. Hollingworth, P., et al., *Common variants at ABCA7, MS4A6A/MS4A4E, EPHA1, CD33 and CD2AP are associated with Alzheimer's disease.* Nat Genet, 2011. **43**(5): p. 429-35.
236. Rice, L.M., et al., *A longitudinal biomarker for the extent of skin disease in patients with diffuse cutaneous systemic sclerosis.* Arthritis Rheumatol, 2015. **67**(11): p. 3004-15.
237. Frankenberger, M., et al., *Transcript profiling of CD16-positive monocytes reveals a unique molecular fingerprint.* Eur J Immunol, 2012. **42**(4): p. 957-74.
238. Kared, H., et al., *CD57 in human natural killer cells and T-lymphocytes.* Cancer Immunol Immunother, 2016. **65**(4): p. 441-52.
239. Pullen, N.A., et al., *The Fyn-STAT5 Pathway: A New Frontier in IgE- and IgG-Mediated Mast Cell Signaling.* Front Immunol, 2012. **3**: p. 117.
240. Weiskopf, K. and I.L. Weissman, *Macrophages are critical effectors of antibody therapies for cancer.* MAbs, 2015. **7**(2): p. 303-10.
241. Krieg, C., et al., *High-dimensional single-cell analysis predicts response to anti-PD-1 immunotherapy.* Nat Med, 2018. **24**(2): p. 144-153.
242. Lee, J., et al., *The MHC class II antigen presentation pathway in human monocytes differs by subset and is regulated by cytokines.* PLoS One, 2017. **12**(8): p. e0183594.
243. Thomas, G., et al., *Nonclassical patrolling monocyte function in the vasculature.* Arterioscler Thromb Vasc Biol, 2015. **35**(6): p. 1306-16.
244. Gunther, P., *Rule-based data informed generation of cellular consensus maps.* 2019: bioRxiv.
245. Böttcher, C., et al., *Multi-parameter immune profiling of peripheral blood mononuclear cells by multiplexed single-cell mass cytometry in patients with early multiple sclerosis.* Sci Rep, 2019. **9**(1): p. 19471.
246. Donnadieu, E., M.H. Jouvin, and J.P. Kinet, *A second amplifier function for the allergy-associated Fc(epsilon)RI-beta subunit.* Immunity, 2000. **12**(5): p. 515-23.